University of Southern Queensland

Faculty of Health, Engineering & Sciences

The Effect of Fibres on the Properties of Concrete with Oil Contaminated Sand

A dissertation submitted by

Ashleigh Braden

in fulfilment of the requirements of

Course ENG4111 Research Project part 1 &
ENG4112 Research Project part 2

Towards the degree of

Bachelor of Civil Engineering (Honours)

Submitted: 29th October 2015

Abstract

The use of oil contaminated materials in construction applications such as concrete could result in a cleaner environment and a cost effective construction material. This research aimed at investigating the physical and mechanical properties of concrete with light crude oil contaminated sand. It focused on evaluating the effects of the addition of short fibres and determining the optimum dosage of short fibres that can enhance the physical and mechanical properties of concrete consisting of sand contaminated with light crude oil. In order to achieve the project objectives, the following experimental programmes were implemented:

1. Characterisation of the physical and mechanical properties of concrete using sand with different levels of oil contamination.
2. Evaluation of the compressive and flexural behaviour of crude oil-impacted sand in concrete with four types of short fibres.
3. Determination of the optimum dosage by volume through investigation of compressive and flexural behaviour.

The results of the experimental investigation showed that concrete density and compressive strength decreases with increased oil content. To maximise options for the use of oil contaminated materials, a maximum oil content of 10% by volume of sand was deemed suitable for use in concrete for construction applications.

The addition of 0.1% by concrete volume of Forta Ferro, polpropylene and ReoShore 45 fibres had an insignificant effect on the mechanical properties of concrete with 10% oil contamination, while steel fibres slightly enhanced the concrete compressive and flexural strength. Thus, it was selected as the best performing fibre.

The steel fibres in 10% oil contaminated concrete at dosages between 0.00115% - 0.5% by concrete volume (0.9 - 39.65 kg/m^3) had minimal effect on oil-impacted concrete mechanical properties. The maximum fibre volume dosage of 0.5% most improved concrete flexural strength while causing minimal reduction to compressive strength.

From the results of this study, it was found that minimal recovery of concrete strength properties with 10% oil contaminated sand was made with the inclusion of fibres. This could be due to concrete saturation due to oil, which greatly affected its bond with fibres. Further investigations should be conducted to determine the maximum level of oil contamination that will not hinder the enhancement provided by short fibres on concrete properties to make this waste material applicable in building and construction.

University of Southern Queensland

Faculty of Health, Engineering and Sciences

ENG4111/ENG4112 Research Project

Limitations of Use

The Council of the University of Southern Queensland, its Faculty of Health, Engineering & Sciences, and the staff of the University of Southern Queensland, do not accept any responsibility for the truth, accuracy or completeness of material contained within or associated with this dissertation.

Persons using all or any part of this material do so at their own risk, and not at the risk of the Council of the University of Southern Queensland, its Faculty of Health, Engineering & Sciences or the staff of the University of Southern Queensland.

This dissertation reports an educational exercise and has no purpose or validity beyond this exercise. The sole purpose of the course pair entitled "Research Project" is to contribute to the overall education within the student's chosen degree program. This document, the associated hardware, software, drawings, and other material set out in the associated appendices should not be used for any other purpose: if they are so used, it is entirely at the risk of the user.

University of Southern Queensland

Faculty of Health, Engineering and Sciences

ENG4111/ENG4112 Research Project

Certification of Dissertation

I certify that the ideas, designs and experimental work, results, analyses and conclusions set out in this dissertation are entirely my own effort, except where otherwise indicated and acknowledged.

I further certify that the work is original and has not been previously submitted for assessment in any other course or institution, except where specifically stated.

Ashleigh Braden

Student Number: 0061033155

_____

Signature

_____

Date

Acknowledgements

This project was carried out under the supervision of Dr Allan Manalo and Dr Weena Lokuge of the University of Southern Queensland along with the assistance of Rajab Abousnina. Without their supervision and guidance this project would not have been possible.

I would also like to thank my Family and Friends for providing continual support and encouragement throughout the process.

Table of Contents

List of Figures

List of Tables

List of Abbreviations

Abbreviations

PHC	Petroleum Hydrocarbon
COIS	Crude Oil-Impacted Sand
FRC	Fibre-Reinforced Concrete
OPC	Ordinary Portland Cement
MDD	Maximum Dry Density
OMC	Optimum Moisture Content
UCS	Unconfined Compressive Strength
S/S	Stabilisation/Solidification
HMA	Hot Mix Asphalt
SFRC	Steel Fibre-Reinforced Concrete
VCC	Vibrator Compacted Concrete
LWC	Light Weight Concrete
SSD	Saturated Surface Dry
GP	General Purpose

Chapter 1

Introduction

1.1 Project Background

Global energy demand is set to increase 37% by 2040, with increased oil use for transport and petrochemicals driving demand higher from 90 million barrels per day (mb/d) in 2013 to a projected 104 mb/d in 2040 (International Energy Agency 2014). The worldwide increase in energy demand is driven by:

1. *Industrialisation due to emerging markets:* As economies industrialise, demand for energy increases.
2. *Increasing wealth in these emerging markets:* When economies grow as does their energy needs.
3. *Forecast global population growth:* Like economy growth, with a larger population to cater for, energy demand increases.
4. *Globalization:* Energy use in transportation increases as we travel more often, further and with greater speed.
5. *Concerns over energy security:* Long-term concerns over energy security around the world have led to an irrational premium paid for energy assets.

Chevron (2014) says that even if the use of renewable energy (wind, solar) triples over the next 25 years, the world is still likely to depend on fossil fuels for at least 50 percent of its energy needs. Figure 1.1 illustrates the final fuel shares of total final consumption by energy source (International Energy Agency 2014). It is clearly seen from the figure that oil is the most in demand energy source making up 40.7% of the world's energy needs.

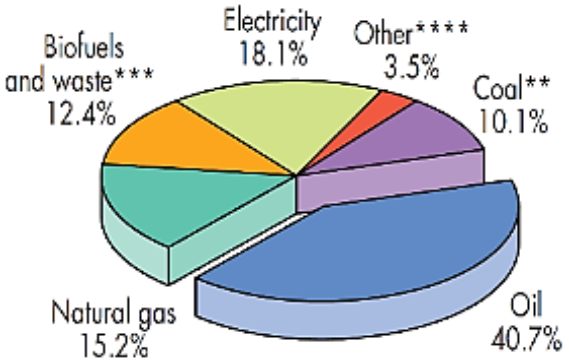

Figure 1.1: Final fuel shares of total final consumption by energy source (International Energy Agency 2014)

Due to the demand for oil as an energy source, hydrocarbon-polluted soils are widespread across the globe and over the past decade sand contamination has increased. Today, petroleum hydrocarbon (PHC) contaminated sand contributes to a significant fraction of waste materials in the environment. Some major causes of crude oil contamination are; oil spills, oil pipe vandalism, leakage from underground oil storage tanks, treatment activities for exploration, drilling, hydrocarbon waste disposed from industries and hydrocarbon production itself. Oil spills are a common event in the Niger Delta region, West Africa's biggest producer of petroleum, leaving the environment oil ridden as shown in Figure 1.2 (Petesch 2013).

Figure 1.2: Oil Contamination in Niger Delta (Petesch 2013)

Similarly, Libya is faced with the significant issue of contamination from crude oil pits, storage facilities, refineries and the petrochemical and chemical plants associated with production and refining operations. Dumping is common practice in remote areas of the country where most of the crude oil and natural gas wells are located (The Telegraph 2008).

Various methods exist for the treatment PHC-polluted soils which range from the conventional methods of excavating affected soils and moving them to landfills, capping of the affected areas in a site, stabilising soil with materials such as lime, apatite and cement to chemical methods like bioremediation. These solutions for contaminated soils are considered unsustainable as treatment technologies are either costly and/or the treated products are sent to land fill without any potential end-use (Almabrok, McLaughlan & Vessalas 2013).

In the past, research has been conducted to review the feasibility of the use of crude oil-impacted sand (COIS) in concrete. On paper, this is a viable solution for contaminated sand – while the use of these waste material in the construction industry would contribute to a cleaner environment, it would also result in a cost effective construction material. However, previous studies have noted that the use of COIS in

concrete effects its mechanical properties resulting in a reduction in compressive strength (Ajagbe et al. 2011; Ayininuola 2008; Osuji & Nwankwo 2015; Almabrok, McLaughlan & Vessalas 2013; Ejeh & Uche 2009). Due to this loss in strength, crude oil-impacted concrete is usually limited to use in non/low-load bearing structures such as sandcrete bricks and binding concrete (Oluremi & Osuolale 2014).

The addition of fibres in oil-impacted concrete may be the compensation solution for this known reduction in concrete strength. Concrete is acknowledged to be a relatively brittle material when subjected to normal stresses and impact loads, where tensile strength is only approximately one tenth of its compressive strength. The introduction of fibres is offered as a solution to modify and enhance the mechanical properties and behaviour of concrete in its applications. Fibre-reinforced concrete (FRC) can enhance impact, abrasives, durability, vibration and specifically crack control properties that ordinary Portland cement (OPC) concrete does not possess (Maccaferri 2015).

Fibres are most generally discontinuous, randomly distributed throughout the cement matrices. They vary in types, geometry, properties and availability in the construction industry (Døssland 2008). The most common are polypropylene fibres, steel fibres and glass fibres (Figure 1.3). The effects of the addition of these types of fibres on the properties of concrete with oil contaminated sand will be investigated in this study.

Polypropylene

Steel

Glass

Figure 1.3: Common fibre types (Exporters India 2015), (Saint-Gobain 2011)

1.2 Project Aim

This project aims to examine the effect of the addition of fibres on the mechanical and physical characteristics of concrete with oil contaminated sand, which will give a better understanding on the properties of concrete with COIS, its potential application as structural concrete and solutions for it to meet strength requirements through the addition fibres.

1.3 Research Objectives

The project aim was reviewed and split into a number of specific objectives defining the project objectives:

1. Review of current and related literature on crude oil contaminated sand, oil contaminated sand in concrete and fibre-reinforced concrete including its applications, properties and mechanical behaviour.
2. Investigate the effect of oil contamination on the physical and mechanical properties of concrete. Determine the maximum oil content that is suitable of use in structural concrete.
3. Evaluate the compressive and flexural behaviour of crude oil-impacted sand in concrete with four different types of fibres and determine the best performing fibre.
4. Determine the optimum dosage of the best performing fibre through investigation of the compressive and flexural behaviour.

1.4 Scope and Limitations

The principle aim of this research project is to improve the knowledge base and offer solutions for the use of oil contaminated materials in construction applications such as concrete. Due to time and budget restrictions, for the purpose of this research, the fine sand in ordinary Portland cement concrete is contaminated with light crude oil before casting, only four types of fibres are considered and the investigation of the behaviour is limited to compressive and flexural testing.

1.5 Dissertation Overview

The dissertation is structured to present the project objectives in chapters:

Chapter 2 – Literature Review

This chapter includes a review of literature relating to crude oil contaminated sand, the use of oil contaminated sand in concrete, the properties and mechanical behaviour of fibre-reinforced concrete.

Chapter 3 – Materials and Methods

This chapter provides a description of the testing programs undertaken in the generation of experimental data for project analysis. The materials and mix design implemented for concrete specimens is outlined along with an overview of test procedures.

Chapter 4 – Properties of Concrete with Oil Contaminated Sand

This chapter reports the results and observations made from the first testing stage, which investigates the physical and mechanical properties of concrete with oil contaminated sand. Experimental findings are outlined and discussed.

Chapter 5 – Properties of Oil Contaminated Concrete with Short Fibres

This chapter reports the results and observations made from the second testing stage, which investigates the physical and mechanical properties of oil-impacted concrete with four fibre types. Experimental findings are outlined and discussed.

Chapter 6 – Optimum Fibre Dosage for Concrete with Oil Contaminated Sand

This chapter reports the results and observations made from the third testing stage, which investigates the optimal fibre dosage volume for oil-impacted concrete. Experimental findings are outlined and discussed.

Chapter 7 – Conclusion

Lastly, this chapter gives a reviewal of research objectives and an overview of project findings. Furthermore, recommendations for further research to improve the prospects of the use of oil contaminated sand in construction is made.

Chapter 2

Literature Review

2.1 Chapter Overview

This literature review provides an overview of the background information relevant to the project along with a number of established past research on the topic. First to be outlined is the basis of this project; the contamination of sand by crude oil (Section 2.2). The section is broken down into components addressing a brief description of the oil production process and oil demand (Section 2.2.1), how soil is contaminated (Section 2.2.2), the geotechnical properties of oil contaminated sand (Section 2.2.3) and a review of the current remediation options for contaminated sand (Section 2.2.4).

The prospect of the use of oil contaminated sand in concrete is then discussed in Section 2.3. The benefits of its use in construction is outlined (Section 2.3.1), followed by a review of past studies that have analysed the effect of contaminated sand on the mechanical properties of concrete (Section 2.3.2).

Based on the findings from Section 2.3.2, an overlook of fibre-reinforced concrete (FRC) is discussed (Section 2.4) as an option to improve the mechanical properties of oil-impacted concrete. The section is an introduction to FRC outlining its historical development (Section 2.4.1), FRC properties (Section 2.4.2), its applications in

modern industries (Section 2.4.3), fibre technology (Section 2.4.4) and fibre types including steel and polypropylene fibres (Section 2.4.5).

Having established an understanding of FRC, the mechanical behaviour of FRC is reviewed in Section 2.5. The mechanism of fibre bridging, fibre-matrix interaction and the mechanics of crack formation and propagation is revised in Sections 2.5.1, 2.5.2 and 2.5.3 respectively. This followed by an outline of the factors affecting the fibre-matrix interaction known as fibre orientation and distribution, fibre mechanical properties and fibre volume dosage in Sections 2.5.4, 2.5.5 and 2.5.6, respectively. Sections 2.5.7 and 2.5.8 then review the strength characteristics of FRC under compressive and flexural loading with referral to relative past investigations.

2.2 Crude Oil Contaminated Sand

2.2.1 Oil Production

The basic process of oil extraction can be classified into four categories which include; exploration, well development, production and site abandonment. Production is the process of extracting hydrocarbons which is processed at a refinery where it is made into marketable products with defined specifications (Devold 2013).

The International Energy Agency's Oil Market Report shows the world's oil demand increasing, with the estimated demand for the fourth quarter of 2016 at 96.82 million barrels per day (refer to Figure 2.1).

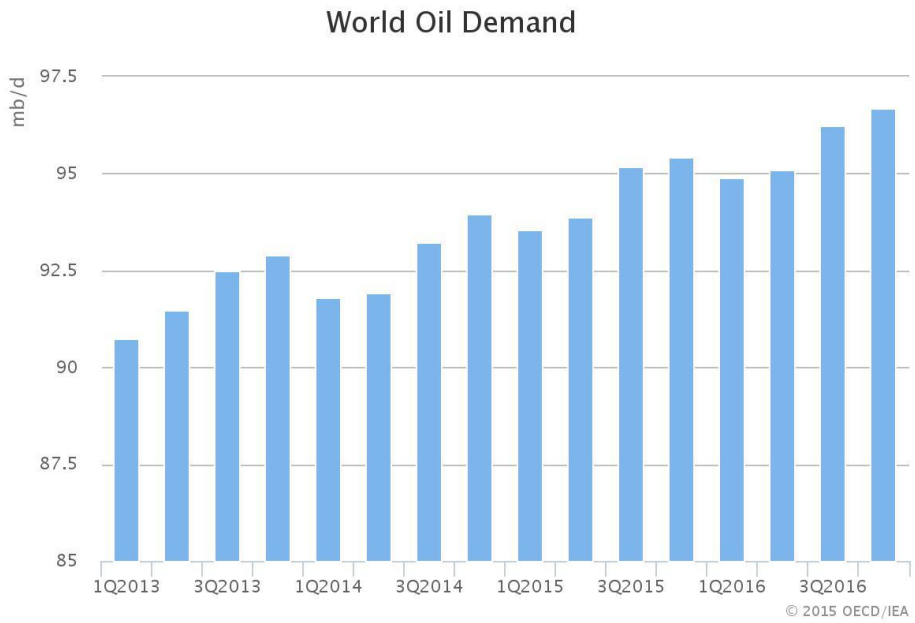

Figure 2.1: World oil supply (International Energy Agency 2015)

As the demand for oil continually increases, the consequential effect on the environment is brought into question. Hydrocarbon-polluted sand is widespread due to increase in the demand of oil and has become a common problem in recent years.

2.2.2 Sand Contamination

The increasing demand for crude oil has resulted in an increase of its production, transportation and refining, which in turn has caused gross hydrocarbon-polluted sand. Currently, approximately 80 percent of land is polluted by products of petroleum origin used as an energy source in the oil industry, as well as chemicals (Calsiu et al. 2001). Crude oil enters the soil through onshore and offshore crude oil exploration, oil pipe leakages and vandalism, oil tank raptures and indiscriminate disposal of refinery products.

Crude oil which is located in the Niger Delta region of Nigeria is spilled on sand primarily as a result of pipeline destruction. Nigeria is Africa's largest oil producer

and the sixth largest in the world, with a maximum crude oil production of 2.5 million barrels per day (Nigerian National Petroleum Corporation 2015). Royal Dutch Shell says that over the past 5 years less than 30 percent of spills are due to operational negligence such as corrosion, human error and equipment failure and the majority have been caused by sabotage or theft. The 2007-2013 oil spill incident data for Nigeria is summarised in Figure 2.2. In 2009 more than 104,000 barrels of oil were spilled into the environment.

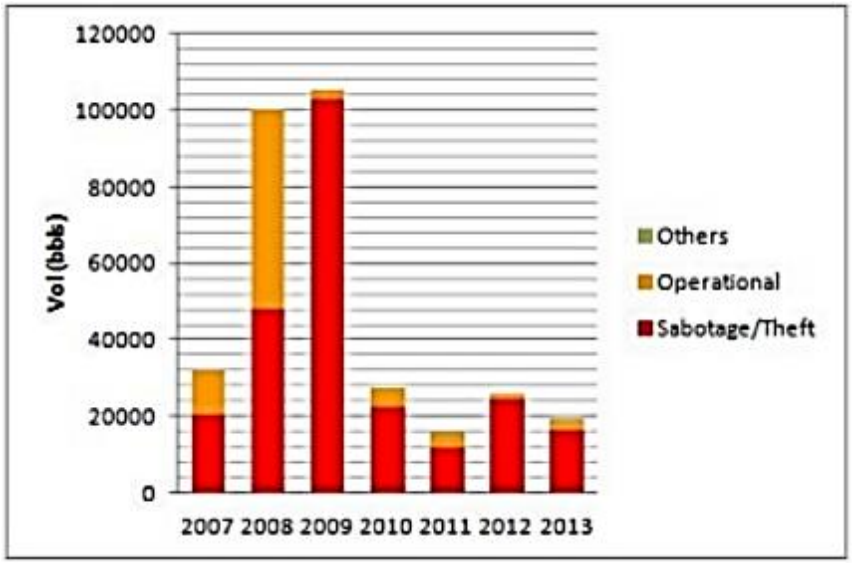

Figure 2.2: Volume of oil spills barrels/year (Shell Nigeria 2015)

Moreover, in August 2008, 450,000 barrels of crude oil was intentionally discharged from an oil-storage tank to avoid an explosion when the tank caught fire due to human error. This occurred during annual maintenance at the Harouge Oil Operation petrochemical and refining complex at the Ras Lanuf Terminal in Libya (T. F. S. B. Products 2008). Libya's economy depends primarily on the oil sector, which represents over 95 per cent of export earnings (Organization of the Petroleum Exporting Countries 2015). While most oil spills are unintentional due to ageing facilities and human error, Libya, being a large oil exporting country, has been affected

by sand contamination by crude oil. Figure 2.3 shows the Libyan major oil and gas facilities.

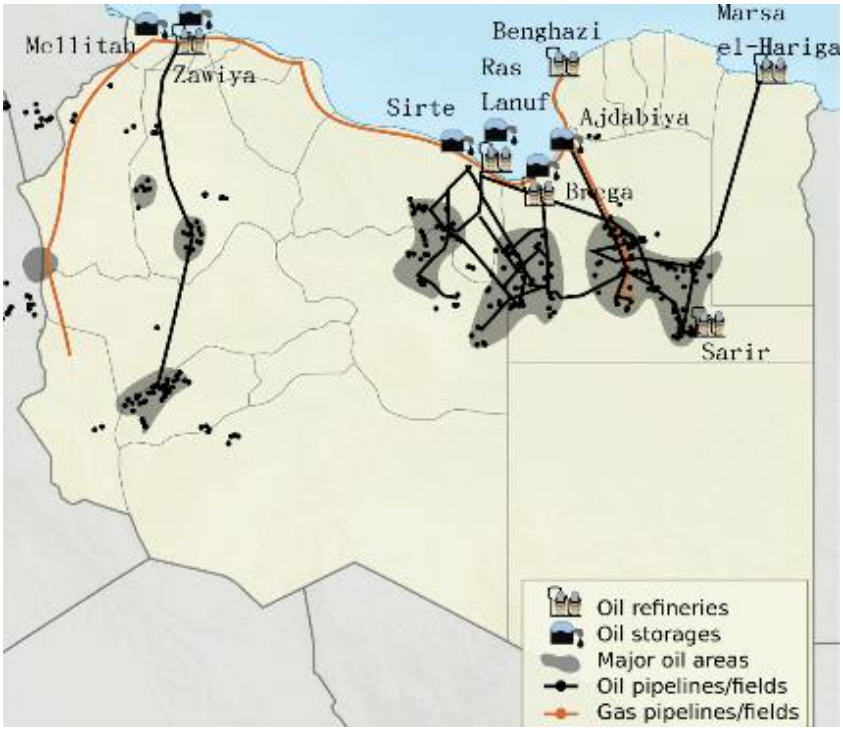

Figure 2.3: Libyan major oil pipelines, refiners and oil fields (Wikipedia 2015)

With oil contamination problems so wide spread, naturally, other industries are affected. It is pertinent to assess the behaviour of sand under the influence of the contaminants to understand the effects of its use as a construction material.

2.2.3 Geotechnical Properties

In order to reuse contaminated sand for construction purposes it is important to research the behaviour of sand under the influence of crude oil.

Abousnina et al. (2014) studied the effect of Mineral Fork w2.5 motor cycle oil (used as crude oil) on the shear strength of fine sand through the direct shear test. Light crude oil was mixed with fine sand at amounts ranging from 0 to 20% by mass of sand. Results showed that the highest sand cohesion of 10.7 kPa occurred at 1% oil

contamination before decreasing as oil contamination exceeded 1%. Additionally, only a slight reduction in friction angle was observed with 1% oil contamination. The results of the cohesion and friction angle are summarised in Table 2.1:

Table 2.1: Cohesion and friction angle results from study by Abousnina et al. (2014)

Oil Content %	**Cohesion kPa**	**Friction Angle ∅°**
0	0.756	38
0.5	9.418	31
1	10.76	31
2	8.911	29
4	6.51	30
6	5.544	32
8	3.718	31
10	3.105	31
15	2.422	31
20	1.823	32

Rahman *et al*., (2010) investigated the geotechnical properties of engine oil contaminated Basaltic residual soil through artificial contamination of up to 4% of the dry weight soil sample. The influence of the oil enhanced the liquid and plastic limits of the soil but reduced maximum dry density (MDD) and optimum moisture content (OMC) when compared to uncontaminated soil.

Similarly, in a study by Shah *et al.* in 2003, fuel oil contamination of foundation soil was found to decrease maximum dry density (-4%), cohesion (-66%), angle of internal friction (-23%) and unconfined compressive strength (UCS) (-35%) while increasing liquid limit (+11%).

In a study by Al-Sanad *et al.* (1995), the geotechnical characteristics of heavy crude oil contaminated Kawaiti sand was investigated of up to 6% oil contamination by weight of sand. It was concluded that "oil contamination leads to decreased permeability and strength" and reduces the friction angle by 2° for specimens mixed

with 6% heavy crude oil. Similar findings were noted by Mashalah *et al*., (2006) where 0-16% crude oil contamination of soil from Bushehr Beach of South Iran was investigated.

This may result from the formation of oil around sand particles which acts as a cushion preventing inter-particle contact. This lack of cohesion would promote slippage as oil content and viscosity increases, consequently, reducing the shear strength and compressibility of contaminated sand. These effects of oil on the properties of sand are undesirable for use in construction materials such as concrete. Often, remediation efforts are made to allow contaminated soils to be used as a viable construction material.

2.2.4 Remediation of Contaminated Soil

While there are many limitations for the disposal of oil contaminated sand, their remediation is also complicated, time consuming and expensive and is also required to comply with strict environmental legislation (Abousnina 2015). Hazardous materials tend to bind, chemically or physically, to silt and clay. Silt and clay, in turn, binds to sand and gravel particles (United States Environmental Protection Agency 1996). Remediation aims to separate these hazardous materials from sand to enable its safe use in construction.

Types of remediation technologies for contaminated sand include (United States Environmental Protection Agency 2006):

- *Physical/Chemical:* Soil vapour extraction (water and organic solvents, surfactants, vegetable oil), solidification/stabilisation, chemical oxidation and soil flushing

- *Biological:* Bioremediation (on-site land farming and composting), aerobic/anaerobic treatment (bioventing) and phytoremediation
- *Thermal:* incineration, vitrification, thermal desorption and thermally enhanced soil vapour extraction

From the flow chart seen in Figure 2.4, remediation solutions for oil contaminated sand include soil washing, thermal treatment, chemical decomposition and bioremediation.

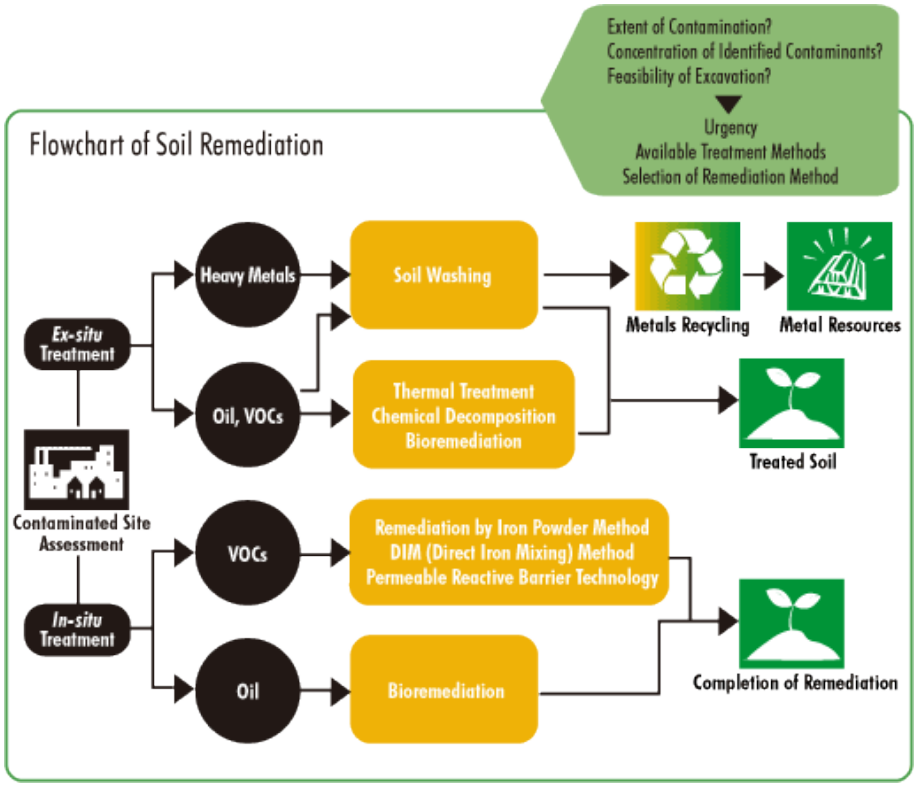

Figure 2.4: Remediation technologies based on contaminant (Dowa Eco-System 2006)

The most common remedial method is excavation and disposal of oil-impacted sand. In South Australia, the relative cost of treatment and long-term management of sand versus dig and dump is prohibitively high and unattractive to land managers (Sinclair Knight Marz 2013). The treatment costs of incineration, thermal desorption, soil washing, vitrification, chemical decomposition, solvent extraction and

solidification/stabilisation are outlined in Figure 2.5. The current solutions for contaminated sand are unsustainable as treatment technologies are either cost prohibitive and/or the treated products are sent to land fill without any potential end-use.

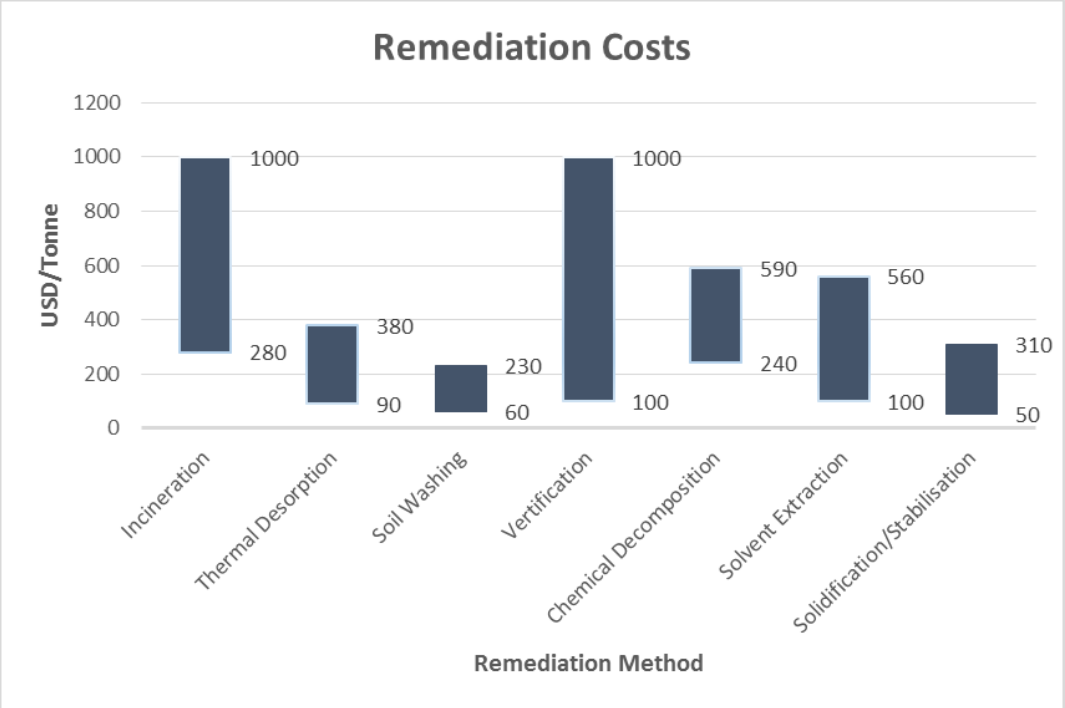

Figure 2.5: Remediation costs in USD/tonne (U. S. E. P. Agency 1997)

The use of contaminated soil as a construction material could be a cost effective solution instead of – or in conjunction with – remediation.

2.3 Oil Contaminated Sand in Concrete

Concrete is a composite material composed mainly of water, cement and aggregates (sand and gravel). It is the most commonly used construction material on earth due to its high strength, ease of production, low cost, good compatibility with other materials and durability under aggressive conditions. Use of crude oil-impacted sand (COIS) in concrete depends on the required properties of the end product. It can be used to alter

and enhance properties of fresh and hardened concrete and also to assist in the remediation of contaminated soil.

2.3.1 Benefits of Reuse in Construction

The use of these waste materials in the construction industry would contribute towards a cleaner environment and can also result in a cost effective construction material. Cement-based stabilisation/solidification (S/S) has emerged as a viable alternative technology due to its improvement on the physical and mechanical properties of petroleum wastes through binding oily materials to produce chemically and physically stable products (Tuncan, Tuncan & Koyuncu 1997). Some possible options for the reuse of contaminated sand is listed below:

1. *Subgrade material in road construction:* Brown field and borrow pit materials are commonly used as road construction material (Shan & Meegonda 1998). Oil contaminated sand can be mixed with crushed stone aggregate in road bases or subgrades (Hassan et al. 2005). However, steps must be taken in order to avoid contamination of the water table.
2. *Production of soilcrete/sandcrete bricks and tiles:* Blocks are commonly used for non-load bearing walls from a mixture of sand and cement. Using contaminated materials in non-load bearing situations, such as this, is ideal as any loss in strength due to contaminants will not affect the integrity of the structure (Shan & Meegonda 1998).
3. *Production of concrete/mortar:* Fresh concrete and mortar using contaminated recycled aggregates as a replacement of sand has been researched in the past. The material could be used in non-load bearing structures such as partition

wall, blinding concrete or masonry in civil engineering construction works (Oluremi & Osuolale 2014).

4. *Production of asphalt concrete*: 5-10% of waste materials such as petroleum contaminated sand can be added to hot mix asphalt (HMA). A study by Al-Matairi and Eid in 1997 found that concrete asphalt with oil contaminated sand was of a quality that can be used for secondary roads, road beds, impermeable layers for landfill and containment facilities or as stabilisers for step embankments.
5. *Parking lots, footpaths, pathways and bus terminals*: pervious concrete ranging from 5-10 MPa is used for these lower load applications (Sriravindrarajah et al. 2011).

Previous research has investigated the effect of oil contaminated sand on the mechanical properties of concrete. It is important to understand its influence on concrete to ensure its safe use in construction.

2.3.2 Effect on Concrete Mechanical Properties

Concrete's drawback is that that its strength cannot be measured prior to it being placed; concrete gains its full strength after 28 days of curing unlike materials like steel and timber. Therefore, it is important to evaluate the effect that any additives, such as oil contaminated sand, have on the properties of concrete prior its use in construction.

Previous research has particularly investigated the effect that oil contaminated sand on the compressive strength of concrete. In general, compressive strength is

considered as the most important property and the quality of concrete is often judged based on its compressive strength.

In a study by Ajagbe *et al.*, (2011) the compressive strength of ordinary Portland cement concrete containing 2.5-25% COIS was investigated experimentally. It was found that sand containing more than 5% crude oil contamination reduced the compressive strength of concrete by more than 50%. It was also noted that crude oil contamination between 5% and 10% should be considered for low strength concrete (<15 MPa).

Similarly, an experimental investigation was conducted by Ayininuola (2008) on the effects of the addition of 0-10% diesel oil contaminated sand in Portland cement concrete. A mix ratio of 1:2:4 and water-cement ratio 0.6 was used. Concrete was tested under compression on a range of curing lengths from 7 to 148 days. It was found that the higher the percentage of oil present in the fine aggregate, the lower the resulting compressive strength irrespective of concrete age (refer to Figure 2.6). It was concluded that the loss in strength was due to the coating of the surface areas of sand particles in oil which hindered the physical bond formation between cement paste and fine aggregate.

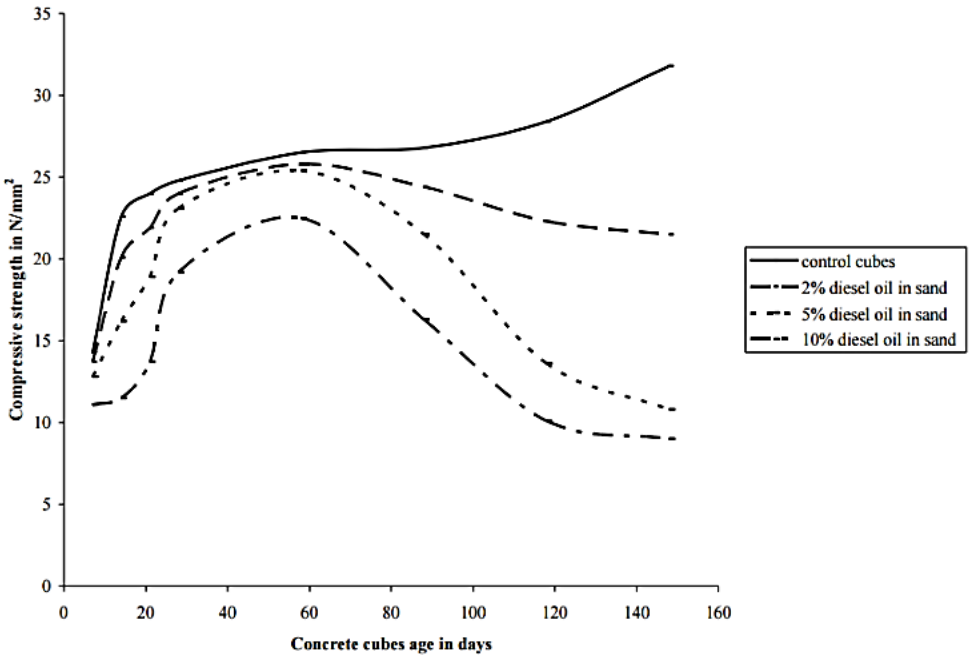

Figure 2.6: Variations of compressive strengths of diesel oil contaminated concrete with age (Ayininuola 2008)

An investigation by Osuji & Nwankwo (2015) also established that the presence of crude oil in concrete made with OPC hinders the bond formation between constituent materials and encourages segregation. Concrete cubes containing 0-5% COIS with a mix ratio of 1:2:4 and water-cement ratio of 0.5 were tested under compressive loads at various ages. It was concluded that the presence of crude oil in fine aggregate lowered the compressive strength of concrete; the higher the percentage of crude oil, the lower the compressive strength obtained (Table 2.2).

Table 2.2: Mean compressive strengths of concrete with or without crude oil contamination (MPa) (Osuji & Nwankwo 2015)

Testing Days	Control Cubes	Crude Oil Contaminated Fine Aggregate				
		1%	2%	3%	4%	5%
7	13.96	11.24	9.82	8.36	7.44	6.82
14	17.90	15.65	13.72	11.24	8.86	7.02
28	22.00	17.61	15.82	12.12	10.24	8.00
56	23.60	18.45	16.24	13.63	11.56	10.46

Almabrok et al. (2013) again made similar conclusions in their investigations of mortar when incorporating mineral oil additions up to 10% of the aggregate mass. It was found that increased oil content in the cement mortar increased setting time and air content. The decrease in compressive strength by 78% compared to the control at 28 days was said to be due to the oil inhibiting cement hydration.

Additionally, Ejuh & Uche (2009) researched on the effect of crude oil spill on compressive strength of concrete materials, subjected specimens to concentrated crude oil solution and simulated water/crude oil mix. The OPC concrete samples were cured in the media at ambient temperature at immersion ages of 3, 7, 28 and 56 days. The results showed that the concrete is susceptible to different aggressiveness of the solutions of crude oil concentrations as they led to low rates of strength development.

Over saturation of a concrete mix causes it to be too weak to hold course aggregate particles in suspension so they move downward with gravity (Madderom 1980). Water (or oil), being lighter, rises to the surface, carrying some cement and fine particles with it. As it rises, vertical water channels are created making the concrete porous and subject to subsequent ingress of water. The suspended fines carried outward weaken the concrete surface. As a result of over saturation, reservoirs are created around aggregate particles which become air pockets after concrete has cured and dried (refer to Figure 2.7).

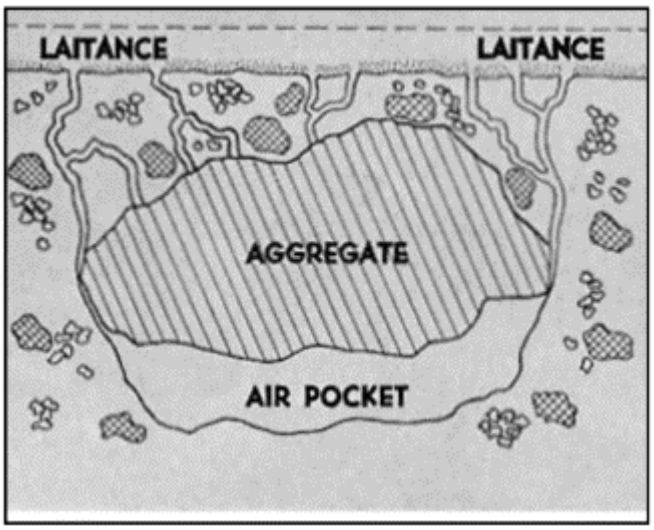

Figure 2.7: Effects of excessive water in concrete mix (Madderom 1980)

From previous studies mentioned, it is clearly shown that COIS effects the mechanical properties of concrete. All research concluded that the higher the oil content in the sand, the higher the loss in compressive strength. For this reason, the effect of the addition of fibres on the mechanical properties of COIS in concrete is investigated.

2.4 Fibre-Reinforced Concrete

Fibre-reinforced concrete (FRC) is a concrete containing dispersed fibres. In comparison to conventional steel reinforcement, the defining characteristics of FRC is that: (1) fibres are generally distributed throughout a cross-section, whereas reinforcement bars are only placed where needed; (2) fibres are relatively short and closely spaced; and (3) generally, it is not possible to achieve the same area of reinforcement with fibres as with reinforcing bars (Löfgren 2005).

2.4.1 Historical Development of FRC

As the structural use of concrete developed in the late 1800's, interest started to focus on reinforcement to enhance the low tensile capacity of concrete. Historically, the concept of using fibres was first recorded when ancient Egyptians used horsehair in mortar and straw in mud bricks as reinforcement (Balaguru & Shah 1992). It was not until the 1900's that asbestos fibres were developed, manufactured and widely distributed to enhance the cement matrix (Bentur & Mindess 1990). Studies investigating the use of steel and glass fibres in concrete date back to the 1950's, while the use of synthetic fibres came about in the 60's (Maccaferri 2015).

Construction industries have led the development of conventional fibres such as steel and glass, as well as newer types of fibres including Kevlar, carbon and low modulus fibres both manmade (polypropylene, nylon) or natural fibres (bamboo, jute, wood pulp and jute). In the early stage of fibre development, straight and smooth steel and glass fibres were used because of their improvement on concrete ductility, flexural strength and fracture toughness. However, difficulty arose with mixing and workability as long fibres at higher volume fractions were found to ball up during the mixing process (Balaguru & Shah 1992). The process, known as 'balling', causes concrete to become stiff and often influences concrete strength.

Over the past 40 years, through research and development, fibre-reinforcement to enhance concrete properties has been gradually accepted for use in construction. Technological advances bought forward the development of fibres with varied geometric shapes and properties to expand their applications.

2.4.2 Properties of FRC

Portland cement concrete is relatively strong in compression but weak in tension and tends to be brittle (Domone & Illston (eds.) 2010). Fibres are added to concrete to reinforce the matrix in order to make the material more capable of carrying tensile loads (Holcim Australia 2015). The presence of fibres having adequate tensile strength and being homogeneously distributed within the concrete builds a micro-scaffolding that; 1) controls crack formation due to shrinkage and 2) leads to concrete ductility (Maccaferri 2015). FRC also exhibits greater durability, fatigue life, resistance to impact and gauging compared to conventional reinforced concrete, thus, expanding its application options.

2.4.3 Application in Modern Industries

Fibres are primarily used as a replacement for conventional reinforcement in non-structural applications in order to control early thermal contraction cracking and drying shrinkage cracking. However, FRC uses have expanded beyond pavement application and into areas where the reinforcing specification has historically been bars or fabric (Radmix 2009). In some types of structures with relatively low reliability levels for structural safety such as slabs on grade, foundation and walls, fibres can replace ordinary reinforcement completely. Recently, fibre-reinforced concrete has been used in applications such as (Wong 2004):

- Buildings subject to shatter, impact, abrasion and shear
- Floors, driveways, walkways and curbs to reduce shrinkage and cracking problems

- Airport runways to improve resistance to fuel spills with decreased permeability and shatter resistant FRC
- Replacement of steel in corrosion prone application such as sanitary sewer tunnels
- Simplify concrete pumping by increasing cohesiveness and preventing segregation
- Varied techniques of shotcrete used to line underground openings, stabilise slopes, prevent spalling and minimise time and labour of placing, particularly in difficult to access areas
- Precast applications to combat early age stresses by preventing development of cracks
- Reduction of permeability in freeze-thaw conditions by controlling cracking and shrinkage for water retaining and reservoir structures

Residential Slabs

Precast

Shotcrete and Underground

Transportation

Figure 2.8: Fibre-reinforced concrete applications (Fibremesh 2011)

2.4.4 Fibre Technology

Fibre-reinforced concrete contains short fibres that are uniformly distributed and randomly orientated. A wide range of fibre types exist, which are made of different materials with varied geometries. Fibres types include (Maccaferri 2015):

- *Metallic fibres*: carbon steels and non-alloy steels, aluminium
- *Synthetic fibres*: asbestos, cellulose, carbon
- *Natural fibres*: nylon, polypropylene, polyacronytrile, polyvinylalcohol

Several important terms, definitions, parameters and features serve to characterise the wide variety of fibres. These terms are generally independent of fibre type and depend on the geometry rather than any material characteristics. Relevant definitions include (Löfgren 2005):

- *Aspect ratio:* the ratio of length to diameter (or equivalent diameter for non-circular fibres) of a fibre
- *Bundled fibres:* strands consisting of several hundreds or thousands of filaments of microfibers
- *Chopped strand:* fibres cut at varied lengths
- *Collated:* bundled fibres through cross-linking or chemical means
- *Fibrillated:* continuous networks of fibre where individual fibres have branching fibrils
- *Filament:* a continuous fibre (aspect ratio approaches infinity)
- *Monofilament:* a large-diameter continuous fibre, generally with a diameter larger than 100μm
- *Multifilament:* yarn consisting of many continuous filaments or strands

From the material characteristics above, each type of fibre can be separated into two groups:

- *Discrete Monofilaments*: each fibre is separate from one another (e.g. steel)
- *Bundles of filaments*: fibres are structured in an assembly, with a diameter of 10 μm or less. Includes majority of manmade fibres (e.g. glass), organic fibres (e.g. carbon) and natural fibres (e.g. asbestos)

Monofilament fibres are commonly used in structural concrete to enhance the fibre-matrix interaction through mechanical anchoring. Filament fibres are rarely a cylindrical shape, but are usually deformed into a desired configuration. They also may be designed to break up into separate filaments after mixing.

The fibre types being investigated as a part of this study are outlined in more detail in the following section.

2.4.5 Fibre Types

The reinforcement in concrete structures can either be continuous or discontinuous or a combination of both. There are numerous fibre types which vary in size, shape and material available for commercial and experimental use. Discontinuous fibre types are outlined in Figure 2.9:

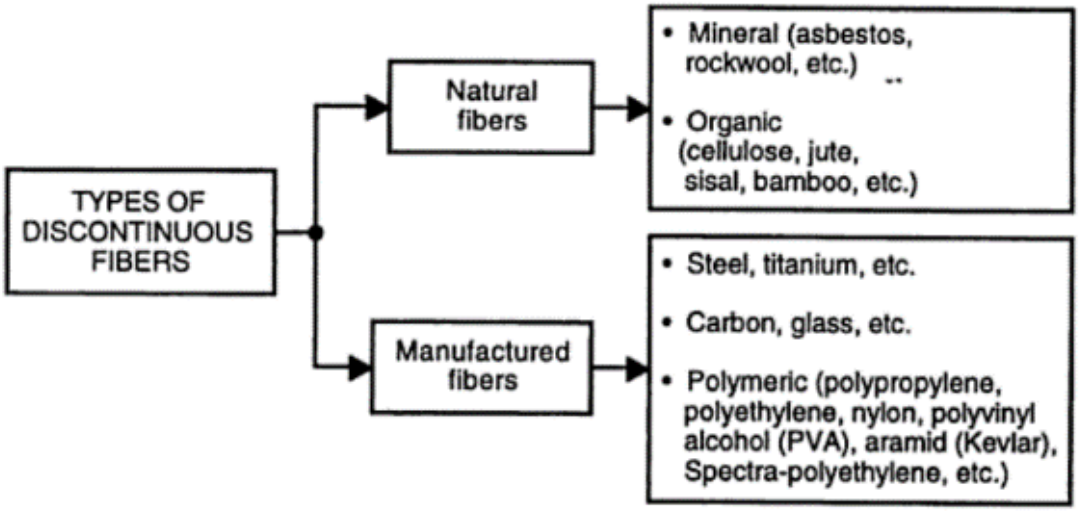

Figure 2.9: Discontinuous fibre types (Naaman 2000)

2.4.5.1 Steel Fibres

Industrial floors and pavements are major applications for steel fibre-reinforced concrete (SFRC) as the stresses are complex depending on the type of load. Other applications include tunnel linings, manholes, curbs, pipes, risers etc. Steel fibres, compared to traditional fabric reinforcement, have a tensile strength typically 2-3 times greater and a significant increase in surface area to develop a greater bond with the concrete matrix (ACIFC 1999).

Many efforts have been made to optimise the shape of steel fibres to enhance fibre dispersibility in the concrete matrix and achieve improved fibre-matrix bond characteristics (Labib & Eden 2006). Common types of steel fibres are shown in Figure 2.10. Each fibre geometry, particularly the varied and irregular shaped, aims to enhance the bond with the concrete matrix through anchorage. If the concrete is well compacted the corrosion of fibres will be limited to the surface of concrete (ACI Committee 54.1R 1996), these fibres will corrode rapidly in exposed conditions.

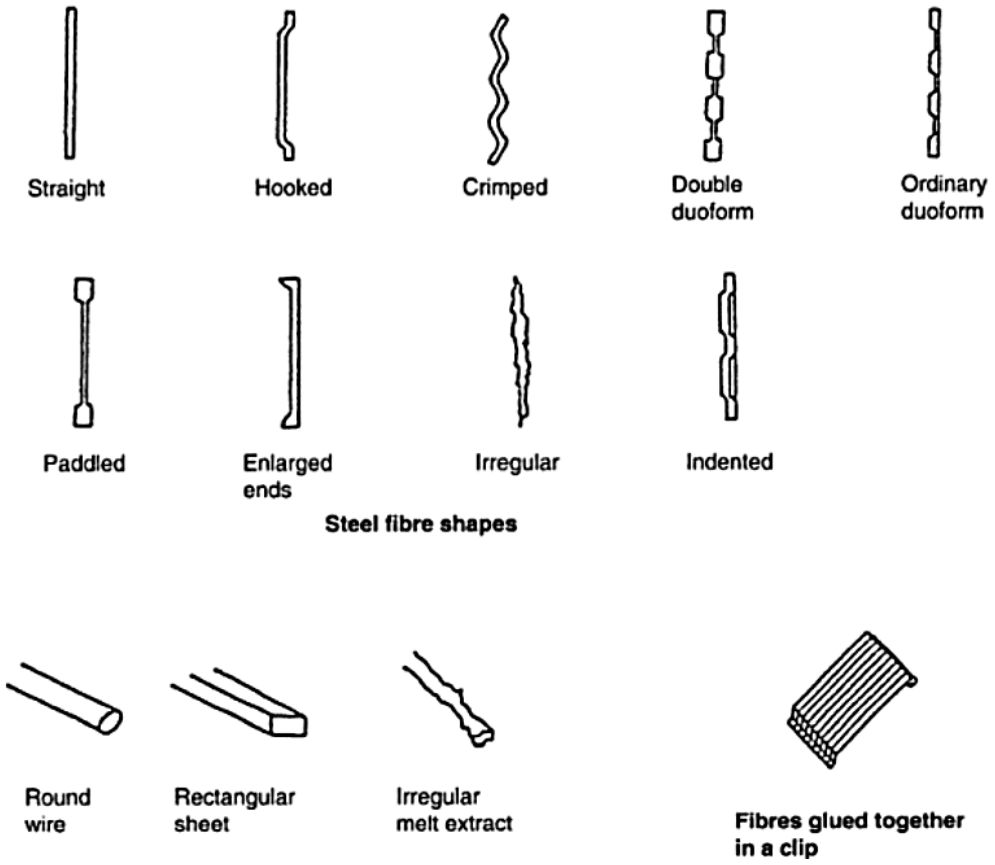

Figure 2.10: Types of steel fibres (Knapton 2003)

Steel fibres improve the ductility of concrete under all modes of loading (Labib & Eden 2006). The recommended steel fibre dosage varies with its applications, depending on the criticality of application and ductility required. Recommended dosages range from 15 to 30 kg/m^3 of concrete (Fibrex 2015). The greater the dosage rate, the greater the flexural strength of the concrete (Knapton 2003). The theory of McKee estimates the minimum fibre dosage permitted is required to give a maximum average spacing factor of 0.45 times the nominal fibre length. This is to ensure adequate overlap between fibres to transfer load. The McKee formula for minimum steel fibre dosage is:

$$Minimum\ Fibre\ Dosage\ (kg/m^2) = 67658/(aspect\ ratio)^2 \quad (2.1)$$

Where the aspect ratio is the fibre length divided by the fibre diameter. This recommendation is a design guideline for SFRC for use with the European Code on concrete structures (Dramix Guidelines 1995).

2.4.5.2 Polypropylene Fibres

Polypropylene fibres have been used in applications ranging from roads and pavements, driveways, overlays and toppings, ground supported slabs, machine foundations, off shore structures, tanks and pools etc. (Madhavi, Raju & Mathur 2014). Polypropylene fibres are gaining significance due to the low price of the raw polymer material and their high alkaline resistance (Keer 1984). They are available in two forms including monofilament or fibrillated manufactured in a continuous process by the extrusion of a polypropylene homopolymer resin (Keer 1984). Figure 2.11 shows various polypropylene fibre geometries.

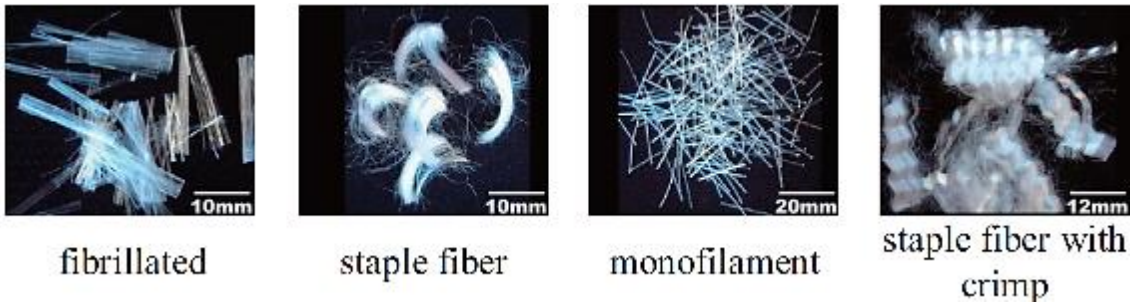

Figure 2.11: Various polypropylene fibre geometries (Song & Tu 2014)

Typical dosages of polypropylene fibres range from 0.6 to 0.9 kg/m^3 (Fibrex 2015; Madhavi, Raju & Mathur 2014). Unlike steel fibres, synthetic fibres should not be used for structural reinforcement (Fibrex 2015). While they can enhance the strength of concrete, the application of polypropylene fibres also reduces the water permeability, plastic shrinkage and settlement of concrete (Madhavi, Raju & Mathur 2014).

2.5 Mechanical Behaviour of Fibre-Reinforced Concrete

The enhancement of the structural performance of FRC depends on the strength properties of the fibres, dispersion and orientation of fibres, fibre geometry and fibre dosage volume (Gambhir 2009). During loading, the matrix transfers part of the load to the fibres before any crack propagation has initiated making it theoretically possible to increase concretes strength by adding fibres. However, pronounced strength improvement is limited for relatively low fibre dosages, which are usually added to concrete, due to the low tensile strain capacity of the cementitious matrix and the increased porosity that the fibre addition may induce (Löfgren 2005).

2.5.1 Fibre Bridging

In general, fibre-reinforcement is not a substitution for conventional steel reinforcement as they are not as efficient in withstanding tensile stresses. However, fibres are more closely spaced than steel bar reinforcement which better controls cracking and shrinkage. The main advantage of fibres is their ability to transfer stresses across a crack, consequently enhancing the toughness and ductility of concrete as well as the absorption capacity under impact (Clarke, Vollum & Swannell 2007).

For most FRC, the reinforcing effect of fibres initiates after matrix cracking. FRC is less brittle in comparison to normal concrete through fibres increasing the fracture energy through fibre bridging of a cracked surface. When a crack is present in the matrix, generally, it approaches an isolated fibre and the following mechanisms may take place to contribute to energy dissipation (Löfgren 2005):

- Fibre fracture
- Post-debonding friction between fibre and matrix (fibre pull-out)

- Fibre-matrix interface debonding
- Matrix fracture and matrix spalling
- Fibre abrasion and plastic deformation (or yielding) of fibre

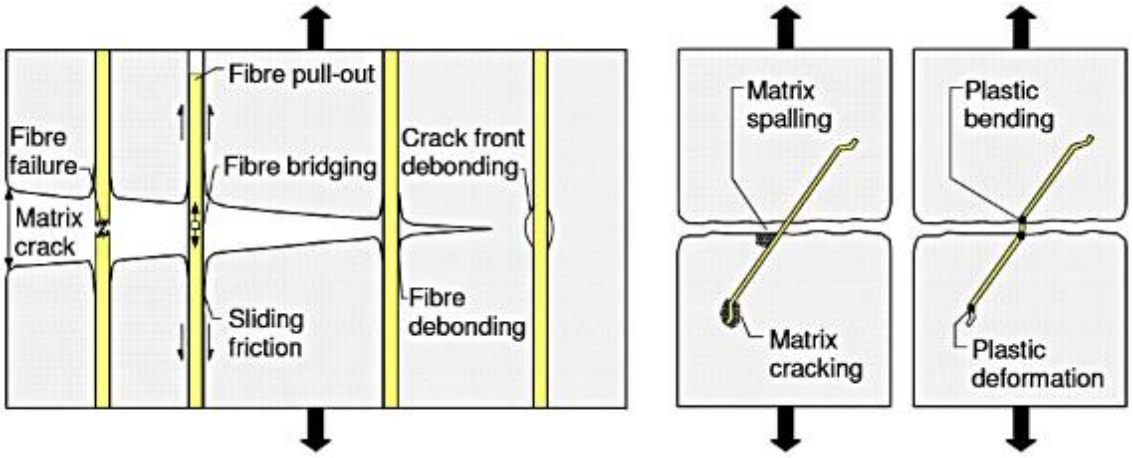

Figure 2.12: A schematic illustrating mechanisms contributing to energy dissipation (Löfgren 2005)

Fibre interaction with the concrete matrix and the transmission of forces between the two are discussed further below.

2.5.2 Mechanism of Fibre-matrix Interaction

In FRC, cracking occurs over a wide range of loading and the debonding of fibres occurs over several stages. Due to the low tensile cracking-strain of the cement matrix, when FRC is loaded the matrix will crack prior to fibre fracture (depending on the yield or ultimate strain of fibres). The composite continues to carry the increasing tensile load when the matrix is cracked.

The idealised stress-strain relationship for steel fibre-reinforced concrete (SFRC) is shown in Figure 2.13. It is assumed that both the fibres and the matrix behave elastically and there is no slippage between the two until the initial cracking of the matrix. Between first cracking and the peak (inelastic stage), the matrix experiences

multiple cracks. Following initial cracking, if the pull-out resistance of fibres is greater than the load of initial cracking, the composite will carry increasing load. In the post-cracking stage, the composite failure is often due to fibre pull-out rather than fibre yielding or fracture (Gambhir 2009). The pull-out resistance of fibres depends on the bond strength of fibres with the matrix, the number of fibres crossing the crack and the length and diameter of fibres (aspect ratio l/d).

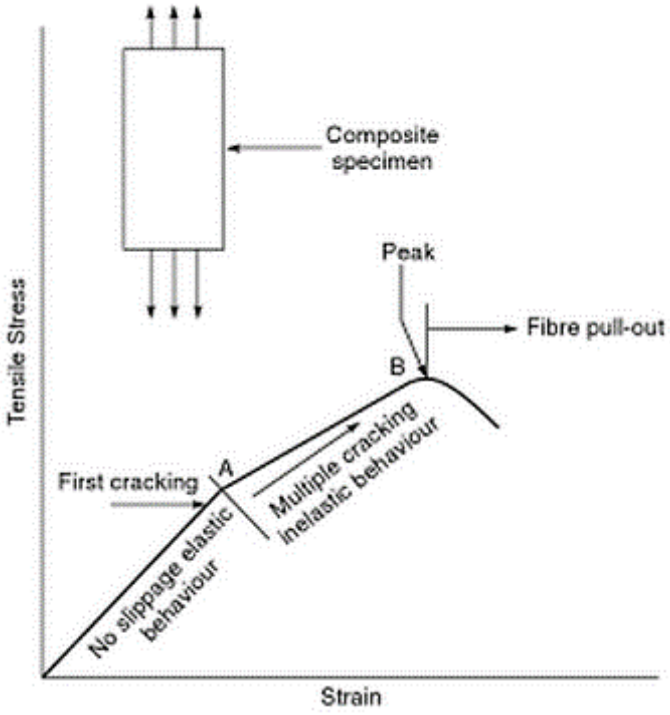

Figure 2.13: Behaviour of SFRC under tensile load (Gambhir 2009)

In FRC, the fracture is a continuous process with several stages. In the cracked state, shear bond strength and frictional shear strength are the two major mechanisms influencing the stress transfer between the fibre and matrix.

High bond strength helps to give a close crack spacing but it is also essential that the fibres debond sufficiently local to the crack to offer ductility to concrete, which will absorb impacts. Three type of bonding are possible in FRC (Domone & Illston (eds.) 2010):

- *Elastic bonding*: fibres adhere to the matrix
- *Frictional Bonding*: friction between fibres and matrix provides pull-out resistance
- *Mechanical bonding*: fibres are purposely deformed along their length to enhance interlocking with matrix, enhancing the frictional bond

In understanding fibre-matrix interaction, it is important to recognise how fibres effect the failure behaviour of concrete.

2.5.3 Mechanics of Crack Formation and Propagation

Concrete is a heterogeneous material with the matrix containing 'stable flaws' in many forms, including; capillary porosity, aggregate-paste interfaces, air bubbles, micro-cracking etc., which act as crack initiators (Døssland 2008). When the strain energy input exceeds the energy required for new surfaces to be formed within the concrete – either by crack formation from a flaw or micro-crack, or by extension of an existing crack – then crack propagation will occur.

To be fully effective, each fibre needs to be completely embedded in the matrix. In FRC, there are three ways in which the presence of fibres can prevent, retard or modify propagation of cracks (Domone & Illston (eds.) 2010):

1. *Fibre-matrix debonding*: fibres act indirectly as crack stoppers through the growth of cracks at the fibre-matrix interface and/or the diversion of propagating matrix cracks along the interface, effectively arresting them.
2. *Crack stabilisation*: fibres suppress further crack growth through crack bridging providing a 'closing force' that resists crack opening and increases energy required for further propagation.

3. *Crack suppression*: dispersed fibres increase the energy required for crack initiation.

Micro-cracks are prevented when they intersect fibres as concrete hardens and shrinks, provided that fibre rapture is avoided (depending on the tensile strength of the fibre). Debonding between fibre and concrete begins on the shortest embedded lengths until full debonding occurs. Past research has indicated that the strain energy release rate associated with debonding (3-7 N/m) is less than that associated with forming new cracks in the matrix (5.12 N/m). Therefore, cracks preferentially propagate along the fibre-matrix interface (Bentur & Mindess 1990). Macro cracks covering several micro cracks form when the initial micro cracks spread. The bridging of fibres across cracks provides concrete with a post-crack tensile strength (Figure 2.14).

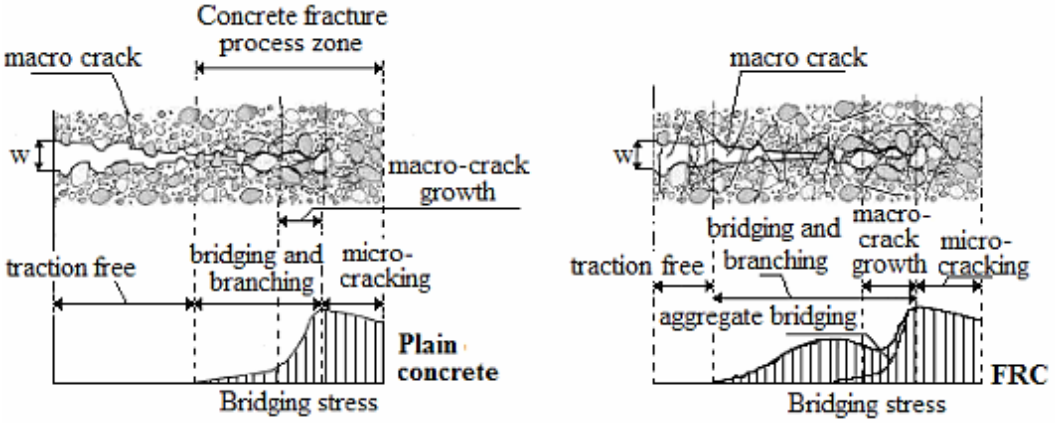

Figure 2.14: Schematic description of stress-crack relationship for plain concrete and for FRC (Löfgren 2005)

Post cracking behaviour of FRC is difficult to predict as it is influenced by fibre orientation and distribution.

2.5.4 Orientation and Distribution of Fibres

The post crack tensile strength of concrete is largely dependent on the distribution and orientation of fibres, which is governed by the casting process and the size and geometry of the specimen. The fibre orientation in vibrator compacted concrete (VCC) is likely to have a planar-random orientation occur perpendicular to the direction of the vibration (Kooiman 2000; Barragán 2002). However, if the specimen is only vibrated for a short time, it will not have a significant effect on fibre orientation (Dupont 2003).

The use of fibres in the concrete matrix is randomly distributed, where the orientation of fibres is unpredictable with either one, two or three-dimensional arrays. Figure 2.15 shows a fibre placed at an angle θ to the applied stress can be more efficient in carrying load as compared to a fibre placed parallel to the load through using vector analysis in the components of x, y and z. Additionally, fibres inclined in three dimensions (inclined angle to the direction of load) carry more bending stress for crack bridging, however, are less efficient in carrying load applied to the concrete (Wong 2004).

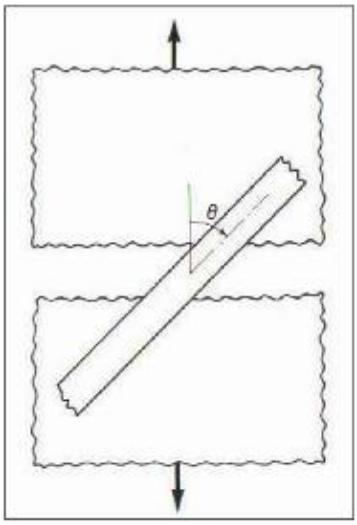

Figure 2.15: The intersection of an inclined fibre across a crack with angle (θ) (Bentur & Mindess 1990)

A study by Neves & Fernandes de Almeida (2005) reported that under compressive loading, steel fibres orientated parallel to the load direction can act like voids. The amount of stress a fibre can carry is largely dependent on its properties. Knowledge of these properties is important for design purposes.

2.5.5 Fibre Mechanical Properties

The post cracking strength of concrete will be dependent on the strength of the fibres themselves, therefore, it is important to understand their properties. The most common types of fibres are steel and polypropylene fibres, due to their low cost and availability (Beaudoin 1990). However, there are many fibres types that may be used in concrete composites depending on requirements and applications. Various types of fibres and their typical respective properties are outlined in Table 2.3:

Table 2.3: Properties of various fibre types (Beaudoin 1990)

Fibre Type	Specific Gravity	Modulus of Elasticity	Tensile Strength	Failure Strain
Steel	7.8	200.0	1.0-3.0	3.0-4.0
Glass	2.6	80.0	2.0-4.0	2.0-3.5
Asbestos	3.4	196.0	3.5	2.0-3.0
Nylon	1.1	4.0	0.9	13.0-15.0
Carbon	1.9	380.0	1.8	0.5
Polypropylene	0.9	5.0	0.5	20.0
Polyester	1.4	8.2	0.7-0.9	11.0-13.0
Polyethylene	0.9	0.1-0.4	0.7	10.0

Beaudoin (1990) stated the high fibre modulus of elasticity would have direct influences on the matrix elasticity due to the stress transfer from the matrix to the fibre.

However, modulus of elasticity and Poisson ratio are generally taken as equal to those of similar non-fibrous concrete when the volume percentage of fibre is less than 2% (ACI Committee 54.1R 1996).

As fibres are used for crack control, fibres with higher tensile strength is essential for effective reinforcement. However, the tensile strength of fibres decreases as fibre length increases (Beaudoin 1990). Furthermore, fibres with a higher failure strain will allow for more prolongation within the composite reducing pull-out force.

Fibres vary in recommended dosage volume due to their geometry, mechanical properties and intended application. Fibre dosage volume therefore effects the mechanical properties of concrete.

2.5.6 Fibre Volume Dosage

The fibre content in cement matrices is a specified volume fraction of the total composite due to the formulation of the mechanics of the composite. The fibre volume dosage of a typical FRC is less than about 2%. Whereas, high performance FRC generally use a 2-15% fibre dosage range (Naaman 2000). The load bearing capacity of the FRC is dependent on the volume dosage rate used in the concrete matrix. As fibre materials vary in density, weight fractions of fibres differ for the same volume fraction of fibres of different materials.

A higher number of fibres in the matrix leads to a higher probability of a micro-crack being intercepted by a fibre. However, fibre addition causes some perturbation of the matrix which can result in more voids (Neves & Gonμalves 2000). Therefore, the influence of fibres on the compressive strength of concrete can be seen as a balance between micro-crack bridging and additional voids caused by fibre addition.

A study by Mansour, Parniani & Ibrahim (2011) investigated the effect of steel fibre dosage on the compressive and flexural behaviours of SFRC. Hook-ended fibres in dosages of 0.0, 0.7, 1.0 and 1.5% were compared at 7, 14 and 28 days. The compressive strength results showed that fibres have a negative effect on compressive strength. A slight reduction with increasing fibre dosage was reported and the rate of strength reduction increased at higher dosages. However, a significant increase in the flexural strength of concrete containing steel fibres was found, as well as enhanced ductility.

Another study by Hsu & Hsu (1994) reported that steel fibres did not contribute to an increase in concrete compressive strength since more voids could be produced in SFRC because of its low workability. On the other hand, Ezeldin & Balaguru (1992) reported that the compressive strength of SFRC increased with increasing steel fibre volume due to the transverse confinement effect of the steel fibres which restrained the lateral expansion of specimens.

Similar findings were reported by Neves & Fernandes de Almeida (2005) who investigated the compressive behaviour of steel fibre-reinforced concrete in fibre volumes up to 1.5%. Test results indicated that the addition of fibres to concrete enhanced its toughness and strain at peak stress, but slightly reduced Young's modulus.

An experimental investigation carried out by Sarbini, Ibrahim & Saim (2013) analysed the enhancement of strength properties of steel fibre-reinforced concrete in fibre volume fractions from 0% to 1.75%. It was concluded that steel fibre dosage has an insignificant effect on SFRC compressive strength but highly contributes to flexural strength. Additionally, using a standard cone test (slump), it was found that increased

steel fibre volume fractions contribute to a reduction in concrete slump which may affect cohesion of SFRC due to difficulty in compacting.

The effect of fibres on concrete compressive behaviour is discussed below.

2.5.7 Compressive behaviour

The compressive behaviour of plain concrete is due to frictional sliding along pre-existing flaws resulting in the formation of tensile cracks at the tip of these flaws (Löfgren 2005). Cracking starts as sliding along the aggregate-cement paste interface and propagates into the matrix as tensile cracks. These cracks are extended parallel to the load direction with increasing compressive loading. The failure mode is a combination of distributed axial splitting and localised deformation and the ultimate failure is due to the interaction of the tensile cracks (Markeset & Hillerborg 1995). The effect of fibres in the presence of cracks is mainly based on providing resistance to these lateral deformations, resulting in a more ductile behaviour (Kooiman 2000) (Figure 2.16).

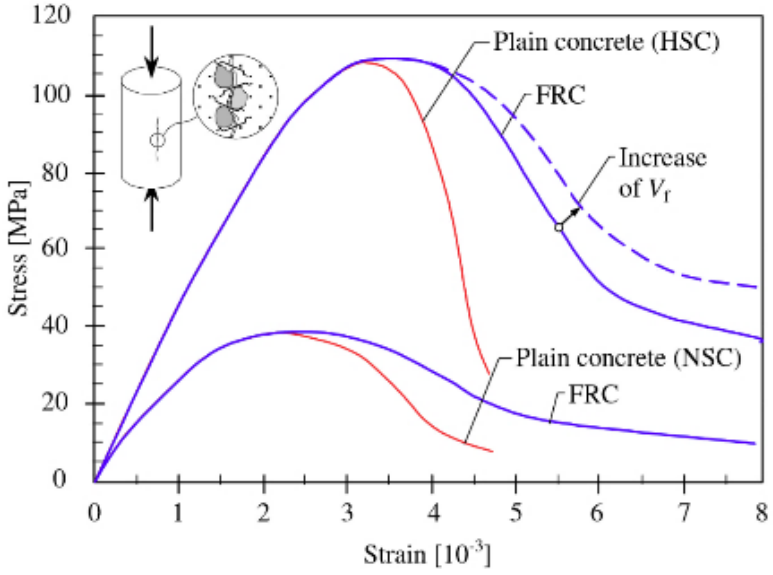

Figure 2.16: Schematic description of the behaviour of concrete and FRC in compression (Löfgren 2005)

Moderate concentrations of fibres do not influence the compressive strength of concrete significantly, rather, the addition causes a less brittle failure (Døssland 2008). Similarly, a study by Rai & Joshi (2014) found that the effect of fibres in concrete (steel, glass and polymer fibres) is minor on the improvement of compressive strength values (0 to 15 percent).

In another study by Ezeldin & Balaguru (1992) normal and high-strength steel fibre-reinforced concrete was tested under compression at fibre dosages of 30 kg/m^3, 45 kg/m^3 and 60 kg/m^3. Only a marginal increase in the compressive strength, the strain corresponding to peak stress and the second modulus of elasticity of FRC was obtained. It was also noticed from the experimental results that fibres have more effective contribution on the compression stress-strain curve in the post failure region.

Similarly, Lee, Oh & Cho (2015) researched the compressive behaviour of fibre-reinforced concrete with end-hooked steel fibres. It was shown that SFRC exhibited ductile behaviour after reaching compressive failure load and that the strain at this load generally increased along with an increase of fibre volumetric ratio and fibre aspect ratio, while the elastic modulus decreased.

Fibres have a diversely different effect on concrete flexural behaviour as they are employed to resist tensile stresses.

2.5.8 Flexural behaviour

The influence of fibres on the flexural strength of concrete is largely dependent on the fibre content and fibre properties. The fibres influence the flexural strength of concrete as the softening response due to fibre bridging leads to a redistribution of stresses, which imposes a new state of equilibrium across the cross-section after cracking. As

a result, the maximum moment capacity may exceed the maximum moment of plain concrete (Kooiman 2000).

A number of past literature agree with this theory. A study by Wang & Wang (2013) found that the flexural strength was largely improved through steel fibre-reinforcement of light weight concrete (LWC) with fibre volume factions of 0.5%, 1.0%, 1.5% and 2.0%. It was observed that the deflection corresponding to ultimate load increases with increase in fibre volume fraction, and the branch of the load-deflection curves after ultimate load tends to descend more gently for higher steel fibre volume fractions. Figure 2.17 is the average load-deflection behaviour of the three test results on identical mix specimens for the four-point bend test.

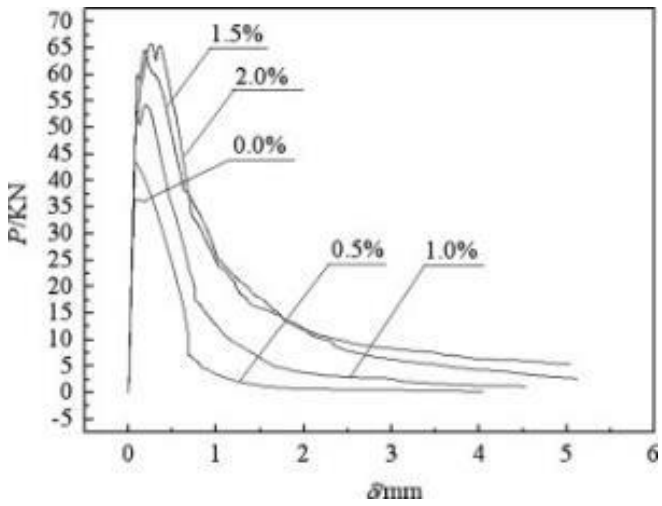

Figure 2.17: Load-deflection curve of SFLWC (Wang & Wang 2013)

Similarly, a study by Yazıcı, İnan & Takak (2007) investigated the effect of aspect ratio and volume fraction of steel fibres on the compressive and flexural strength of SFRC at fibre dosages of 0.5, 1.0 and 1.5% by volume of concrete. It was concluded that steel fibres significantly improve the flexural strength of concrete compared to the compressive strength improvement. Moreover, flexural strength was improved with increasing aspect ratio and dosage volume.

Another study by Alhozaimy, Soroushian & Mirza (1996) investigated the mechanical properties of collated fibrillated polypropylene fibres at dosages below 0.3% by concrete volume. It was found that polypropylene fibre volume fraction did not affect the flexural strength of concrete but rather increased its flexural toughness.

2.6 Summary

This section has covered a large amount of information regarding crude oil contaminated sand. Oil production and sand contamination was discussed followed by a review of oil contaminated sand's geotechnical properties and current remediation technologies. Remediation technologies were found to be expensive and often time consuming.

The use of oil contaminated sand in concrete was then reviewed. This section discussed the benefits of its use in construction, outlining possible applications following a detailed discussion of past studies which have investigated the effects of oil contamination on concrete mechanical properties. All investigations concluded that oil contaminated reduced concrete strength.

A general review of fibre-reinforced concrete was then outlined. Firstly, the historical development of FRC was reviewed followed by its properties and applications in modern industries. Fibre technology in relation to concrete enhancement and fibre types relating to this study were then discussed.

Finally, FRC mechanical properties were researched in depth. The mechanism of fibre bridging, fibre-matrix interaction and mechanics of crack formation are summarised. It has described the effects of fibre orientation and distribution, fibre mechanical properties and fibre volume dosage on concrete properties. Additionally, a review of

the effects of fibres on concrete compressive and flexural strength was undertaken. All studies concluded that fibres had marginal effect on concrete compressive strength, however, largely improved flexural strength.

Chapter 3

Materials and Methods

3.1 Introduction

This section details the methods that were implemented to complete the experiments for the analysis. An outline of all resources is provided, as well as details of the mix designs, casting and curing of specimens followed by a summary of test setups and procedures.

The effect of oil contamination on concrete properties is important to understand before introducing fibres. Mainly, the extent of oil contamination that is still viable for use in construction needs to be determined. This is because fibres can usually only enhance the mechanical properties of concrete. If oil contamination effected concrete physical properties to an extent that it was unsuitable for practical use, the introduction of fibres would be impractical. It is also important to determine how oil alters the mechanical properties of concrete in order to predict any possible hindrance of fibre interaction with the concrete matrix.

The experimental program includes three stages:

- *Programme 1:* Determine maximum oil content that is suitable for use in construction with concrete specimens containing 0%, 1%, 2%, 6%, 10% and 20% oil contaminated sand
- *Programme 2:* Determine the mechanical performance of four different types of fibres to find the best performing in concrete containing the maximum sand oil content found in programme 1
- *Programme 3:* Determine optimum dosage rate of best performing fibre with concrete containing the maximum oil content found in programme 1

3.2 Materials

3.2.1 Aggregate

The main concern was the material used as fine aggregate as it varies from place to place. Fine sand was chosen because it is similar to sand in the Libyan Desert. A sieve analysis carried out by Abousnina (2015), who used the same fine sand in his investigation, found that grain size of the sand particle is less than 2.36 mm.

In order to contaminate sand, oil was added to dry sand at least 72 hours before it was used in casting to allow absorption.

Figure 3.1: Oil contaminated sand

As course aggregate, 10 mm crushed gravel from USQ was used. The aggregate was washed to remove any dirt and debris at least 24 hours before casting in order to achieve saturated surface dry (SSD) condition.

Figure 3.2: Saturated surface dry (SSD) course aggregate

3.2.2 Cement

General purpose (GP) Portland cement in 20 kg bags from Bastion Building Materials was used. The cement properties are outlined in Table 3.1:

Table 3.1: GP cement properties (Cement Australia 2012)

Property		GP Cement
Setting Time	Min	45 min
	Max	10 hrs
Soundness	Max	5 mm
SO_3	Max	3.50%
ISO Mortar Compressive Strength	3 Day (min)	-
	7 Day (min)	25 MPa
	28 Day (min)	40 MPa

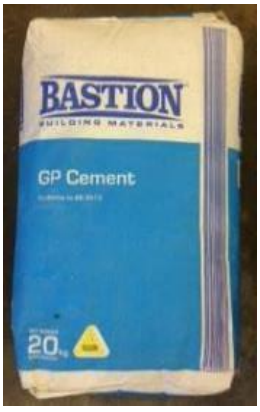

Figure 3.3: General purpose Bastion cement

3.2.3 Oil

Crude oil also varies from place to place. Mineral Fork w2.5 motorcycle oil was selected because its density and viscosity are very similar to light crude oil (Table 3.2).

Table 3.2: Comparison of light crude oil and Fork w2.5 Motorcycle oil (ChampionMotoUK Ltd 2009, Simetric 2011)

Property	Light Crude Oil	Fork w2.5 Motorcycle Oil
Density (kg/L)	0.825	0.827
Viscosity (mm^2/s)	5.96	6.74
Temperature (°C)	40	40

Figure 3.4: Mineral Fork w2.5 motorcycle oil (ChampionMotoUK Ltd 2009)

3.2.4 Fibres

The programme investigated the effect of four types of fibres. All fibres types varied in properties in terms of material, strength and geometry. The fibres used are shown in Figure 3.5:

Figure 3.5: Fibre types investigated

3.2.4.1 Forta Ferro

Forta Ferro is a bundle twisted fibre which ensures that fibre mixes well into the concrete and distributes evenly throughout the concrete matrix (Figure 3.6). The fibre is designed to provide excellent resistance to impact forced and is designed to retain its cross sectional shape. Its properties are outlined in Table 3.3:

Table 3.3: Forta Ferro properties (BASF 2015)

Material	100% virgin co-polymer/polypropylene
Form	Twisted bundle non-fibrillated monofilament and a fibrillated network
Fibre Count	161,900/kg
Length	38 mm
Estimated Diameter	0.8 mm
Specific Gravity	0.91
Tensile Strength	570 MPa – 660 MPa
Colour	Grey

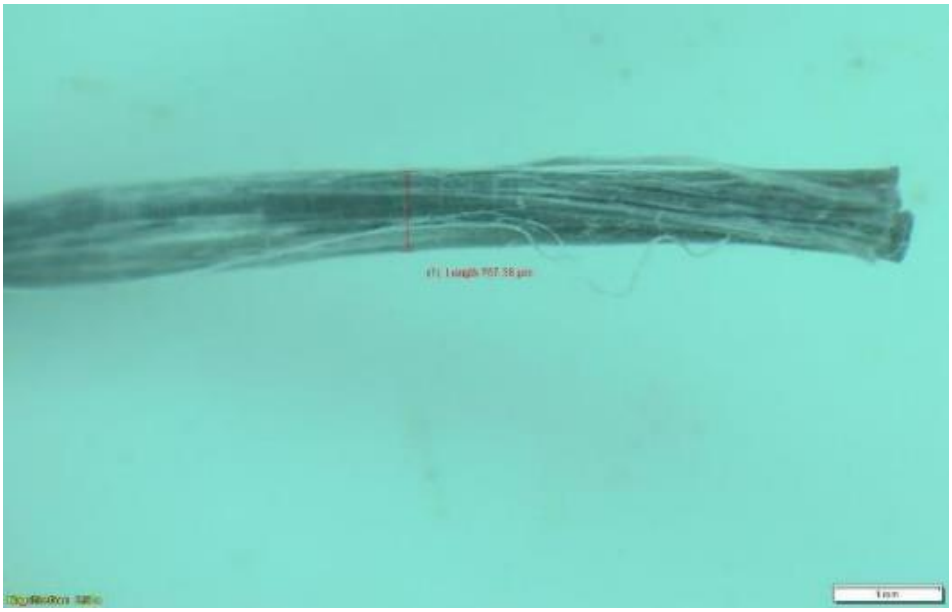

Figure 3.6: Microscopic screenshot of Forta Ferro fibre

3.2.4.2 ReoShore 45

ReoShore 45 is a structural polypropylene fibre with a unique surface design to provide anchorage. The surface design exhibited evenly spaced extruded treads down the length of the fibre (Figure 3.7). Its properties are outlined in Table 3.4:

Table 3.4: ReoShore 45 properties (BASF 2015)

Material	100% virgin polypropylene
Form	Monofilament fibre system
Fibre Count	31,000/kg
Length	45 mm
Estimated Diameter	0.8 mm
Est. Anchorage Spacing	0.8 mm
Specific Gravity	0.91
Acid/Alkali Resistance	Excellent
Tensile Strength	750 MPa – 850 MPa
Absorption	Nil
Colour	Black

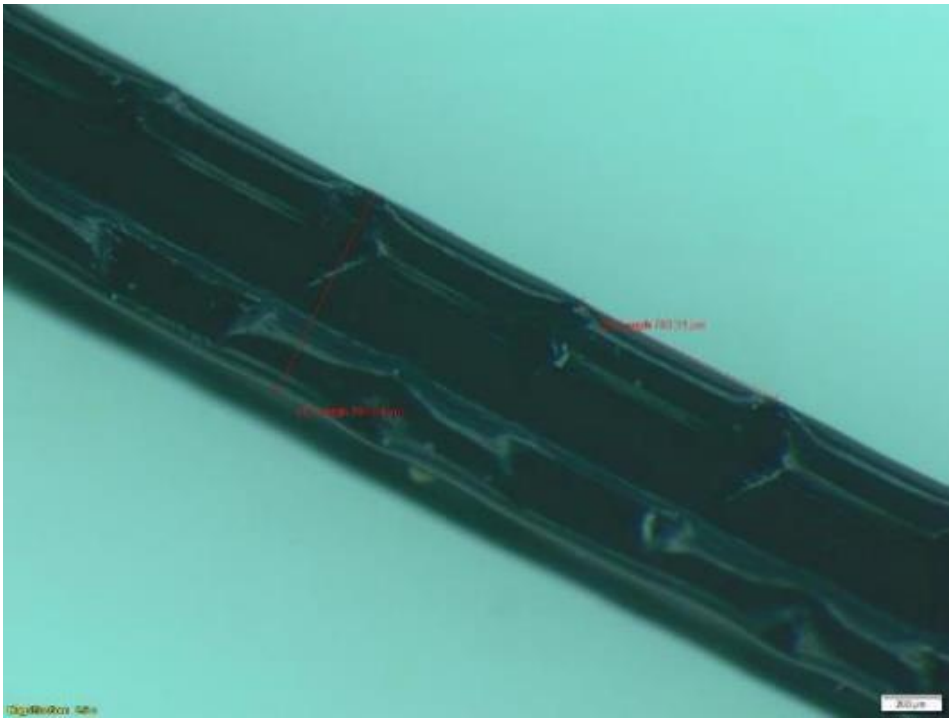

Figure 3.7: Microscopic screenshot of ReoShore 45 fibre

3.2.4.3 Masterfibre Econo-Net (Polypropylene)

Masterfibre Econo-Net is a polypropylene fibre micro-reinforcement system in a network form (Figure 3.8). It is used to reduce plastic and hardened concrete shrinkage, improve impact strength, increase fatigue resistance and concrete toughness. Its properties are outlined in Table 3.5:

Table 3.5: Masterfibre Econo-Net properties (BASF 2015)

Material	Virgin homopolymer polypropylene
Form	Collated fibrillated fibre
Length	19 mm
Specific Gravity	0.91
Acid/Alkali Resistance	Excellent
Tensile Strength	570 MPa – 660 MPa
Absorption	Nil
Colour	White

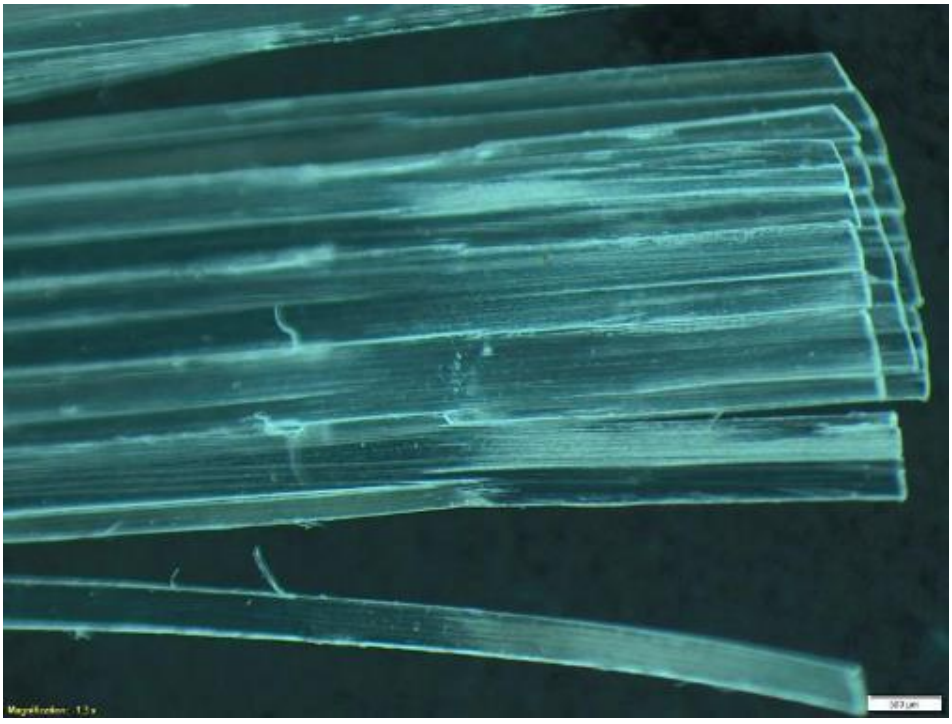

Figure 3.8: Microscopic screenshot of polypropylene fibre

3.2.4.4 Reoco 65/35 (Steel)

Reoco 65/35 is a cold drawn hook-ended fibre used for concrete crack control and reinforcing (Figure 3.9). It is designed to provide excellent resistance to rupture forces and guarantee strata stability. Its properties are outlined in table 3.6:

Table 3.6: Reoco 65/35 properties (BASF 2015)

Material	Bright low carbon steel wire
Form	Round wire, hook shape
Fibre Count	15,318/kg
Length	35 mm
Diameter	0.55 mm
Est. Diagonal Hook Length	2.4 mm
Est. Outer Hook Length	2.5 mm
Specific Gravity	7.93
Tensile Strength	1250 MPa – 1350 MPa
Absorption	Nil
Colour	Silver

Figure 3.9: Microscopic screenshot of steel fibre

3.3 Mix Design

3.3.1 Base Mix Quantities

For all programmes a mix ratio of 3:3:1 (course aggregate : fine aggregate : cement) with a water-cement (w/c) ratio of 0.5 is implemented. A course aggregate ratio of 3 is based on previous research by Abousnina (2015), where a mix ratio of 3:1 was implemented to investigate the effects of oil contaminated sand on the properties of mortar. Likewise, a w/c ratio of 0.5 was selected based on the same investigation on the effect of w/c ratio on mortar containing light crude oil where the highest compressive strength was observed with a w/c ratio of 0.5. Therefore, for all programs the base concrete mix per batch is:

Table 3.7: Base mix design

Material	Quantity (kg)
OPC	5.32
Water	2.66
Fine Aggregate	15.97
Course Aggregate	15.97

3.3.2 Properties of concrete with oil contaminated sand

Programme 1 investigates the physical and mechanical properties of concrete with oil contaminated sand. The study analyses the compressive strength of concrete with oil contaminated sand up to 20% by dry volume of sand. The programme's aim is to determine the maximum oil content in sand that is suitable for use in structural concrete. It is important to take strength characteristics into account, but specifically the physical properties will be the determining factor.

Table 3.8: Programme 1 testing outline

Test	Sand Oil Content	Number of Specimens
Compression	0%	3
	1%	3
	2%	3
	6%	3
	10%	3
	20%	3

3.3.3 Properties of oil contaminated concrete with short fibres

Programme 2 investigates the effect for short fibres on the physical and mechanical properties of concrete with oil contaminated sand. The found maximum oil content determined from programme 1 is tested under compressive and flexural loading with the addition of four types of fibres outlined in Section 3.2.4. A dosage of 0.1% by volume of concrete is implemented to enable a comparative study. This based on the recommended dosage of polypropylene fibres which is the lowest recommended dosage of the four fibre types. As well as flexural and compressive testing, a microscopic analysis will be undertaken to analyse the matrix-fibre bond. The aim of this study is to determine the fibre type which most improves concrete's mechanical properties.

Table 3.9: Programme 2 test outline

Test	Fibre Type	Dosage		Number of Specimens
		% by Volume	kg/m^3	
Compression	Forta Ferro	0.1	0.91	3
	ReoShore 45	0.1	0.91	3
	Polypropylene	0.1	0.91	3
	Steel	0.1	7.93	3
Flexural	Forta Ferro	0.1	0.91	3
	ReoShore 45	0.1	0.91	3
	Polypropylene	0.1	0.91	3
	Steel	0.1	7.93	3

3.3.4 Optimum fibre dosage for concrete with oil contaminated sand

Programme 3 investigates the best performing fibre determined from programme 2 at varied dosage rates. The dosage rates are dependent on the recommended dosage of the best performing fibre from the literature. For steel fibres, the recommended dosage is 15-30 kg/m^3 (Section 2.4.5.1). Additionally, from the McKee theory presented in Section 2.4.5.1, the minimum recommended steel fibre dosage with an aspect ratio (l/d) of 63.64 is 16.71 kg/m^3 to give a maximum average spacing factor of 0.45 times the nominal fibre length. The 0.9 kg/m^3 dosage is based on the same percentage by weight for the other three types of fibres in Programme 2.

As well as compressive and flexural loading, a slump test for each dosage batch will be performed prior to preparing specimens to compare concrete workability. The aim of the study is to determine the optimum fibre dosage which most improves concrete's mechanical properties.

Table 3.10: Programme 3 test outline

Test	**Fibre Type**	**Dosage**		**Number of Specimens**
		% by Volume	**kg/m^3**	
Compression	Steel	0.00115	0.9	3
		0.2	15.86	3
		0.3	23.79	3
		0.4	31.72	3
		0.5	39.65	3
Flexural	Steel	0.1	0.9	3
		0.2	15.86	3
		0.3	23.79	3
		0.4	31.72	3
		0.5	39.65	3

3.4 Mixing of Concrete Batches

3.4.1 Apparatus

Mixer – a useable portable cement mixer.

Buckets – buckets capable of storing water for mix before casting.

Plastic bags – large plastic bags capable of storing cement and course aggregate and small plastic bags capable of storing fibres.

Wheel Barrow – capable of storing fresh concrete before slump test and placement of fresh concrete into moulds.

Mason's Towel – a useable mason's towel made from non-absorbent material.

3.4.2 Casting Process

1. Materials were weighed according to mix design.
2. Mixing:
    a. Programme 1: water was added first followed by cement, when cement is mixed with water sand was added followed by aggregate. Materials were mixed thoroughly.
    b. Programmes 2 and 3: Fibres were added before aggregates were introduced to ensure optimum bond with mortar.
3. Continued mixing for approximately 3 minutes.
4. Once mix was uniform, batch was poured into wheel barrow and mixed manually using a mason's towel to ensure sand was mixed.

Figure 3.10: Mixing concrete batches

3.5 Preparation of Specimens

3.5.1 Apparatus

Moulds – 100 x 200 mm cylindrical and 100 x 100 x 300 mm square prism moulds.

Scoop and mason's towel – for concrete placement and levelling made for non-absorbent material.

Immersion vibrator – electric immersion vibrator for concrete compaction.

Vibrating table – electric vibrating table for concrete compaction.

Glad wrap – for covering cast specimens.

Plastic bags – large plastic bags capable of storing concrete specimens.

Incubator – a curing room with a controlled environment of 25℃ and 85% humidity.

Cement paste mixer – electric mixer capable of mixing cement paste.

Plastic and glass squares – for levelling of cement paste.

3.5.2 Preparation Process

1. Fresh concrete is placed into moulds with a scoop in layers of three, compacting using an immersion vibrator for 20 seconds between layers.
2. Place moulds on vibrating table for 20 seconds to remove any excess air voids and ensure concrete is level with mould.
    a. Programme 1: compression moulds are filled with concrete to top.
    b. Programme 2 and 3: compression specimens filled 2 mm from the top of the moulds to allow space for cement paste capping.
3. Specimens are covered with glad wrap to prevent seepage and left overnight to set.
4. Moulds are removed the following day and specimens are placed in plastic bags in the incubator for the remaining 27 days of curing.
5. Programme 2 and 3 compression specimens were left in the moulds to allow cement paste to be placed:
    a. Mix water and cement in cement paste mixer until workable.
    b. Clean top surface of specimens to optimise bond with cement paste.
    c. Add workable cement paste until level with top of cylinder.
    d. Place plastic film followed by glass on top of moulds to level the cement mortar and leave overnight.
    e. Remove moulds the following day, place specimens in plastic bags in incubator for the remaining 26 days of curing.

Figure 3.11: Use of immersion vibrator

Figure 3.12: Cement paste application

Figure 3.13: Specimens before mould removal

3.6 Slump Test

The slump test is the most common test to evaluate the workability of fresh concrete. The empirical test measures the workability of fresh concrete, but specifically, it measures the consistency of concrete detecting variations in the uniformity of a concrete mix. Concrete workability is mainly affected by water content, along with other factors including aggregate grading and particle shape. A low slump concrete has a stiff consistency, therefore, the concrete may be difficult to place. However, a more workable mix does not necessarily mean a more fluid mix as segregation and honeycombing can occur if the mix is too fluid.

Fibres impart considerable stability or cohesion to FRC mixtures which may cause them to appear unworkable when judged only on terms of slump, which is a measure primarily of stability under static conditions. However, when properly proportioned, FRC mixtures flow readily under dynamic conditions produced by vibrators usually used for placement in practice. Accordingly, they are satisfactory from a mobility point of view (Lamond & Pielert (eds.) 2006). Therefore, this test will be used as a comparison of fibre dosages analysed rather than an indication of FRC consistency.

The apparatus for the test is simple and portable, making it suitable for either on-site or laboratory testing. The test procedure was carried out in accordance with AS1012.3.1 (2014) after concrete was casted.

3.6.1 Apparatus

Mould – a hollow frustum of a cone made of non-reactive rigid material at least 1.5 mm thick. The bottom and top of the mould are open at right-angles to the axis of the cone with internal dimensions as follows:

Bottom diameter = 200 ± 5 mm

Top diameter = 100 ± 5 mm

Vertical height = 300 ± 5 mm

Rod – a metal rod of 16 ± 10 mm in diameter, a length of 600 ± 10 mm and having at least one end tapered for a distance of approximately 25 mm to a spherical shape having a radius of approximately 5 mm.

Conical collar – a detachable collar to facilitate filling the mould made of non-reactive rigid material.

Scoop – the scoop shall be made from non-absorbent material of appropriate size.

Base plate – the base plate shall be of smooth, rigid, non-absorbent material with a thickness of at least 3 mm.

Ruler – appropriate steel ruler is required for measurement of slump height.

Figure 3.14: Slump test apparatus

3.6.2 Test Procedure

The procedure of testing was conducted as follows:

1. The internal surface of the mould is cleaned and moistened with a damp cloth before beginning each test.
2. The mould is placed on the base plate and held in place by standing on the foot-rests while the mould is filled and compacted.
3. The mould is filled in layers of three. As each scoopful of concrete is placed, move scoop around the top edge of the mould to ensure symmetrical distribution of concrete within the mould.
4. Rod each layer with 25 strokes of the rounded end of the rod. Ensure the strokes are distributed uniformly over the mould cross-section. Rod the second

and top layers throughout their depths, so that the strokes just penetrate into the underlying layer.

5. Heap concrete above mould for the top layer. If rodding results in subsidence of concrete below the top edge of the mould, add more concrete to keep excess above mould. The excess concrete after compaction is removed by using a screeding and rolling motion of the rod so that the mould is filled exactly.
6. Remove mould by raising it slowly and carefully in a vertical direction, allowing the concrete to subside.
7. Immediately measure slump by determining the difference between the height of the mould and the average height of the top surface of the concrete.

3.7 Compressive Strength Test

Compressive strength of concrete is a measure of its ability to resist static load. It is the most common test performed on hardened concrete as it is easy to perform. The compressive strength of concrete is usually regarded as its most important property as concrete is designed to resist compressive stresses. The compressive strength gives a clear indication of how oil contamination affects concrete strength along with the effect of fibres.

Compression testing followed ASTM C39 (2015) standard test method for compressive strength of cylindrical concrete specimen's guidelines. The test method applies a compressive axial load to moulded cylinders at a prescribed rate until failure. The compressive strength (MPa) of the specimen is calculated by dividing the maximum load (N) attained during the test by the cross-sectional area (mm^2) of the specimen. In Australia, concrete cylindrical specimens are 100 mm diameter and 200

mm height. The test was conducted in the engineering laboratory of University of Southern Queensland after the specimens were cured for 28 days.

3.7.1 Test Setup

The test setup consisted of a hydraulic loading machine. Programme 1 testing used rubber capping to promote symmetrical loading of the specimen (Figure 3.1 (a)), however, programme 2 and 3 specimens were capped with a cement paste to eliminate the need for external capping (Figure 3.15 (b)).

(a) (b)

Figure 3.15: Compression test setup (a) using rubber capping and (b) using cement paste capping

3.7.2 Test Procedure

The procedure of testing was conducted as follows:

1. All moist cured specimens are tested and measured immediately after they are removed from the curing room.
2. The mass of each specimen is weighed and recorded.

3. Placing of specimen: the lower bearing plate is placed on the platen of the testing machine directly under the seated (upper) spherical bearing block. Bearing faces are wiped clean and the specimen is placed on the lower bearing block.
4. When using external rubber capping, the top cap of the specimen is wiped clean and bearing cap is centred on the top cap of the specimen.
5. Carefully align the axis of the specimen with the centre of thrust of the spherically seated block.
6. Prior to proceeding with test ensure the load indicator is zero and in the case that the indicator is not properly set to zero, adjust the indicator.
7. When using external rubber caps, verify the alignment of the specimen after application of load, but before reaching 10% of the anticipated specimen strength. The axis of the cylinder should not depart from the vertical by more than 0.5°. If the cylinder alignment does not meet requirements, release load and carefully re-centre the specimen before reapplying the load and rechecking.
8. Apply the load continuously and without shock at a rate corresponding to a stress rate on the specimen of 0.25 ± 0.05 MPa/s.
9. Apply compressive load until load indicator shows that the load is decreasing steadily and the specimen displays a well-defined fracture pattern.

3.8 Flexural Strength Test

Flexural strength of concrete is a measure of its ability to resist bending. Flexural strength can be expressed as the 'modulus of rupture'. While the modulus of rapture is important, the load-deflection behaviour will say more about the effect of each fibre on the concrete.

The test procedure was carried out accordance with ASTM C1609 (2012). The test method loads a simply supported beam under four-point loading using a closed loop, servo-controlled testing system and evaluates the flexural performance of fibre-reinforced concrete using parameters derived from the load-deflection curve. The first-peak and peak loads and the corresponding stresses can be determined through the formula for modulus of rapture (ASTM International 2012):

$$f = \frac{PL}{bd^2} \tag{3.1}$$

Where; $f =$ Strength (MPa)

$P =$ Load (N)

$L =$ Span length (mm)

$b =$ Average width of specimen at fracture (mm)

$d =$ Average depth of specimen at fracture (mm)

The first peak stress characterises the flexural behaviour of fibre-reinforced concrete prior to cracking, while the residual strengths at specified deflections characterise remaining capacity after cracking. In some cases, fibres may increase the residual load and toughness at specified deflections while producing a first-peak strength equal to or only slightly greater than the flexural strength of concrete without fibres. In other

cases, the effect can be opposite. The test was conducted in the engineering laboratory of University of Southern Queensland after the specimens were cured for 28 days.

3.8.1 Test Setup

Concrete specimens had a cross-sectional area of 100 mm x 100 mm and a length of 350 mm. The specimen is subjected to bending through four-point loading until failure. Figure 3.16 shows the test setup. The loading point spacing's (l) is 100 mm having a support span (L) of 300 mm.

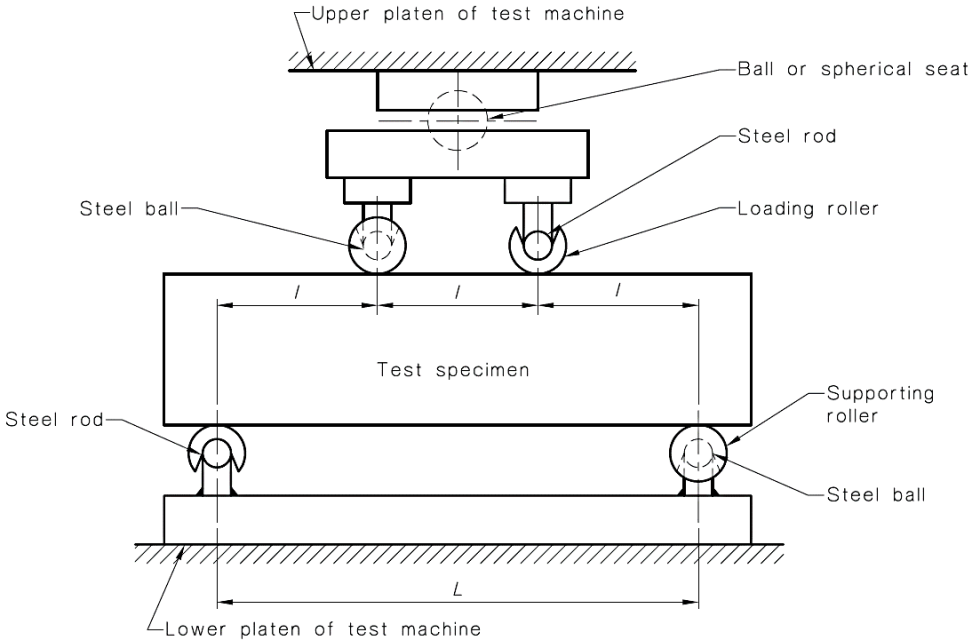

Figure 3.16: Diagrammatic view of flexure testing apparatus (Standards Australia 2000)

3.8.2 Test Procedure

The procedure of testing was conducted as follows:

1. All moist cured specimens are tested and measured immediately after they are removed from the curing room.
2. The mass of each specimen is weighed and recorded.

3. Mark specimens where the support and first loading roller should align (l) to ensure symmetrical loading.
4. Input the measured geometry of the specimen being loaded into the machine.
5. Arrange the specimen and the loading system. Centre the specimen in relation to the applied force and bring the load-applying blocks in contact with the surface of the specimen.
6. Load the specimen continuously and without shock. The load shall be applied at a constant rate of 1 mm/min to the breaking point.

3.9 Safety

Due to the experimental nature of this study a number of safety precautions were taken:

- Breathing masks when weighing cement in preparation for casting
- Rubber gloves during casting to avoid contact with oil
- Thick fabric gloves when handling cured specimens, particularly containing fibres
- Safety glasses during compressive and flexural testing
- All laboratories required steel cap safety boots were to be worn

3.10 Summary

This chapter has described the testing programs being undertaken in the generation of experimental data for the project analysis. The experimental programme includes 3 stages:

- Properties of concrete with oil contaminated sand
- Properties of oil contaminated concrete with short fibres
- Optimum fibre dosage for concrete with oil contaminated sand

The concrete materials and mix design was outlined followed by the processes undertaken to mix concrete batches and prepare test specimens. The tests undertaken as part of the experimental investigation including the slump test and the compressive and flexural strength tests have been discussed with referral to test standards.

Chapter 4

Properties of Concrete with Oil Contaminated Sand

4.1 Introduction

The contamination of sand by crude oil was discussed in Section 2.2. As oil pollution worsens due to increasing demand sand contamination becomes more widely spread. Previous investigations discussed in Section 2.3 found that the altered geotechnical properties of sand due to oil contamination would lead to a decrease in the compressive strength of concrete if used as a constituent. However, its use in concrete would contribute towards a cleaner environment as well as proposing a cost effective construction material. Remediation remedies for contaminated sand can be costly and often time consuming. Therefore, this programme has been developed to determine the maximum oil content in sand that is suitable, in terms of its physical and mechanical properties, for use in structural concrete.

Concrete cylinders are tested under compressive loading following the procedure outlined in Section 3.7 to determine the effect of oil contaminated sand on concrete compressive behaviour. Compressive strength of concrete is one of its most important and useful properties because, as a construction material, concrete is employed to

resist compressive stresses. While, when tensile or shear strength is of importance, the compressive strength is used to estimate the required property. The test consists of three specimens for each oil content of 0%, 1%, 2%, 6%, 10% and 20% by volume of sand (Section 3.3.2).

The purpose of the programme is to determine the percentage of oil contamination that significantly decreases the compressive strength of concrete while still retaining adequate physical properties. With the aim of maximising the options for the use of oil contaminated sand in construction, the found percentage of oil will be used in future testing with the addition of fibres.

4.2 Results and Observations

4.2.1 Physical Properties

After curing, a number of visual and physical differences were noticed between the varied percentages of oil content in the cast specimens. It can be seen from Figure 4.1 that as oil contamination increases as does the porosity and saturation of the specimens. The increase in voids is apparent from 6% oil contamination where large voids can be seen on the surface.

Figure 4.1: Compression specimens (1%, 2%, 6%, 10%, 20% oil contamination left to right)

Likewise, the saturation of concrete due to oil is noticeable from 6% oil contamination where dark patches of oil appear on the surface, the specimens are increasingly viscous and excess oil could be smelt. The 20% oil contaminated specimen was excessively saturated with oil causing it to be a dark brown colour with excessive surface voids.

Through keeping the specimens in plastic bags while curing, any seepage that occurred over the 28 days could be identified. Excess water was found in bags which contained specimens with higher oil contents (≤ 6% by sand volume). As oil content increased, more water was found in the bags due to excess oil preventing water absorption during curing.

Typical normal strength Portland cement concrete usually has a density of approximately 2400 kg/m^3 and varies depending on the amount and density of aggregate, air voids, cement-water ratio and maximum size of aggregate used (Dorf 2004). The density of test specimens was estimated through the measured mass and volume of each specimen. Table 4.1 shows the density of specimens containing varied oil contents.

Table 4.1: Density of specimens with varied oil content (kg/m^3)

Oil Content	**Specimen Density (kg/m^3)**			**Average**	**Standard Deviation**
	1	**2**	**3**		
0%	2443.5	2445.9	2429	2439.5	9.1
1%	2429.5	2451.7	2420.9	2434.0	15.9
2%	2423.2	2426.4	2389.9	2413.2	20.2
6%	2403.9	2391.8	2379.3	2391.7	12.3
10%	2339	2331.3	2337.9	2336.1	4.2
20%	2248.7	2230.7	2242.6	2240.7	9.2

As oil content increases, the density of concrete decreases; with the exception of 1% oil contaminated specimens, where the average density showed an insignificant decrease to the non-contaminated average.

4.2.2 Compressive Behaviour

The compressive behaviour results of the influence of oil contamination on concrete are outlined below in sections. Results will be discussed further is Section 4.3.2.

4.2.2.1 Failure Load

Table 4.2 outlines the ultimate compressive strength of specimens with varied oil content. There is a close correlation in strength between specimens of each oil content, with 1% oil contaminated specimens having the largest standard deviation due the premature failure of specimen 2. The average strength of the non-contaminated specimens is 24.5 MPa as compared to the 1% oil contaminated specimens average strength of 25.5 MPa. However, when oil contamination exceeded 1% the average strength of concrete decreases.

Table 4.2: Compressive strength (MPa) of specimens with varied oil content

Oil Content	Specimens Strength (MPa)			Average	Standard Deviation
	1	2	3		
0%	25.15	24.06	24.26	24.49	0.47
1%	26.52	23.83	26.13	25.49	1.19
2%	21.26	-	22.48	21.87	0.61
6%	17.57	18.72	18.31	18.20	0.48
10%	13.65	13.51	14.22	13.79	0.31
20%	4.53	4.91	4.78	4.74	0.16

4.2.2.2 Stress-Displacement Behaviour

The stress-displacement relationship of specimens was plotted to compare their behaviour at varied oil contents. The stress-displacement behaviour was presented as this is the available data obtained from the machine. Overall, at all oil contents the specimens deformed linearly at lower stresses before decreasing after maximum stress is reached. It is also noted that as oil content increases, the corresponding displacement at ultimate stress increases.

The stress-displacement behaviour of non-contaminated specimens can be seen in Figure 4.2. Specimens 1 and 2 deform similarly, with the ultimate stress of specimen 2 being slightly lower, however, the post-peak response of specimen 3 is comparatively more brittle. The control specimens reached ultimate load at displacements of 1.85 mm, 1.89 mm and 1.65 mm, respectively.

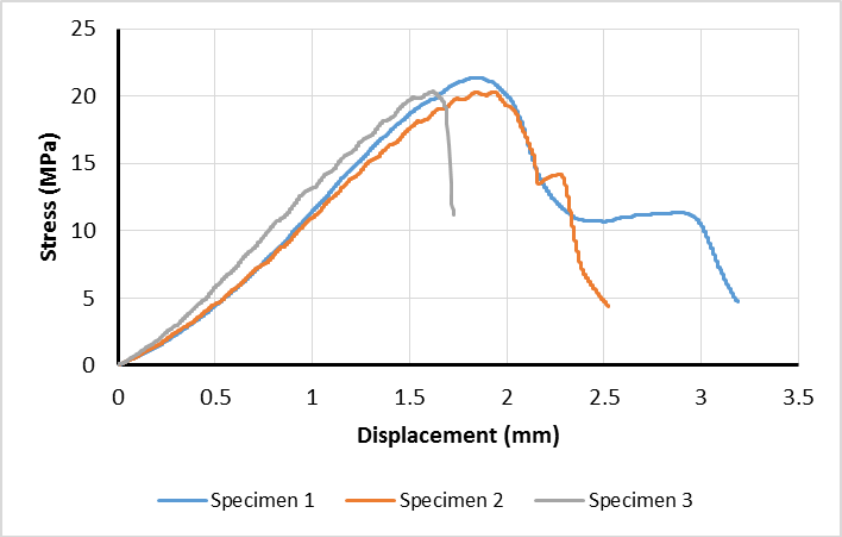

Figure 4.2: Stress-displacement behaviour of specimen with 0% oil contamination

Specimens with 1% oil contamination displayed similar elasticity as noted by the comparable initial linear region in the stress-displacement plot (refer to Figure 4.3). Moreover, the post-peak behaviour of all specimens is brittle. The displacement at ultimate load of specimens is 1.95 mm, 1.91 mm and 2.5 mm, respectively.

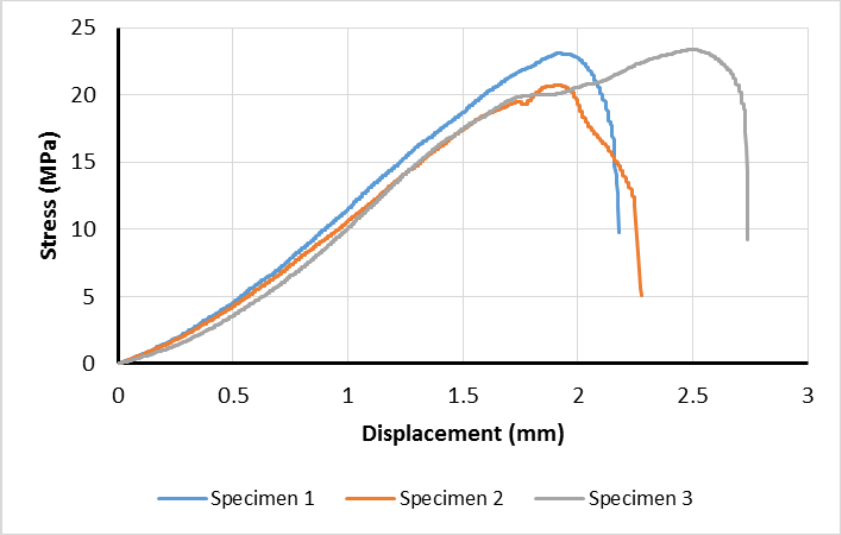

Figure 4.3: Stress-displacement behaviour of specimen with 1% oil contamination

Due to experimental problems there is only two specimens with 2% oil contamination. The linear region of specimens is comparable, with the ultimate stress of specimen 3 being slightly bigger (Figure 4.4). The displacement corresponding to ultimate stress is 1.79 mm and 1.95 mm, respectively. The post-peak response of specimens is brittle rather than exhibiting the typical displacement-softening response of concrete.

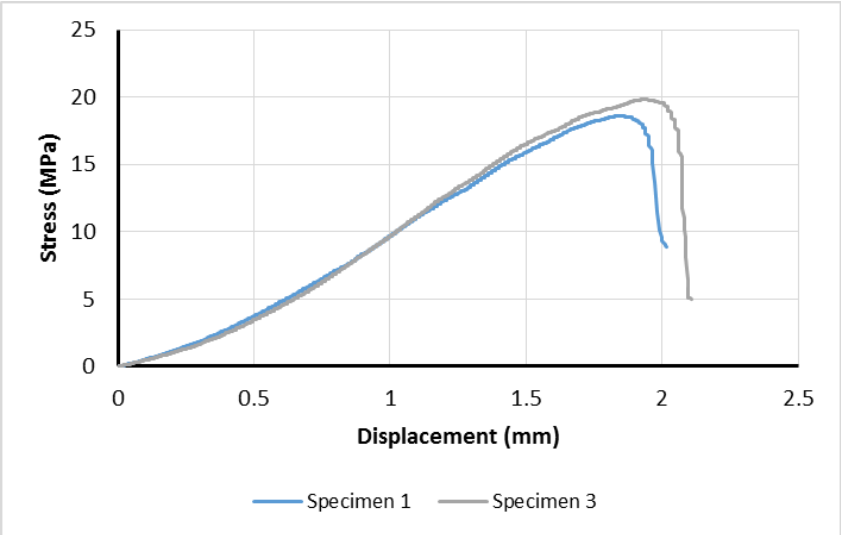

Figure 4.4: Stress-displacement behaviour of specimen with 2% oil contamination

The behaviour of all 6% oil contaminated specimens is similar, with specimen 1 yielding at a lower stress than the other specimens (Figure 4.5). It is noticed that the

yield stress approaches the ultimate stress (or first peak) of specimens as oil content increases. At ultimate stress the displacement of specimens is 2.31 mm, 2.03 mm and 2.13 mm, respectively.

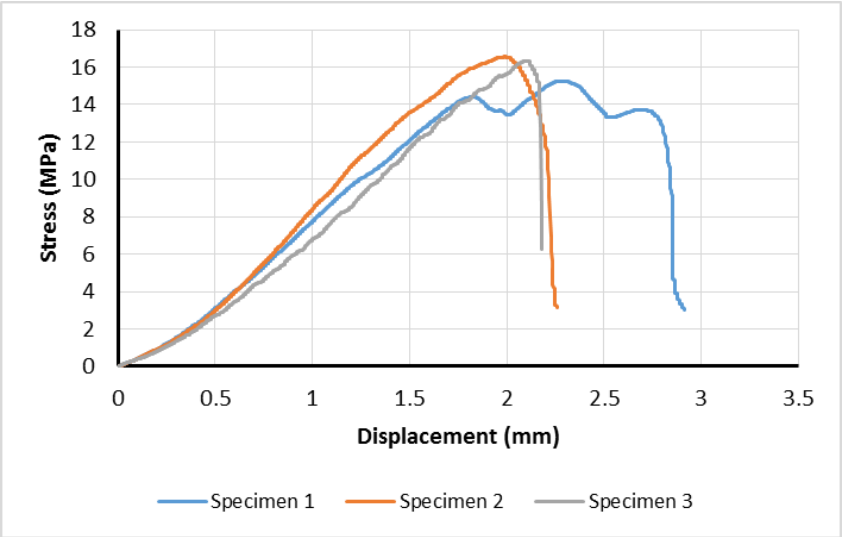

Figure 4.5: Stress-displacement behaviour of specimen with 6% oil contamination

The stress-displacement behaviour of specimens contaminated with 10% of oil by volume of sand is shown in Figure 4.6. The elasticity of specimens is comparable and the yield strength of all specimens is the first peak stress. Following the first peak, specimens decrease in stress without any increase in displacement, before increasing in stress and displacement to peak again. The corresponding displacement at ultimate stress of specimens is 2.43 mm, 2.13 mm and 1.87 mm, respectively.

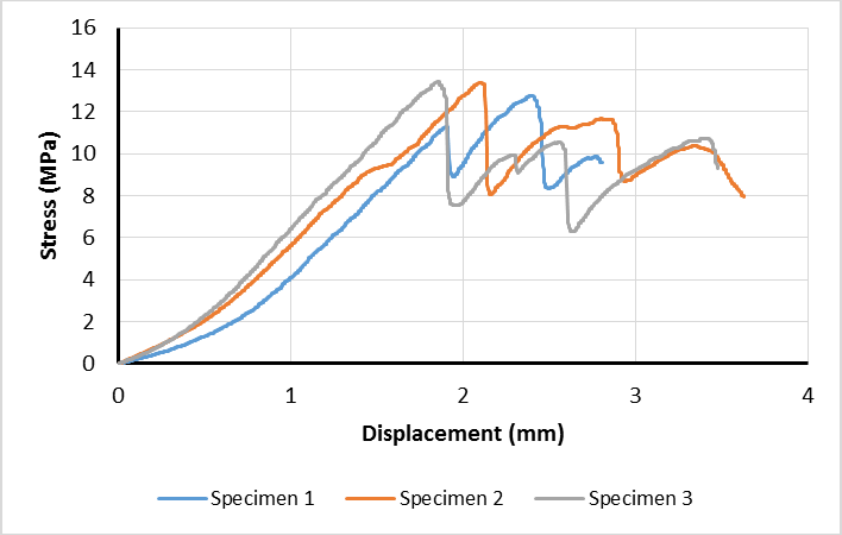

Figure 4.6: Stress-displacement behaviour of specimen with 10% oil contamination

The only similarity from the stress-displacement relationship of specimens with 20% oil contamination is the linear behavior upto approximately 1 mm displacement (Figure 4.7). Specimen 3 may have experienced crushing at this point as stress decreased after first peak. Specimens 2 and 3 did not reach ultimate load until a displacment of 4.15 mm and 4.38 mm, respectively, before showing a brittle post-peak response. While specimen 1 displayed a relatively brittle behavior, having a displacement of 1.51 mm at ultimate stress.

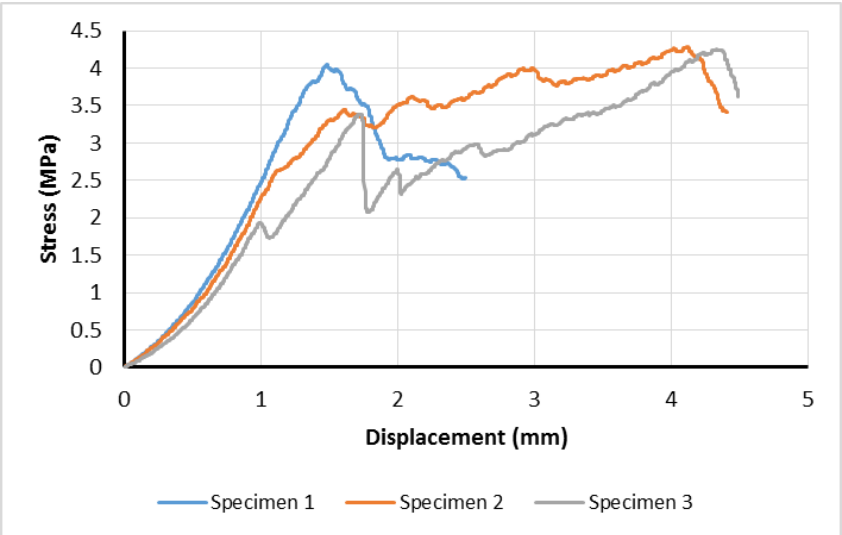

Figure 4.7: Stress-displacement behaviour of specimen with 20% oil contamination

The relative stiffness of specimens was found through fitting a linear tread line to the specimen stress-displacement curves to determine the linear slope. The elasticity of specimens are outlines in Table 4.3:

Table 4.3: Relative stiffness of specimens with varied oil content (MPa/mm)

Oil Content	Specimen Stiffness (MPa/mm)			Average	Standard Deviation
	1	2	3		
0%	14.67 $R^2=0.9989$	13.18 $R^2=0.9988$	14.13 $R^2=0.9986$	13.99	0.75
1%	14.33 $R^2=0.999$	13.39 $R^2=0.9994$	14.27 $R^2=0.9956$	14.00	0.53
2%	12.27 $R^2=0.9985$	-	13.34 $R^2=0.9984$	12.81	0.76
6%	8.94 $R^2=0.9991$	10.33 $R^2=0.9959$	9.02 $R^2=0.9982$	9.43	0.78
10%	7.98 $R^2=0.9996$	6.94 $R^2=0.994$	8.53 $R^2=0.9996$	7.82	0.81
20%	3.73 $R^2=0.9988$	3.12 $R^2=0.9954$	2.59 $R^2=0.993$	3.15	0.57

It is noted that across the entire spectrum of results that there is a close correlation to a linear fit, as noted by R^2 being close to 1 (perfect linear fit), ensuring an accurate approximation of specimen stffness. Of interest is that the average elasticity of specimens decreases as oil content increases, with the exeption of 1% oil contamination.

4.2.2.3 Proportional Limit

The proportional limit is the highest stress at which stress is directly proportional to displacement. From the stress-displacement relationship, the proportional limit is the highest stress at which the curve is linear (elastic). Table 4.4 outlines the obtained proportional limit estimated from the stress-displacement curves for each specimen.

Table 4.4: Proportional limit of specimens with varied oil content (MPa)

Oil Content	Specimen Proportional Limit (MPa)			Average	Standard Deviation
	1	2	3		
0%	19.4	18.13	19.9	19.14	0.91
1%	21.66	18.3	19.83	19.93	1.68
2%	18.02	-	18.14	18.08	0.08
6%	14.2	15.72	16.34	15.42	1.10
10%	11.3	13.4	13.43	12.71	1.22
20%	3.77	2.62	1.93	2.77	0.93

As noted by the standard deviation, there is a close correlation between the proportional limit of specimens at each oil content. Overall, proportional limit decreases as sand contamination increases, with the exception of 1% oil contaminated specimens.

4.2.2.4 Failure Behaviour

The failure mechanisms of compressed concrete can be an initial indication of the compressive strength of the cylinder. Typically, conical failure will occur, however, most specimens displayed splitting failure. When unbonded neoprene caps are used cylinders rarely fracture conically. This is because load applied may be concentrated on one side of the cylinder if requirements for vertical alignment during loading are not satisfied due to the capping (ASTM 2014).

Specimens containing sand was an oil content from 0% to 6% primarily exhibited splitting failure (refer to Figure 4.8). The splitting occurred from the bottom cap and travelled perpendicular to the load.

(a) (b) (c)

Figure 4.8: Splitting failure of specimens containing 0% (a), 2% (b) and 6% (c)

However, some specimens experienced short shear failure due to poor cap placement causing the load concentration to be on one side of the specimen. This type of failure indicates that the cylinder has failed prematurely and the actual strength may not have been attained. The specimens which exhibited this type of failure included specimen 1 at 0% oil contamination, specimen 2 at 1%, specimens 1 and 2 at 2% and specimen 3 at 6%. The 1% and 6% oil contaminated specimens short shear failures can be seen in Figure 4.9.

(a) (b)

Figure 4.9: Short shear failures of specimens with 1% (a) and 6% (b) oil contamination

From 10% oil contamination, crushing at the top cap of specimens was evident due to saturation. The specimens also began to exhibit conical failure rather than splitting (refer to Figure 4.10).

(a) (b)

Figure 4.10: Conical failure of 10% oil contaminated specimens

All specimens with 20% oil contamination failed due to crushing. The load concentration becomes uneven as a result of crushing causing premature failure. Specimens 1 and 3 also displayed shear failure in conjunction with crushing (refer to Figure 4.11 (a)/(b)). The shear path is shown on the figures.

(a) (b) (c)

Figure 4.11: 20% oil contaminated specimens 1-3 after compressive failure

4.2.2.5 Other Observations

On further inspection, excess oil within concrete was noticed from 6% oil contamination. At 6% and 10% oil contamination the oil was in the form of crystallised yellow particles (Figure 4.12 (a)/(b)). It is less noticeable on the 10% contamination sample due to concrete saturation. Whereas, the oil in the 20% contaminated specimen was in liquid form in the indents formed by aggregates (refer to Figure 4.12 (c)).

(a) (b) (c)

Figure 4.12: Excess oil found on 6% (a), 10% (b) and 20% (c) oil contaminated specimens

4.3 Discussion

The discussion was divided into sections for clarity, making reference to the findings outlined in the previous section.

4.3.1 Effect of Oil Contamination on Density

The results of the effect of oil contamination on concrete physical properties was outlined in Section 4.2.1. From Figure 4.1 it was noted that increased oil contamination effected concrete porosity and saturation. As oil content increased, concrete porosity was induced and the physical wetness of specimens worsened. After 28 days of curing, 20% oil contaminated specimens were excessively porous and saturated to a point where concrete was a dark brown colour. The surface of specimens also felt weak and viscous to touch, at times crumbling through handling. Additionally, dark patches could be seen on the surface of specimens containing 6% and 10% oil contamination.

The increased porosity is a result of water seepage during curing. Water was found in plastic bags in which specimens were cured. As oil contamination increased, more excess water was found in the bags. This finding supports literature reported by Almabrok et al. (2013) in Section 2.3.2, that concluded that oil contamination

increased mortar setting time and air content and inhibits cement hydration. Therefore, it is suspected that water absorption during curing was prevented due to over saturation by oil. The effects of both water seepage and lack of cement hydration increased air voids within concrete (refer to Figure 4.1).

Additionally, research by Madderom (1980) (Section 2.3.2) suggests that water seepage increases concrete porosity as reservoirs that are formed around aggregate as a result of over saturation are left as air pockets after seepage. The surface of concrete is also porous due to the vertical water channels created by water (or oil) seeping from the concrete surface. Madderom also mentioned that the cement and fine particles carried outwards with seepage weakens the concrete surface, explaining why 20% contaminated specimens felt weak to handle.

As a result of porosity, concrete density deceased as oil content increased. Figure 4.13 is a graphical representation of Table 4.1 showing the average density of specimens with varied oil content. The average density of 1% oil contaminated specimens is 2434 kg/m^3 compared to the non-contaminated average of 2439.5 kg/m^3. With almost a negligible decrease in density, 1% oil contaminated sand had little effect on concrete porosity, therefore, not causing over saturation of sand particles. However, oil contaminated sand in excess of 1% on average decreases concrete density. From the non-contaminated average density, the 2% oil contaminated specimens decreased 1.08% in density. At 6% contamination a 1.96% decrease was seen, a 4.24% decrease at 10% contamination and an 8.15% decrease in specimens containing 20% of oil (by volume of sand) in comparison to the non-contaminated average.

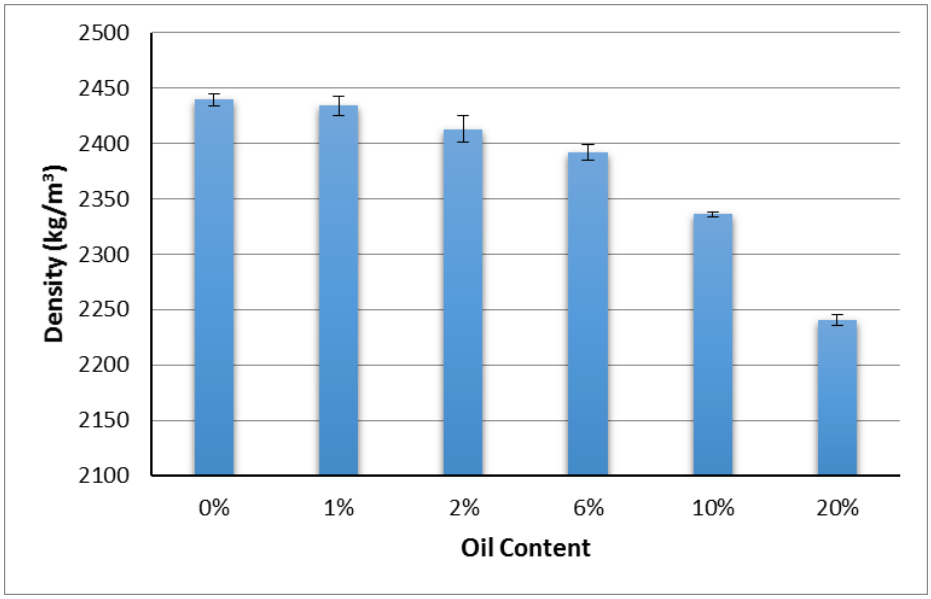

Figure 4.13: Average density of specimens with varied oil content (kg/m^3)

With these findings, it is assumed that sand with an oil content in excess of 1% induces concrete porosity by oil coating sand particles and decreasing concrete cohesion.

4.3.2 Effect of Oil contamination of Compressive Behaviour

4.3.2.1 Effect on Compressive Strength

The findings from the compressive failure load results are graphically summarised in Figure 4.14. The average strength of the non-contaminated compressive specimens is 24.5 MPa (refer to Table 4.2). In general, oil contamination decreases concrete compressive strength. However, sand containing 1% of oil increased concrete average strength by 4.09%, yielding an average strength of 25.5 MPa. The increase in strength may be due to oil optimising concrete cohesion, without causing water seepage. From Section 2.2.3, a study by Abousnina et al. (2014) found that sand contaminated with 1% of light crude oil achieved an optimum sand cohesion of 10.76 kPa. Therefore, the introduction of oil bound sand particles without over saturating them and preventing their bond with other materials during mixing.

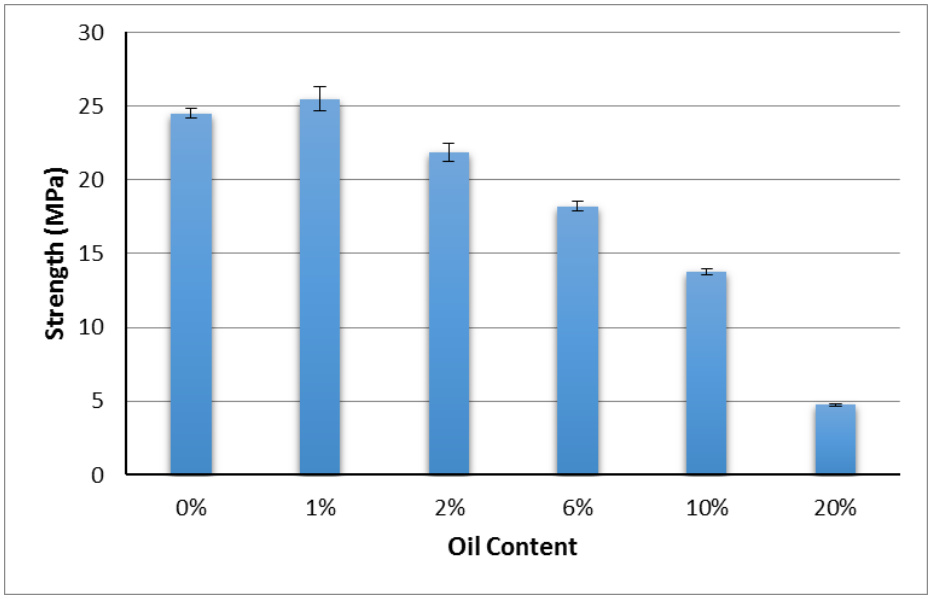

Figure 4.14: Average compressive strength of specimens with varied oil content (MPa)

However, as sand oil content increased from 1%, sand became over saturated. When compared to non-contaminated concrete average strength, the 2%, 6%, 10% and 20% oil contaminated specimens decreased in strength by 10.7%, 25.7%, 43.7% and 80.7%, respectively. Meaning that the use of 20% oil contaminated sand in concrete would, on average, reduce concrete compressive strength to 19.3% of non-contaminated concrete strength.

From literature outlined in Section 2.3.2, studies by Ayininuola (2008), Osuji & Nwanko (2015) and Almabrok et al. (2013) all found that the presence of oil decreased the compressive strength of ordinary Portland cement concrete. All investigations concluded that oil hinders the bond formation between mortar and aggregate by coating sand particles. Referring to Figure 4.12 (c), excess oil was found in the indents left by aggregates. When aggregates exceed saturated surface dry (SSD) state the surface area that is able to bond with mortar is decreased, leaving aggregates surrounded by a barrier of liquid. The formation of oil around sand particles act as a cushion preventing inter-particle contact and the lack of cohesion promotes slippage

as oil content and viscosity increase. After seepage, air voids are left and the result is a relatively porous cement paste that has decreased internal strength, hence, limiting the ultimate compressive strength of concrete.

4.3.2.2 Effect on Stress-Displacement Behaviour

The stress-displacement relationship of concrete is an important aspect of comparison through behaviour analysis. The specimens of each oil content displayed similar behaviour (refer to Figure 4.2-4.7). As oil content increased, it was noticed that yield stress approached ultimate stress; i.e. the linear region of elasticity approaches first peak stress. This trend was observed from 6% oil contamination and above. The specimens, on average, also experienced increased displacements at ultimate stress as oil content increased. The increased displacement is a result of the decrease in specimen density due to oil content (Section 4.3.1); as porosity increased weakening the concrete it became more ductile, hence, displacing more at lower loads.

Additionally, it was observed that, following the first peak stress, specimens containing 10% and 20% oil contamination experienced a decrease in stress without any increase in displacement (Figures 4.6 & 4.7). From observations made through failure behaviour analysis (Section 4.2.4), specimens began to exhibit failure through crushing due to over saturation from oil in excess of 10% (Figures 4.11 & 4.12). Therefore, the drop is stress is assumed to be a result of the specimens crushing. When crushing stopped load resistance is regained and the specimen then increases in stress and displacement to peak again.

A comparison of the most representative stress-displacement curve for each oil content is shown in Figure 4.15. The slope of the non-contaminated specimen and 1%

contaminated specimen displayed comparable elastic displacement. However, the 1% oil contaminated specimen exhibited improved ductility having a displacement of 1.95 mm as compared to the non-contaminated 1.85 mm displacement at failure load.

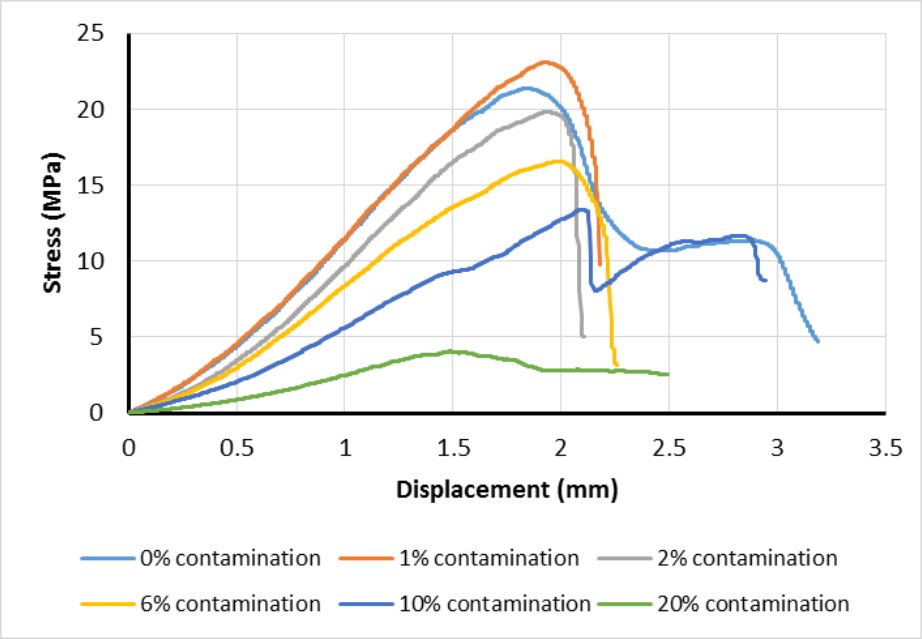

Figure 4.15: Stress-deformation relationship of specimens with varied oil content

The post-peak behaviour of concrete changes from 10% contamination where failure is more brittle due to crushing as a result of saturation. The 20% oil contaminated specimen showed minimal resistance to compressive stress noted by the comparitively gradual behaviour at peak load in conjunction with a displacement of 1.51 mm at failure load.

4.3.2.3 Effect on Relative Stiffness

The relative elasticity (stiffness) of each specimen was calculated by dividing the compressive stress by the displacement in the elastic (linear) proportion of the stress-displacement curves. Figure 4.16 is a graphical representation of the stiffness' outlined in Table 4.3.

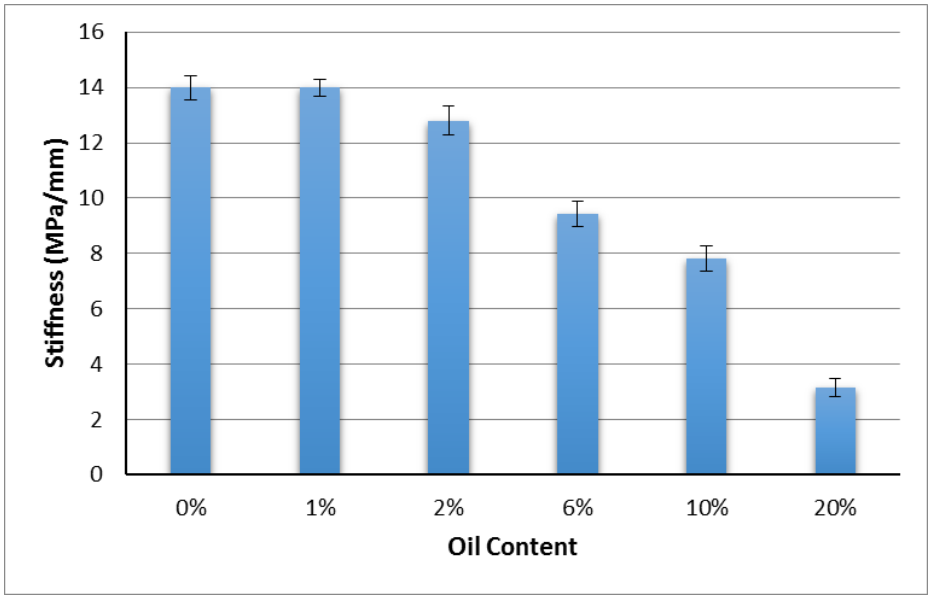

Figure 4.16: Average stiffness of specimens with varied oil content (MPa/mm)

The general trend follows that elasticity of concrete decreases as oil content increases. With the exception of 1% oil contaminated specimens where an average elasticity of 14 MPa/mm was seen as compared to the non-contaminated average of 13.99 MPa/mm. The stiffness decreases by up to 77.5% at 20% oil contamination when compared to the control stiffness and by 44.1% for 10% contaminated specimens. While specimens containing 2% and 6% of oil decreased in stiffness by 8.43% and 32.6%, respectively.

The declining slope of the initial linear region as oil content increases lead to the decrease in stiffness results (Figure 4.15). Therefore, it can be concluded that oil contamination exceeding 1% by volume of sand reduces the elastic limit of concrete and hence experiences increased plastic deformation.

4.3.2.4 Effect on Proportional Limit

The proportional limit is the ultimate stress of concrete elastic behaviour, after which point the concrete begins to deform plastically (permanently). It is used to establish

the limit in repeated applications of the load (service loading). Figure 4.17 is a graphical representation of Table 4.4. Interestingly, as a result of the higher ultimate stress, the average proportional limit for 1% oil contaminated specimens is 4.11% bigger than the non-contaminated proportional limit average. The specimens hold a proportional limit above 10 MPa up to 10% sand contamination, with 20% contaminated specimens having an average proportional limit of 2.77 MPa. A proportional limit of 2.77 MPa may be suitable for sandcrete blocks, however, its uses are limited. While concrete with a proportional limit above 10 MPa can be used for the construction of parking lots, footpaths, pathways and bus terminals (refer to Section 2.3.1).

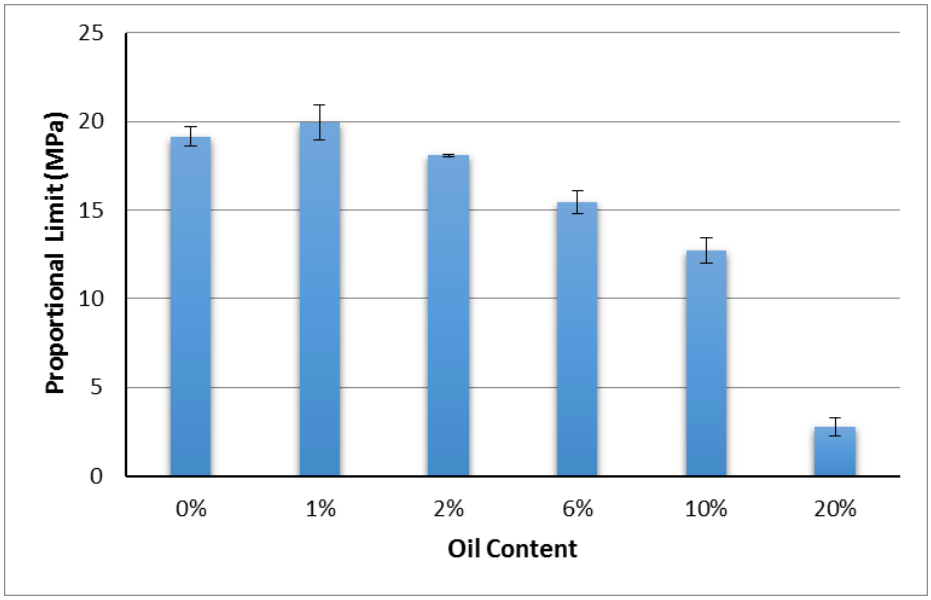

Figure 4.17: Average proportional limit of specimens with varied oil content (MPa)

Figure 4.18 is a comparison of the average proportional limit to the average ultimate strength at each oil content. It is noticed that as oil content increases the proportional limit of concrete approaches ultimate strength. This supports the trend noticed in the analysis of the stress-displacement curves where yield stress approached ultimate stress as oil content increased.

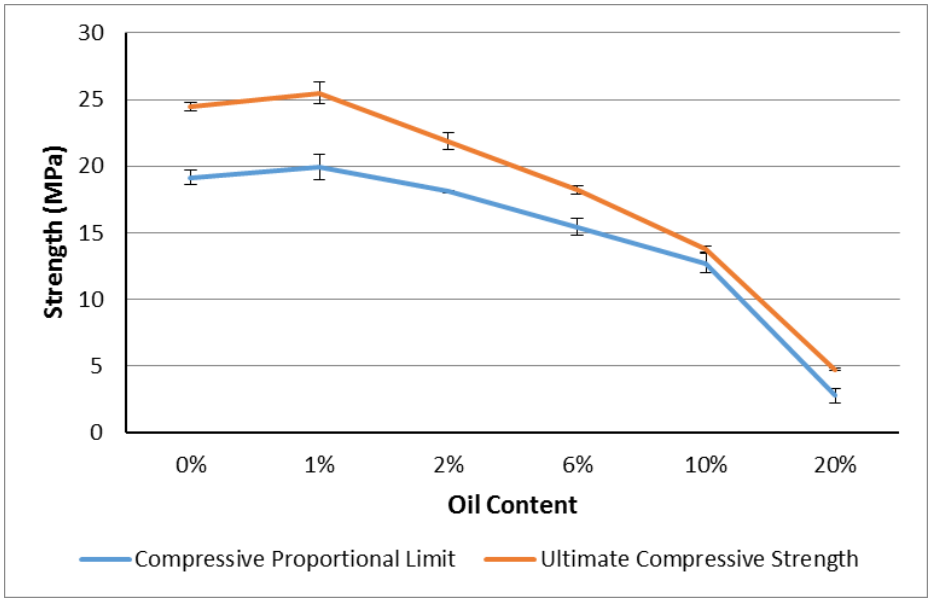

Figure 4.18: Average ultimate strength compared to average proportional limit of specimens with varied oil content (MPa)

From a design perspective, the use of a material where the ultimate and proportional stresses are relatively close is dangerous because if service loading is ever exceeded failure may occur. Therefore, for oil contaminated sand in excess of 6% being used in concrete, the service load should be lower than the proportional limit stress.

4.4 Summary and Conclusion

This chapter has provided insight into the properties of concrete with oil contaminated sand.

It has been noted that the introduction of oil effects the physical properties of concrete, increasing its porosity and saturation. It was found that increased oil contamination restricts cement hydration by preventing water absorption. At 20% contamination the specimens were excessively saturated and porous with a weakened surface. As a result of over saturation by oil hindering concrete cohesion, concrete density decreased as oil content increased.

It was interesting to note that the average compressive strength of concrete with 1% oil contamination increased by 4.09% compared to the non-contaminated average strength. The increase in strength was attributed to the sand reaching optimum cohesion as a result of oil binding sand particles. However, oil in excess of 1% by sand volume however decreased concrete compressive strength. It was concluded that the loss in concrete density in conjunction with over saturation coating sand particles and hindering the physical bond formation between mortar and aggregate led to the loss in compressive strength.

The stiffness was derived from the stress-displacement relationship of specimens. The average stiffness of specimens followed a similar trend to the ultimate failure load findings. It was concluded that the excess porosity caused by oil contamination in excess of 1% decreased concrete elasticity.

The proportional limit can indicate possible applications of concrete through estimating its service strength. Specimens up to 10% oil contamination attained a proportional limit above 10 MPa. However, the application options for 20% contaminated concrete is limited with a proportional strength of 2.77 MPa. For specimens with 6% oil contamination and higher, it is recommended to use a service load lower than the proportional limit as it approaches ultimate stress at higher oil contents due to increased ductility.

For the purpose of the next stage, a maximum of 10% oil contamination is considered suitable for use in construction. The physical properties of concrete at 20% oil contamination is unsuitable for practical use due to over saturation causing excessive air voids leading to a low concrete density. The loss in strength due to these physical characteristics also limits its applications. Therefore, the effect of fibres will be

investigated in concrete with 10% oil contaminated sand. The results of this study are presented in the next section.

Chapter 5

Properties of Oil Contaminated Concrete with Short Fibres

5.1 Introduction

The investigation into the properties of concrete with oil contaminated sand in Chapter 4 concluded that concrete contaminated up to 10% by volume sand is suitable for use in construction. However, it was found that there is up to a 26% compressive strength reduction compared to the non-contaminated specimens. This chapter investigates the possibility of the inclusion of fibres to regain or enhance this reduction in mechanical properties.

Fibre-reinforced concrete (FRC) is reviewed in Section 2.4 while past research on the mechanical behaviour of FRC is revised in Section 2.5. As fibres are added to concrete to reinforce the matrix through load transfer and crack bridging, the enhancement of structural performance of oil contaminated concrete through fibres could be a viable option. The fibre types considered include; Forta Ferro, polypropylene, ReoShore 45 and steel fibres and their structural properties are outlined in Section 3.2.4.

The FRC, as well as non-fibrous specimens, are tested under compressive and flexural loading following the procedures outlined in Sections 3.7 and 3.8, respectively. Flexural testing is included in this programme as fibres are expected to improve the flexural strength of concrete significantly in comparison to compressive strength from literature reported in Sections 2.5.7 and 2.5.8. The testing program is outlined further in Section 3.3.3. The purpose of this study is to determine the fibre type which most improves the mechanical properties of oil contaminated concrete.

5.2 Results and Observations

5.2.1 Physical Properties

Figure 5.1 shows the specimens after curing. From the figure, the physical properties of FRC compared to non-fibrous concrete is visually unaffected.

Figure 5.1: Compressive specimens (Forta Ferro, polypropylene, steel, ReoShore 45 and control left to right)

The density of specimens was estimated through their weight after curing, the results are outlined in Table 5.1:

Table 5.1: Density of compressive specimens with varied fibre types (kg/m^3)

Fibre Type	Specimen Density (kg/m^3)			Average	Standard Deviation
	1	2	3		
Control	2322.7	2322.5	2329.1	2324.8	3.8
Forta Ferro	2330.6	2329.0	2333.7	2331.1	2.4
Polypropylene	2323.0	2323.0	2320.9	2322.3	1.2
ReoShore 45	2321.7	2322.0	2331.4	2325.0	5.5
Steel	2324.4	2320.8	2322.0	2322.4	1.8

From Table 5.1, a close correlation between specimen densities can be noted by the low standard deviation.

5.2.2 Compressive Behaviour

The compressive behaviour results of the influence of fibres on oil-impacted concrete are outlined below in sections. Results will be discussed further is Section 5.3.2.

5.2.2.1 Failure Load

The recorded ultimate compressive stress of specimens is outlined in Table 5.2. The deviation in strength of the control and polypropylene specimens is larger due to outliers. Referring to the stress-displacement curves, the control specimen 1 (Figure 5.2) and polypropylene specimen 2 (Figure 5.4) exhibited greater displacements at lower stresses, having a lower linear slope than their respective specimens. Therefore, these specimens are considered unreliable and not included in average strength calculations.

Table 5.2: Compressive strength (MPa) of specimens with varied fibre types

Fibre Type	Specimen Strength (MPa)			Average	Standard Deviation
	1	2	3		
Control	13.39	16.30	16.29	16.30	1.68
Forta Ferro	18.51	17.17	17.18	17.62	0.77
Polypropylene	18.31	15.64	17.06	17.69	1.34
ReoShore 45	16.38	16.03	15.16	15.86	0.63
Steel	19.01	17.64	17.49	18.05	0.84

All fibres, excluding ReoShore 45, enhanced the compressive strength of oil contaminated concrete. Steel fibres improved the compressive strength of concrete the most, yielding an average strength 1.75 MPa higher than the control average.

5.2.2.2 Stress-Displacement Behaviour

The stress-displacement curve of specimens was plotted to compare the behaviour of fibres and their interaction with the cement matrix. Overall, specimens displayed linear elastic behaviour at lower stresses before deforming plastically after yield stress was reached.

The stress-displacement curves for non-fibrous specimens are shown in Figure 5.2. Specimens 2 and 3 displayed comparable elastic behaviour while specimen 1 experienced increased displacements at lower stresses. The specimens reached ultimate stress at displacements of 0.831 mm, 1.099 mm and 1.793 mm, respectively.

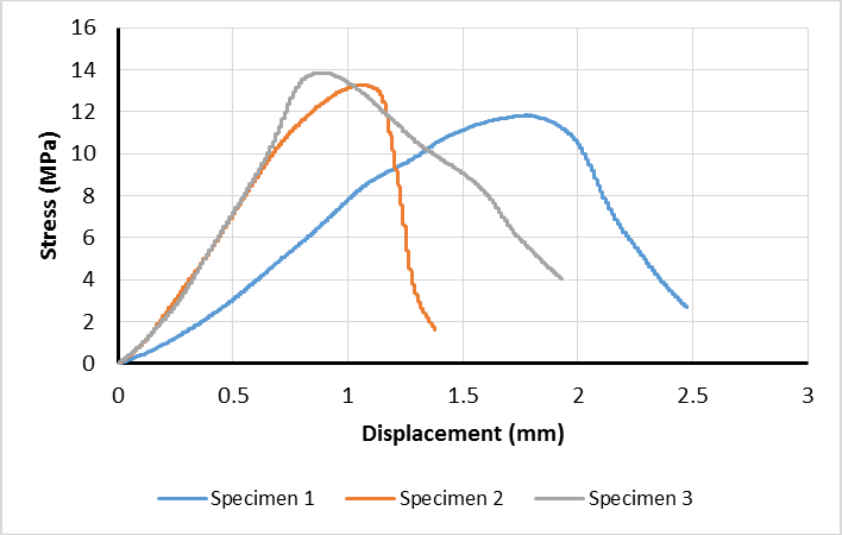

Figure 5.2: Stress-displacement behaviour of control specimens

Specimens containing Forta Ferro fibres deformed at varied rates (Figure 5.3). However, all specimens displayed displacement-softening post-peak behaviour. Specimen displacement at maximum stress is 0.718 mm, 1.134 mm and 0.863 mm, respectively.

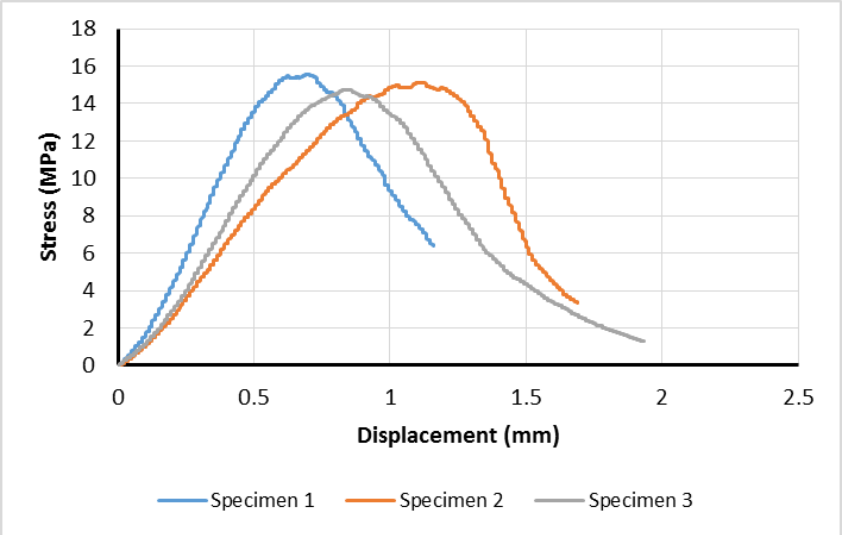

Figure 5.3: Stress-displacement behaviour of Forta Ferro fibre-reinforced specimens

The stress-displacement behaviour of polypropylene specimens can be seen in Figure 5.4. The elasticity of specimens 1 and 3 is comparable, while specimen 2 resisted displacement and failed prematurely before presenting a displacement-softening post-

peak behaviour. The displacement of specimens at ultimate stress is 1.367 mm, 0.754 mm and 1.294 mm, respectively.

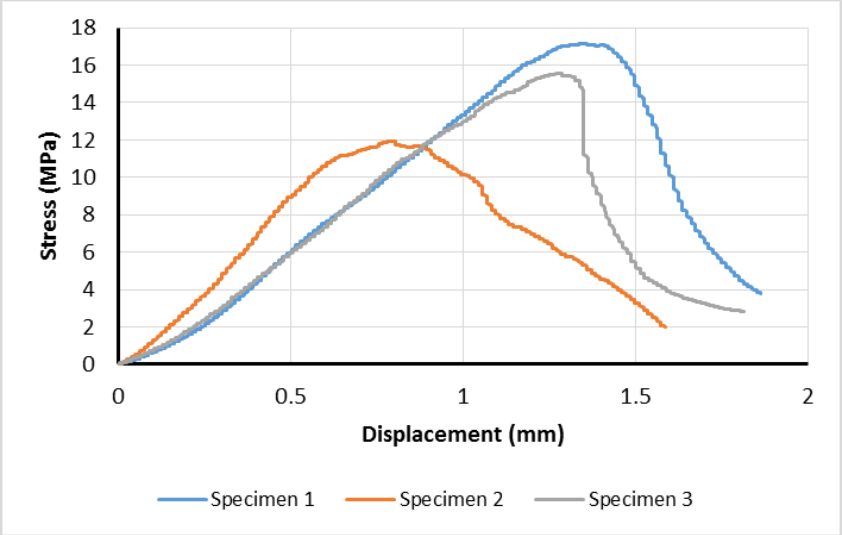

Figure 5.4: Stress-displacement behaviour of polypropylene fibre-reinforced specimens

The stress-displacement curves of concrete containing ReoShore 45 fibres is shown in Figure 5.5. Specimens 2 and 3 deformed similarly, while specimen 1 showed increased resistance to displacement. At maximum stress, the specimen's displacement is 0.679 mm, 1.008 mm and 1.033 mm, respectively.

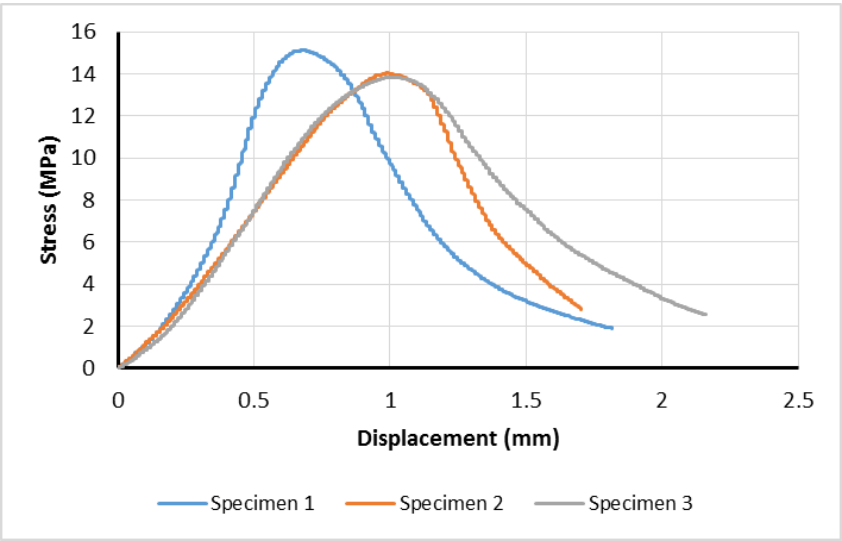

Figure 5.5: Stress-displacement behaviour of ReoShore 45 fibre-reinforced specimens

Steel fibre-reinforced specimens displayed comparable elastic deformation as indicated from the initial linear region in the stress-displacement curves (Figure 5.6). Additionally, all exhibited displacement-softening post-peak behaviour. Moreover, these specimens exhibited the most consistent stress-deformation behaviour among all fibres considered. Specimens reached an ultimate compressive stress at displacements of 1.121 mm, 1.051 mm and 1.240 mm, respectively.

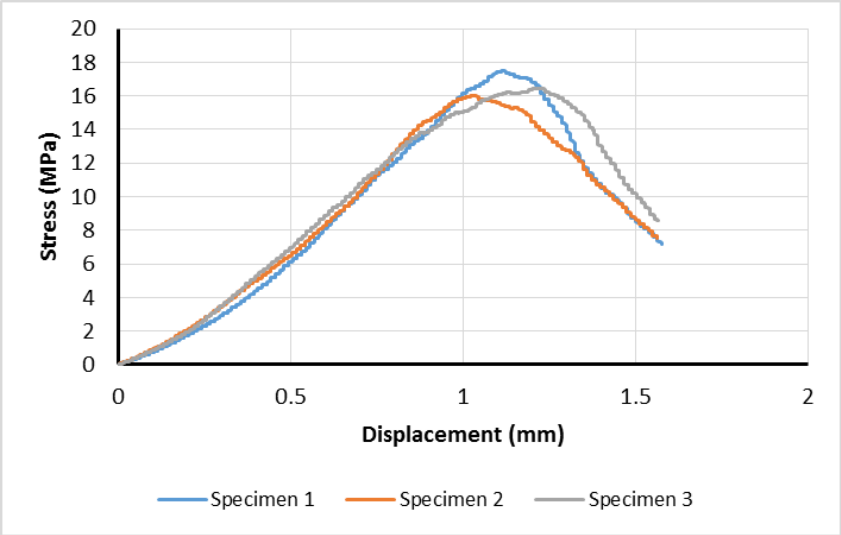

Figure 5.6: Stress-displacement behaviour of steel fibre-reinforced specimens

The relative stiffness of specimens determined through the linear slope of the elastic region from the above curves is outlined in Table 5.3. Specimen 1 of control and specimen 2 of polypropylene FRC are not included in the average stiffness calculation.

Table 5.3: Relative stiffness of specimens with varied fibre types (MPa/mm)

Fibre type	Specimen Stiffness (MPa/mm)			Average	Standard Deviation
	1	2	3		
Control	9.42 $R^2=0.999$	16.39 $R^2=0.9991$	18.00 $R^2=0.9993$	17.20	4.56
Forta Ferro	32.78 $R^2=0.9981$	19.19 $R^2=0.9986$	24.67 $R^2=0.9987$	25.55	6.48
Polypropylene	14.94 $R^2=0.9994$	20.90 $R^2=0.9973$	14.86 $R^2=0.9989$	14.90	3.46
ReoShore 45	41.77 $R^2=0.9932$	17.53 $R^2=0.9994$	19.40 $R^2=0.9992$	26.23	13.49
Steel	19.81 $R^2=0.9992$	20.68 $R^2=0.9954$	18.00 $R^2=0.9994$	19.50	1.37

Across the entire spectrum of results there is a close correlation to a linear fit ensuring an accurate approximation of concrete stiffness. It is noted that the average elasticity of specimens is highest for ReoShore 45 fibre-reinforced concrete due to the high stiffness of specimen 1. Forta Ferro and steel fibres also increased the stiffness of concrete while polypropylene fibres decreased concrete stiffness.

5.2.2.3 Proportional Limit

Analysis of the proportional limit will determine if fibres improve the service strength of oil contaminated concrete. As control specimen 1 and polypropylene specimen 2 are considered unreliable they are not included in the average proportional limit. The estimated proportional limits derived from the stress-displacement curves is outlined in Table 5.4:

Table 5.4: Proportional limit of specimens with varied fibre types (MPa)

Fibre Type	Specimen Proportional Limit (MPa)			Average	Standard Deviation
	1	2	3		
Control	8.60	10.63	10.12	10.38	1.06
Forta Ferro	12.71	10.27	10.91	11.30	1.27
Polypropylene	16.04	10.06	12.55	14.30	3.00
ReoShore 45	12.56	11.44	10.94	11.65	0.83
Steel	16.37	14.34	13.34	14.68	1.54

5.2.2.4 Failure Behaviour

Analysis of failure behaviour can serve as an initial indication of a specimen's ultimate strength. All specimens for control and ReoShore 45 fibre-reinforced concrete exhibited splitting failure from the top cap which travelled perpendicular to the load direction (Figure 5.7).

(a) (b)

Figure 5.7: Splitting failure of control (a) and ReoShore 45 fibre-reinforced (b) specimens

While Forta Ferro, steel and polypropylene fibre-reinforced concrete predominantly displayed shear failure (Figure 5.8):

Figure 5.8: Shear failure of polypropylene fibre-reinforced specimens

Moreover, steel fibre-reinforced specimens controlled cracking more effectively than other fibre types as crack widths and crumbling due to saturation by oil was decreased (Figure 5.9).

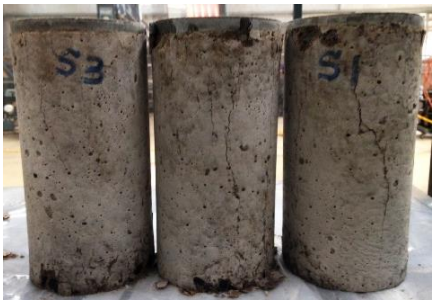

Figure 5.9: Decreased cracking of steel fibre-reinforced specimens

It is noted that failure behaviour may have been affected by the thickness of cement mortar capping. The mortar strength may have surpassed concrete strength which caused crushing at the top cap of concrete and splitting failure (Figure 5.10).

Figure 5.10: Cement mortar capping causing crushing

5.2.2.5 Failure Surface

The surfaces of failed specimens were inspected to analyse the orientation and dispersion of fibres within the matrix. Steel and ReoShore 45 fibre-reinforced specimens are shown in Figure 5.11. Referring to Figure 5.11 (a), steel fibres can be seen intersecting tensile cracking with good dispersion. While in Figure 5.11 (b), ReoShore 45 fibres are in a horizontal alignment also intersecting tensile cracking but show poor dispersion as noted by inspection.

(a) (b)

Figure 5.11: Steel (a) and ReoShore 45 (b) failure surfaces

From inspection, Forta Ferro and polypropylene fibres were well dispersed within concrete. However, due to the small nature of fibres pictures could not adequately show this.

5.2.3 Flexural Behaviour

The flexural behaviour results of the influence of fibres on oil-impacted concrete are outlined below in sections. Results will be discussed further is Section 5.3.3.

5.2.3.1 Failure Load

The flexural failure load of specimens is outlined in Table 5.5. The standard deviation of Forta Ferro fibre-reinforced concrete is larger due to the premature failure of specimen 3. Therefore, this specimen was considered an outlier and not included in the estimation of average flexural strength. Due to testing problems, specimen 1 of steel fibre-reinforced concrete could not be included in the flexural analysis.

Table 5.5: Flexural strength (MPa) of specimens with varied fibre types

Fibre Type	Specimen Strength (MPa)			Average	Standard Deviation
	1	2	3		
Control	5.93	6.83	6.71	6.49	0.49
Forta Ferro	5.92	4.89	2.46	5.41	1.78
Polypropylene	6.29	5.94	5.96	6.06	0.20
ReoShore 45	4.84	6.58	5.12	5.51	0.93
Steel	-	6.76	6.84	6.80	0.06

Fibres showed an insignificant influence on oil-impacted concrete flexural strength. The only fibres that improved concrete flexural strength was steel.

5.2.3.2 Load-displacement Behaviour

The load-displacement relationship of specimens under four-point flexural loading was plotted for a comparison of the fibre-matrix interaction. Overall, concrete

experienced sudden failure after peak load was reached which is evident in the load decrease at a constant displacement after ultimate load.

The load-displacement behaviour of control specimens is shown in Figure 5.12. Although specimens failed at comparable loads, the corresponding displacement at failure is disparate for all specimens. Specimen 1 experienced failure at a displacement of 1.32 mm, specimen 2 at 0.99 mm and specimen 3 at 0.70 mm.

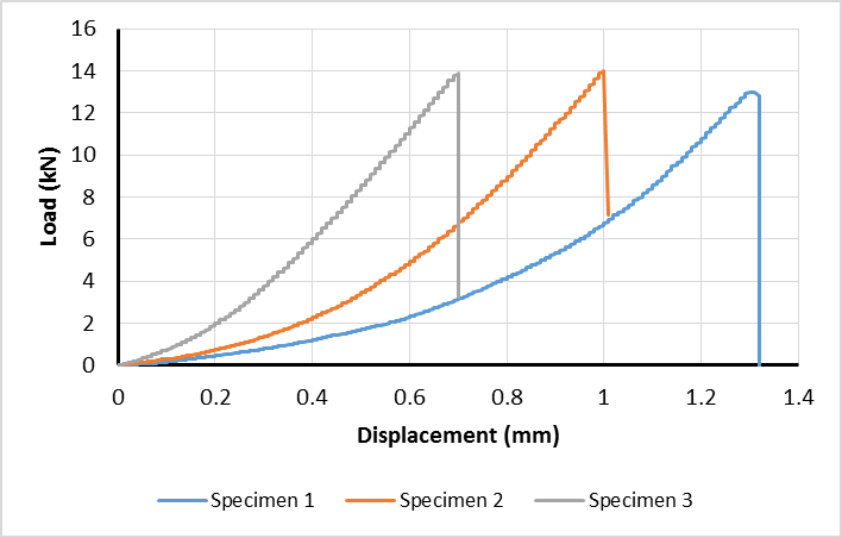

Figure 5.12: Load-displacement behaviour of control specimens

Similarly, Forta Ferro specimens exhibited differing displacements at failure loads (Figure 5.13). Specimen 3 is considered as an outlier due to premature failure, while specimen 1 experienced failure at a displacement of 0.64 mm and specimen 2 at 1.01 mm. The initial cracking of specimen 1 can be seen at a displacement of 0.35 mm, from here, displacement rate decreases until failure load due to fibres stabilising cracks.

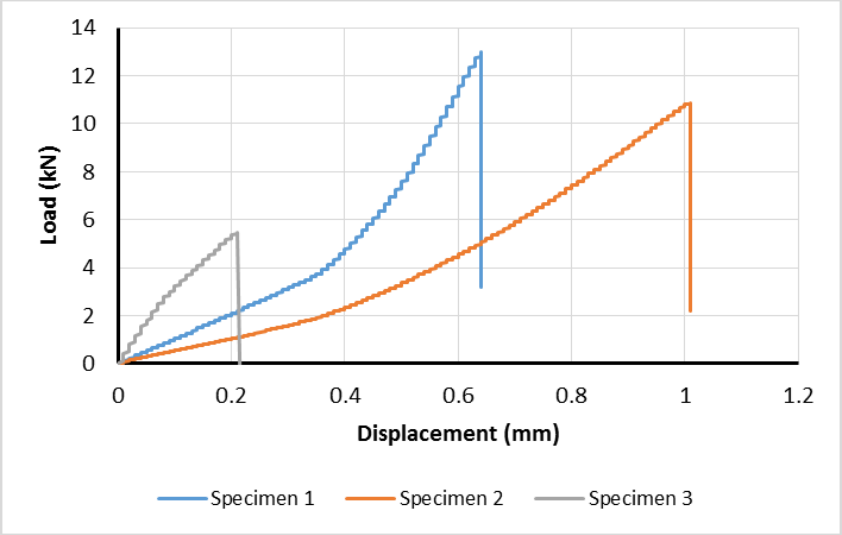

Figure 5.13: Load-displacement behaviour of Forta Ferro specimens

The load-displacement behaviour of polypropylene specimens can be seen in Figure 5.14. These specimens exhibited the most consistent load-displacement behaviour among all fibres considered with failure displacements of 0.76 mm, 0.84 mm and 0.78 mm, respectively. There is minimal indication of crack stabilisation by polypropylene fibres.

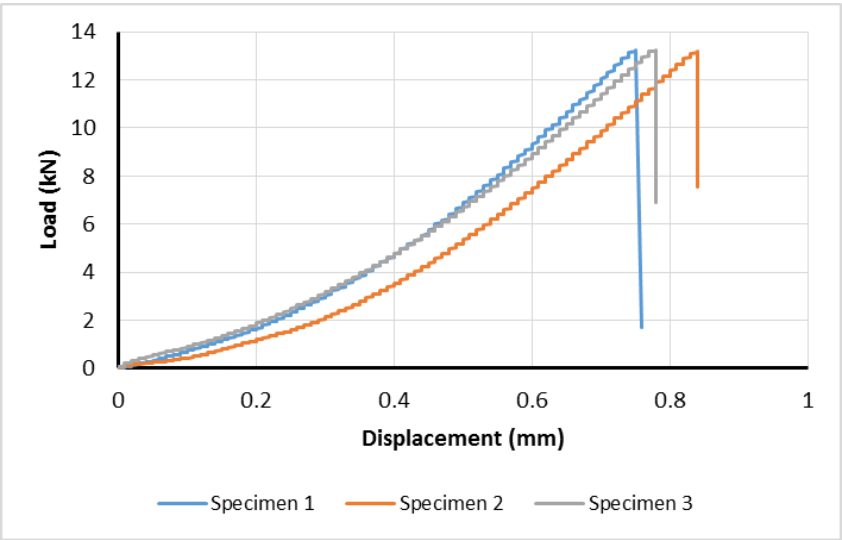

Figure 5.14: Load-displacement behaviour of polypropylene specimens

The load-displacement relationship of concrete containing ReoShore 45 fibres can be seen in Figure 5.15. Specimens 1 and 3 showed a similar linear load-displacement

behaviour, both having a corresponding displacement of 0.46 mm at ultimate load. Specimen 2 exhibited increased ductility experiencing failure at a displacement of 1.27 mm.

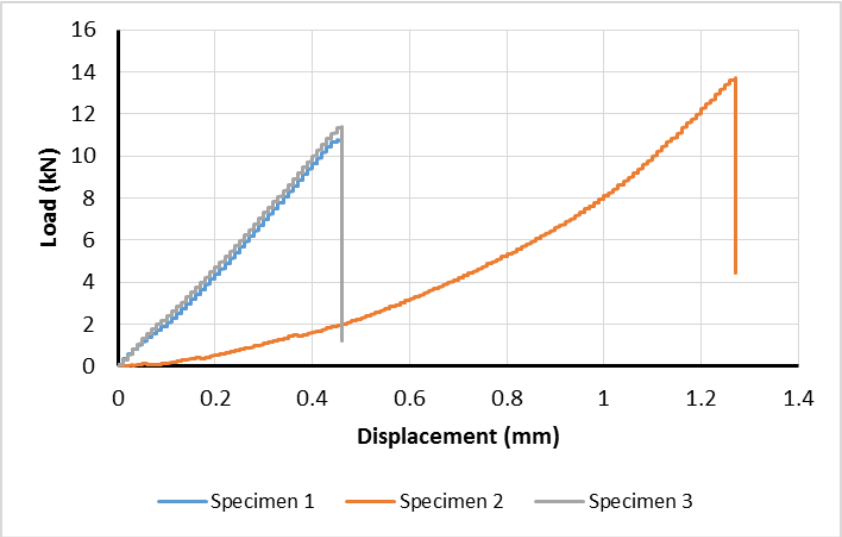

Figure 5.15: Load-displacement behaviour of ReoShore 45 specimens

The load-displacement curves for steel fibre-reinforced specimens is shown in Figure 5.16. Due to data machine problems the data collected showed the same behaviour. Specimens experience failure at a common displacement of 1.61 mm.

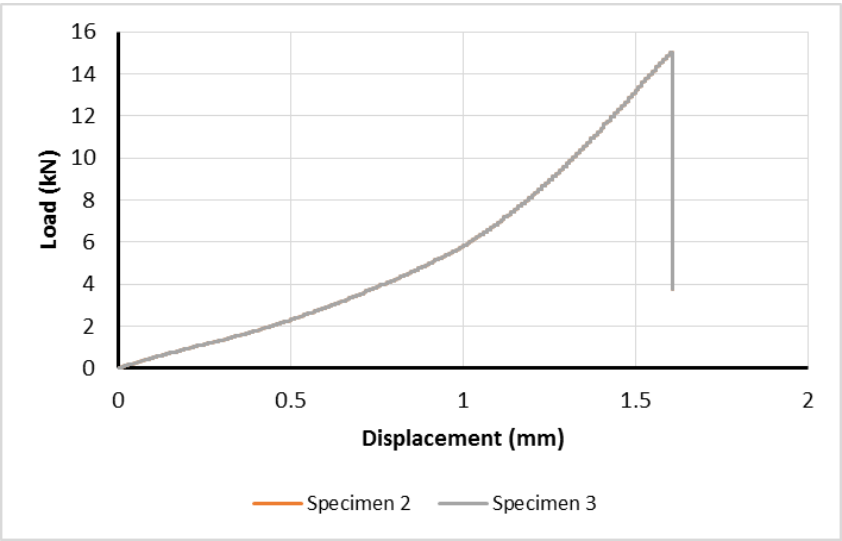

Figure 5.16: Load-displacement behaviour of steel specimens

5.2.3.3 Failure Behaviour

When specimens are loaded in bending setup, maximum tensile stress occurs at the bottom centre where the first crack develops. In the case of specimens without fibre reinforcement, cracks develop at the centre and suddenly collapse at failure (Figure 5.17).

Figure 5.17: Control flexural failure behaviour

Whereas, FRC exhibited increased ductility. Specimens with fibre reinforcement did not collapse suddenly and exhibited reduced crack widths and crack propagation which at times originated off-centre (Figure 5.18). It can be noted steel fibre-reinforced concrete experienced the least propagated tensile cracking when compared to specimens containing other fibres.

Forta Ferro

Polypropylene

ReoShore 45

Steel

Figure 5.18: FRC flexural failure behaviour

Crack bridging is evident due to decreased crack width for all FRC. Crack bridging after failure of Forta Ferro fibre-reinforced specimen 2 is evident in Figure 5.19:

Figure 5.19: Crack bringing of Forta Ferro fibre

5.2.3.4 Failure Surface

Analysis of the failure surfaces of flexural specimens is shown in Figure 5.20. Polypropylene fibres showed to have the best dispersion and fibre orientation was dominantly perpendicular to the failure plain enabling crack bridging. Forta Ferro also exhibited good dispersion through their separation during casting. ReoShore 45 showed poor dispersion, having 5 fibres within the failure surface shown with only 2 having an orientation perpendicular to the failure plane. Steel fibres dispersed well within the matrix and tended to have an orientation perpendicular to the failure surface ensuring crack suppression.

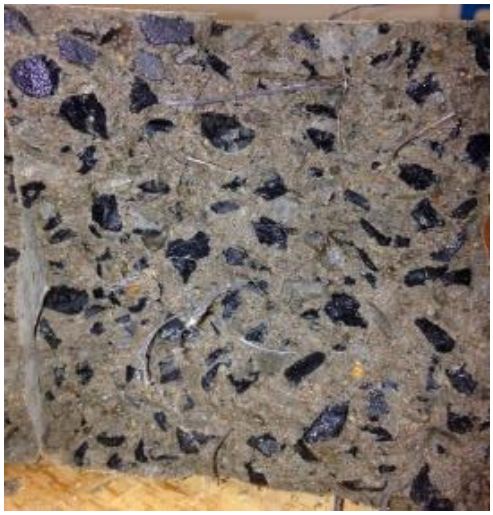

Forta Ferro

Polypropylene

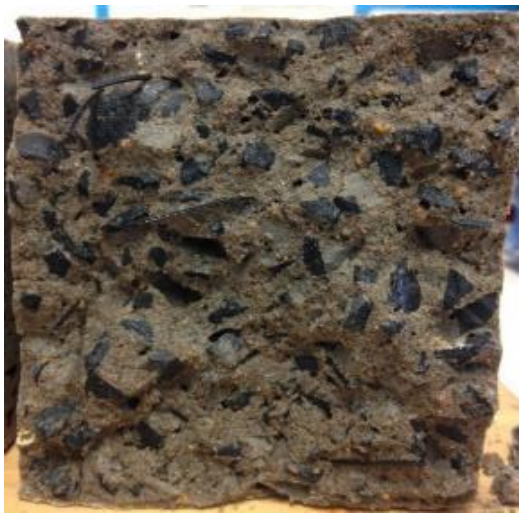

ReoShore 45

Steel

Figure 5.20: Failure surface analysis of flexural specimens

5.2.4 Microscopic Analysis

A microscopic analysis was undertaken to analyse fibre-concrete bond which could draw conclusions to specimen compressive and flexural behaviour. Individual fibres were removed after testing to allow microscopic inspection of the fibre-matrix bond.

Forta Ferro's bond with concrete was assisted by its bundle twisted nature. After mixing, the fibre monofilament breaks up into separate filaments and the fibrillated structure of filaments intertwined with concrete. This interlock with concrete particles can be seen in Figure 5.21 (b). Figure 5.21 (a) shows the filaments external bond with concrete where air voids can be seen at the fibre-concrete interface.

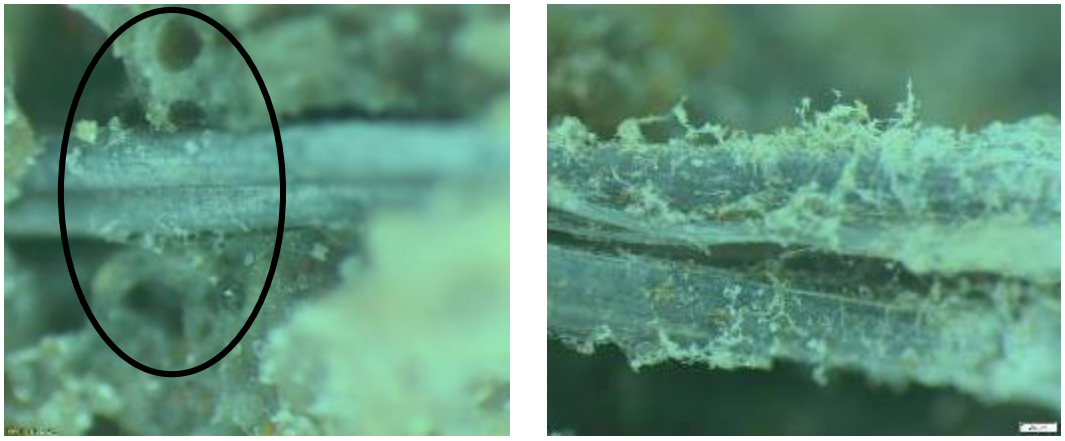

(a) (b)

Figure 5.21: Forta Ferro-matrix interaction microscopic images

Polypropylene fibres were the shortest in length out of the fibres considered. However, the collated fibrillated form of the fibre offered good bonding power with concrete. From Figure 5.22, a continuous bond around the individual fibre can be seen enabling fibre-matrix interaction.

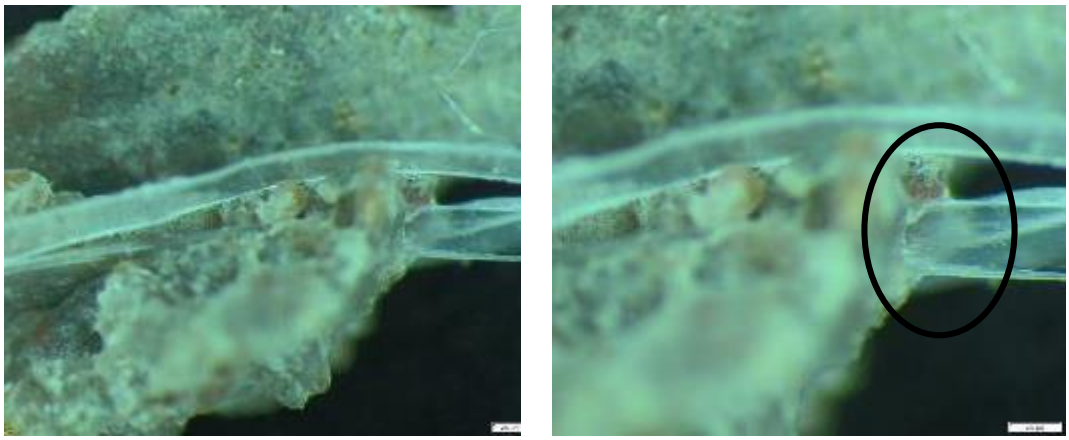

(a) (b)

Figure 5.22: Polypropylene-matrix interaction microscope images

Being a monofilament, ReoShore 45 fibres depend on its tread surface design as an anchorage to enhance its bond with concrete. Figure 5.23 shows voids surrounding the fibre-matrix interface and in Figure 5.23 (a) oil saturation can be seen along the top of the fibre which may have affected its anchorage with concrete.

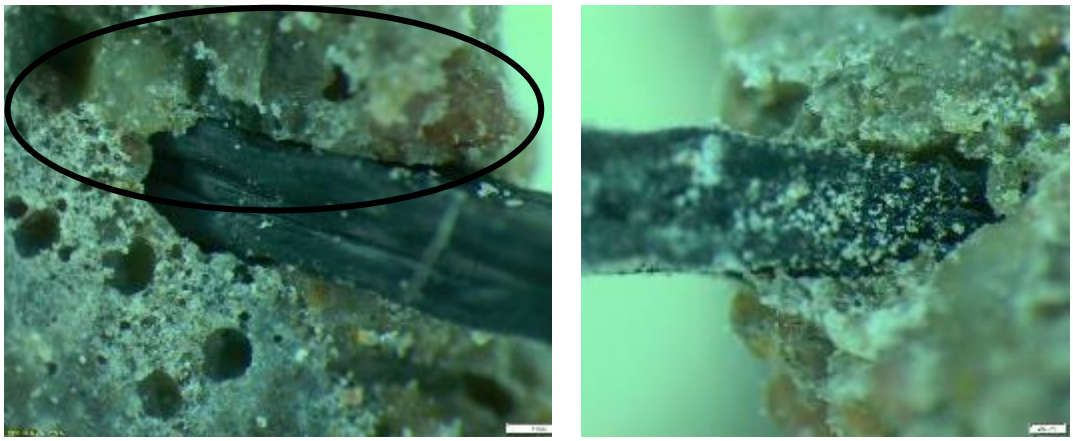

(a) (b)

Figure 5.23: ReoShore 45-matrix interaction microscope images

Steel fibres showed to have a good bond with concrete as indicated by Figure 5.24. Cement mortar can be seen fixed to the surface of the steel fibre in Figure 5.24 (a), while Figure 5.24 (b) displays the formation of mortar around the fibre without any discontinuities weakening the interface.

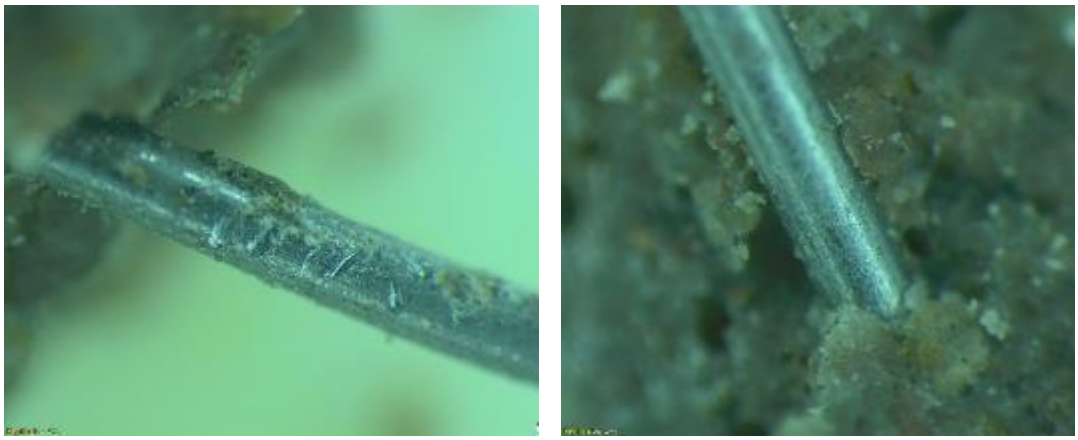

(a) (b)

Figure 5.24: Steel-matrix interaction microscope images

5.3 Discussion

The discussion is outlined in sections for clarity, making reference to the findings outlined in the previous section.

5.3.1 Effect of Fibres on Density

The effect of fibres on oil contaminated concrete physical properties was analysed in Section 5.2.1. As illustrated in Figure 5.1, fibres had no visual effect on concrete as the surface porosity and saturation remained unchanged. Moreover, the density of compressive specimens deviated minimally with fibre type. Table 5.1 is graphically represented in Figure 5.25 showing the average density of specimens with varied fibre types. Steel and polypropylene fibres showed an average density decrease of 0.10% and 0.11%, respectively, while ReoShore 45 fibre-reinforced concrete remained relatively unchanged with a 0.01% increase in density compared to the control

average. Forta Ferro increased concrete density by 0.27% on average compared to the non-fibrous average density.

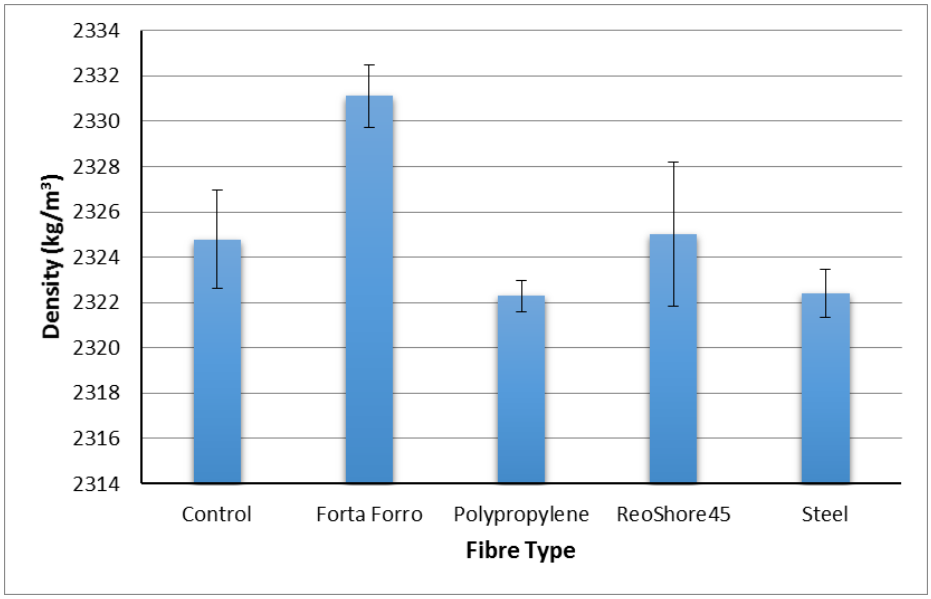

Figure 5.25: Average density of specimens with varied fibre types (kg/m^3)

The average density of fibre-reinforced specimens did not differ from the non-fibrous average density by more than 0.27%. Therefore, it can be concluded that fibres do not have an effect on concrete density and the deviation is due to natural inconsistencies in concrete. This could be due to the relatively low amount of fibres that were added to concrete specimens.

5.3.2 Effect of Fibres on Compressive Behaviour

5.3.2.1 Effect on Compressive Strength

The findings from the compressive failure load results are graphically summarised in Figure 5.26. The average strength of non-fibrous specimens is 16.30 MPa. Forta Ferro, polypropylene and steel fibre-reinforced concrete on average increased concrete strength by 8%, 9% and 11%, respectively, when compared to the control average. While ReoShore 45 decreased concrete strength by 3% on average.

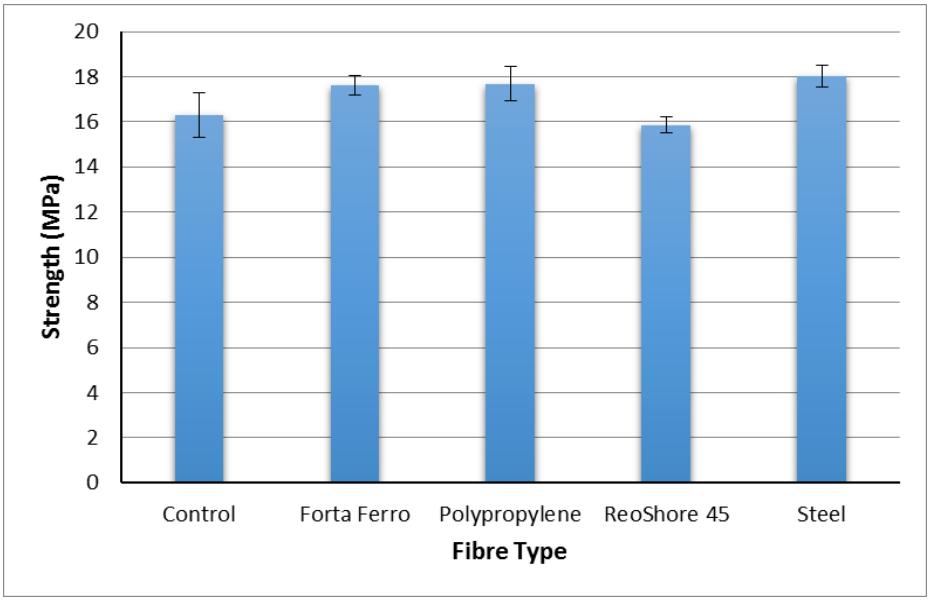

Figure 5.26: Average compressive strength of specimens with varied fibre types (MPa)

In agreement with reported literature by Døssland (2008), Rai & Joshi (2014) and Ezeldin & Balaguru (1992) in Section 2.5.7, results show that the presence of fibres did not significantly affect the compressive strength of concrete. It is suspected that steel fibres most improved concrete strength due to their higher tensile strength and hooked geometry which enhanced their bond with concrete (refer to Section 3.2.4). The ReoShore 45 fibre tread surface design did little to maximise energy absorption in compression. From microscopic analysis, it is suspected that coating by oil hindered fibre anchorage with concrete due to the small prominence of treads from the fibre surface (Figure 5.23).

Furthermore, from analysis of failure behaviour, it is noted that non-fibrous and ReoShore 45 specimens, which yielded the lowest compressive strength, exhibited splitting failure; while steel, polypropylene and Forta Ferro fibre-reinforced specimens exhibited shear failure (Section 5.2.2.4). From investigations by Markeset & Hillerborg (1995) (Section 2.5.7), the resulting shear failure is an indication that fibres

efficiently controlled axial splitting and failure occurred as a result of the interaction between axial cracks.

Moreover, analysis of the compressive failure surfaces showed that steel, polypropylene and Forta Ferro fibres had good dispersion within concrete. From Figure 5.11, steel and ReoShore 45 fibres can be seen intersecting tensile cracks. From literature reported by Löfgren (2005) in Section 2.5.7, the intersection by fibres of tensile cracks can reduce lateral deformation of concrete under compressive loading, however, has minimal effect on concrete compressive strength as seen in results.

5.3.2.2 Effect on Stress-Displacement Behaviour

The stress-displacement relationship of specimens is an important aspect of comparison, particularly for FRC. A comparison of the representative stress-displacement curve for each fibre type is shown in Figure 5.27. An improvement in the descending or softening branch of FRC compared to plain concrete is noticed. ReoShore 45, although not improving concrete strength, significantly extended the softening branch of post-peak concrete behaviour. Steel and Forta Ferro fibres also experienced a more displacement-softening post-peak behaviour when compared to plain concrete.

In agreement with findings from Døssland (2008), Ezeldin & Balaguru (1992), Lee, Oh & Cho (2015) and Kooiman 2000 (Section 2.5.7), the presence of fibres modified the failure mode of concrete from a brittle to a less brittle failure mode. The concrete behaviour seen from results follows a similar trend presented by Löfgren (2005) in Figure 2.16, where fibres had no significant effect on concrete pre-peak behaviour, but

extended the post-peak behaviour by resisting lateral expansion through arresting the failure plane (axial splitting) of concrete.

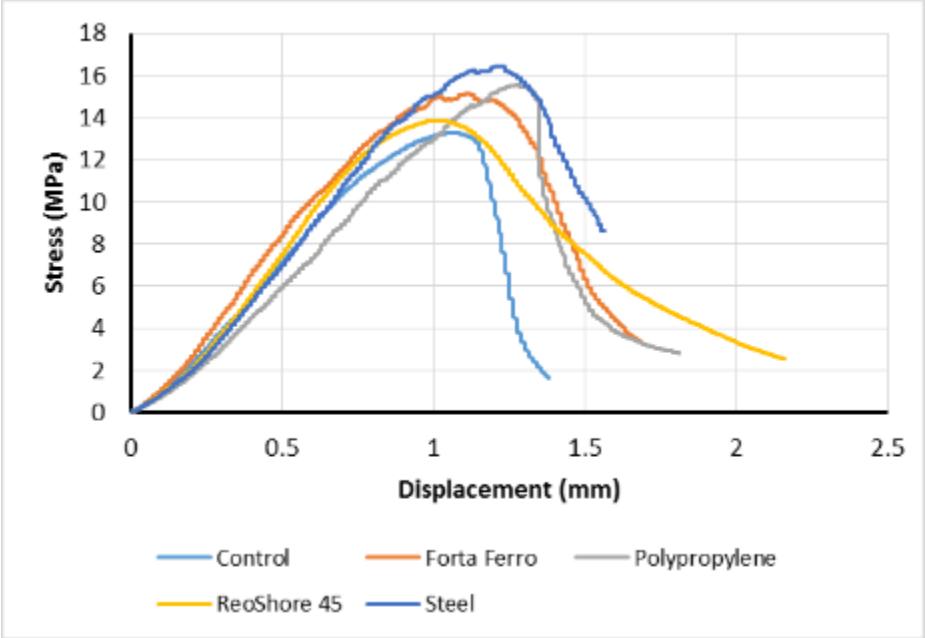

Figure 5.27: Stress-displacement relationship of compressive specimens with varied fibre types

Additionally, Forta Ferro, polypropylene and steel fibres increased the corresponding displacement to ultimate stress of concrete. This agrees with literature reported by Maccaferri (2015) in Section 2.4.2, which found that the presence of fibres having adequate tensile strength and being homogeneously distributed within the concrete built a micro-scaffolding that controls crack formation due to shrinkage and leads to increased concrete ductility. Fibres increased the ductility of concrete under compression through crack suppression increasing the energy required for crack propagation.

5.3.2.3 Effect on Relative Stiffness

The relative elasticity of specimens outlined in Table 5.3 is graphically presented in Figure 5.28. Compared to the control average stiffness, Forta Ferro increased concrete

stiffness by 48.6%, ReoShore 45 by 52.6% and steel by 13.4%. While polypropylene decreased concrete stiffness by 13.3% of the control average.

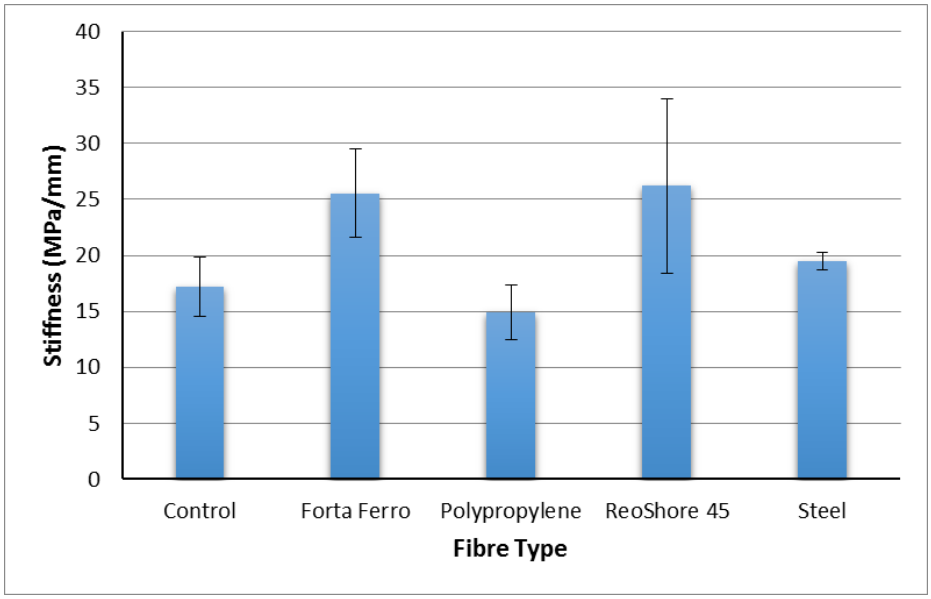

Figure 5.28: Average stiffness of specimens with varied fibre types (MPa/mm)

In Section 2.5.5, Beaudoin (1190) stated that high fibre modulus of elasticity would have direct influences on the matrix elasticity due to the stress transfer from the matrix to the fibre. However, results show that concrete elasticity was not significantly altered which is assumed to be due to the relatively low fibre dosage applied. The variation in results is assumed to be due to the expected deviation among different concrete mixes.

5.3.2.4 Effect on Proportional Limit

While the ultimate compressive strength of concrete is an important factor, analysis of the proportional strength can determine if fibres increase the design strength of concrete in its applications. Figure 5.29 outlines the average proportional limit of FRC derived from the stress-displacement plots (refer to Table 5.4).

Overall, fibres increased the proportional limit of concrete. Forta Ferro fibre-reinforced concrete yielded the lowest proportional limit out of the fibres considered,

having an 8.9% increase to the control average. ReoShore 45 reinforced concrete, although having a negative effect on ultimate strength, increased the proportional limit of concrete by an average of 12.3%. Steel and polypropylene fibres most improved concrete proportional strength, having a 41.5% and 37.8% increase, respectively, to plain concrete's average. The 14.68 MPa proportional strength attained with the addition of steel fibres approaches the average proportional limit of 15.42 MPa for 6% contaminated concrete found in Chapter 5 (refer to Figure 4.17).

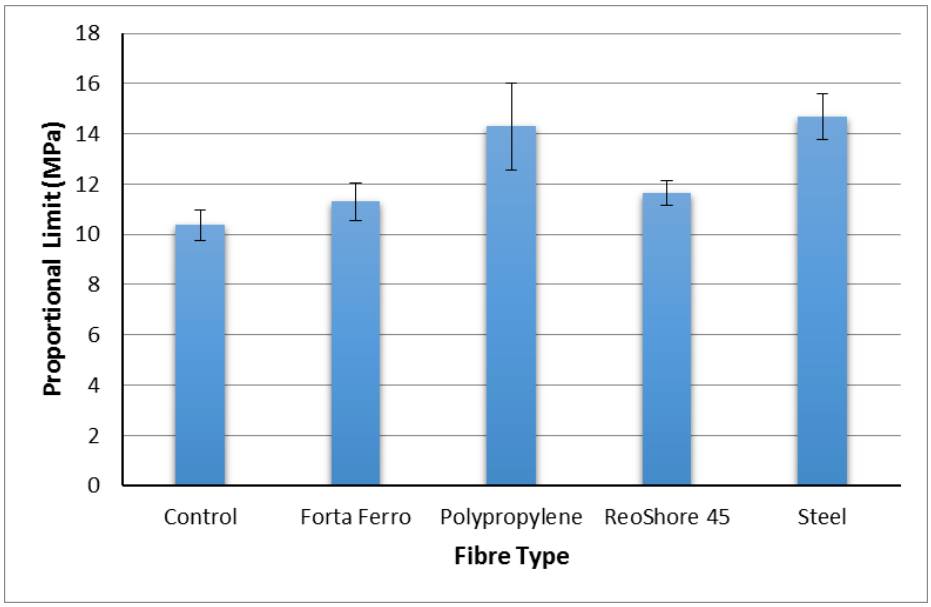

Figure 5.29: Average proportional limit of specimens with varied fibre types (MPa)

Although concrete elasticity is unaltered with the inclusion of fibres, the increase in proportional strength is relative to the increase in FRC ductility in the elastic region.

5.3.3 Effect of Fibres on Flexural Behaviour

5.3.3.1 Effect on Flexural Strength

The ultimate flexural strength results of FRC is summarised in Figure 5.30. The average flexural strength of non-fibrous concrete is 6.49 MPa (refer to Table 5.5). Overall, fibres showed to have a negative effect on oil-impacted concrete flexural

strength. Forta Ferro, ReoShore 45 and polypropylene fibre-reinforcement on average decreased concrete strength by 16.7%, 15% and 6.6%, respectively, when compared to the non-fibrous average. While steel fibre-reinforcement slightly increased concrete flexural strength by 4.8% on average.

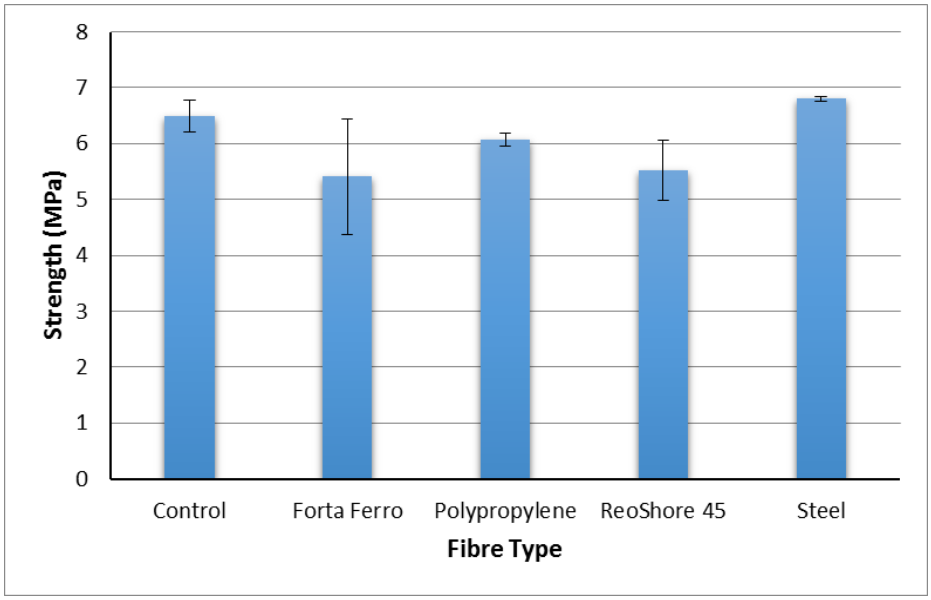

Figure 5.30: Average flexural strength of specimens with varied fibre dosage (MPa)

Results agree with the study by Alhozaimy, Soroushian & Mirza (1996) (Section 5.5.8) where the flexural strength of concrete was not affected by polypropylene fibres at dosages below 0.3% by concrete volume. Forta Ferro, polypropylene and ReoShore 45 fibres did not have the ability to significantly increase concrete flexural strength due to their comparatively low tensile strength to steel fibres (refer to Section 3.2.4) in conjunction with the low fibre dosage applied (0.1% by volume).

However, studies by Wang & Wang (2013) and Yazıcı, İnan & Takak (2007) (Section 5.5.8) found that steel fibres significantly improve concrete flexural strength. However, the minimum fibre dosage considered in these studies is 0.5% by volume of concrete, which is the maximum dosage analysed in this study, which may be why only a minimal improvement was seen.

From microscopic analysis, polypropylene and steel fibres showed to have a good bond with concrete which was evident from the continuous fibre-matrix interface (Figure 5.22 & 5.24). While microscopic analysis of Forta Ferro and ReoShore 45 fibres exposed air voids surrounding the fibre-matrix interface (Figure 5.21 & 5.23). Moreover, oil saturation could be seen surrounding the ReoShore 45 fibre.

It is suspected that excess oil coated fibres like it did aggregate in Programme 1 (Chapter 4), which in turn prevented fibre-matrix interaction. If a sufficient bond was achieved with fibres, it is assumed that the saturated state of oil-impacted concrete would cause a bond-slip effect between the matrix and fibres under tensile stresses. Crack bridging is evident from the decreased crack widths and crack propagation of FRC after failure in Figure 5.18. However, because its efficiency was hindered due to matrix saturation, concrete flexural strength was not improved significantly.

5.3.3.2 Effect on Load-Displacement Behaviour

The load-displacement behaviour of concrete under flexural loading is an indication of its ductility. Figure 5.31 depicts the typical load-displacement relationship of each fibre type. It is evident that the fibres considered, excluding ReoShore 45, increase the ductility of concrete under flexural loading. Polypropylene, Forta Ferro and steel fibre-reinforced concrete experienced increased displacements at failure loads of 0.78 mm, 1.01 mm and 1.61 mm, respectively, through the crack bridging effects of fibres.

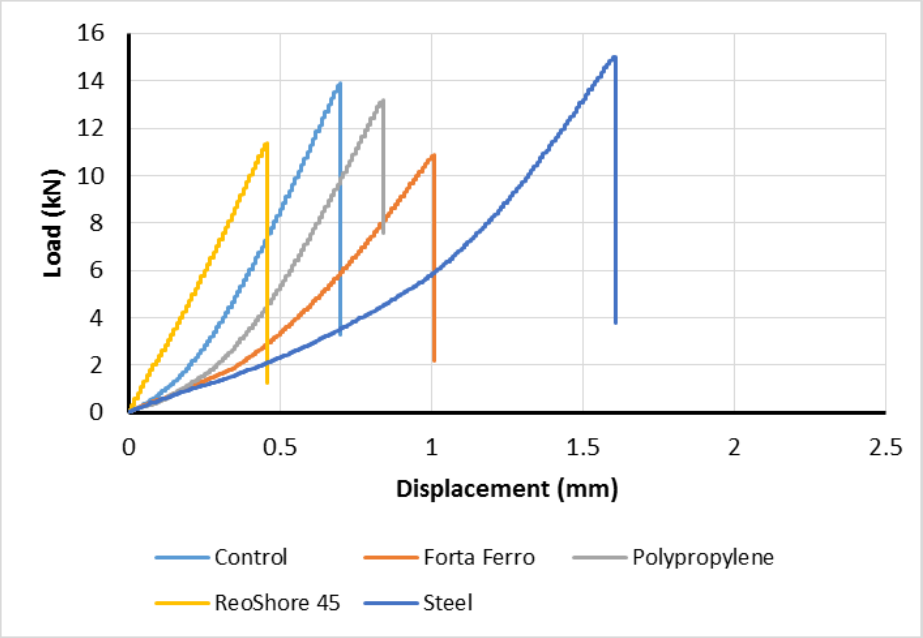

Figure 5.31: Load-displacement relationship of flexural specimens with varied fibre types

Literature by Kooiman (2000) in Section 2.5.8 indicated that fibres influence on the softening response of concrete through fibre bridging, which causes a redistribution of stresses. After cracking initiates, the redistribution of stress imposes a new state of equilibrium across the cross-section. Referring to Figure 5.17, non-fibrous specimens failed suddenly at the centre of the specimen where tensile stress is critical. Whereas, fibre-reinforced specimens did not fail abruptly, crack widths were reduced and at times originated off-centre due to the increased tensile strength of FRC (Figure 5.18).

As steel and ReoShore 45 fibres are monofilaments, they rely on their geometry and tensile strength to enhance concrete bond and its mechanical properties, while polypropylene and Forta Ferro fibres, being fibrillated, rely on their dispersion ability and geometry. With the tread of ReoShore 45 compromised due to saturation by oil (refer to Figure 5.23), its poor bond ability offers minimal ductility to concrete. Moreover, from analysis of the failure surface it was found ReoShore 45 fibres had poor dispersion along the flexural failure plane (refer to Figure 5.20).

Furthermore, analysis of FRC failure surfaces showed that polypropylene and Forta Ferro fibres had good dispersion along the failure plain, while steel fibres were also well dispersed in comparison to ReoShore 45 fibres (refer to Figure 5.20). The high tensile strength and hooked geometry of steel fibres increased concrete ductility, while polypropylene and Forta Ferro fibres' uniform dispersion along the failure surface allowed efficient load transfer under tensile stress.

5.4 Summary and Conclusion

This chapter has provided insight into the properties of fibre-reinforced concrete with oil contaminated sand.

It has been noted that the introduction of fibres does not affect the physical properties of oil-impacted concrete, nor its density, due to the relatively low fibre dosage volume implemented. As a result, minimal change in concrete porosity or saturation by oil with the introduction of fibres was assumed.

The effect of fibres on the compressive behaviour of oil-impacted concrete was analysed. Results showed that fibres had no significant effect on concrete 28 day compressive strength. Forta Ferro, polypropylene and steel fibres improved concrete compressive strength, with steel fibre-reinforcement resulting in the optimal improvement of 11% compared to the control average. While ReoShore 45 decreased concrete strength by 3% on average.

Analysis of the stress-displacement behaviour of compressive specimens showed an improvement in the softening branch of FRC compared to plain concrete. ReoShore 45 most significantly extended the softening branch of post-peak concrete behaviour.

While Forta Ferro, polypropylene and steel fibres enhanced concrete ductility as noted by the increased displacement corresponding ultimate stress.

Additionally, fibres increased the proportional limit of oil-impacted concrete due to the micro-scaffolding of FRC which led to increased concrete ductility in the elastic region, without inducing voids within the matrix. However, fibres showed to have an insignificant effect on the relative stiffness of concrete. Although ReoShore 45 had no effect on concrete ultimate strength, an 8.9% increase in proportional limit was seen due to enhanced ductility. Steel fibres attained the highest proportional strength increase of 41.5% to plain concrete's average. Additionally, steel fibre-reinforced concrete at 10% contamination approached the average proportional limit determined for 6% contaminated concrete found in Chapter 5.

Overall, the addition of fibres had a negative effect on oil-impacted concrete flexural strength. The only fibre that enhanced concrete flexural strength was steel, with a 4.8% increase compared to the control average. It is believed that the saturation and porosity of oil contaminated concrete caused bond-slippage between fibres and the concrete matrix which effected its ability to hold fibres under tensile stress. This in turn hindered the crack stabilisation features of fibres which usually increase concrete flexural strength.

From analysis of the flexural load-displacement behaviour it is evident that all fibres, excluding ReoShore 45, increase concrete ductility through exhibiting increased displacements at failure loads. Moreover, from failure analysis, fibre-reinforced specimens did not fail abruptly, crack widths were reduced and at times originated off-centre due to the redistribution of tensile stresses. The high tensile strength and hooked geometry of steel fibres most improved concrete ductility out of the fibres considered.

While polypropylene and Forta Ferro fibres' uniform dispersion along the failure surface optimised fibre bridging under tensile stress. The tread of ReoShore 45 fibres offered minimal anchorage with concrete due to oil saturation and in turn the poor bond ability offered minimal ductility (or strength) to concrete under flexural loading.

Although fibres in low dosage volumes were found to have minimal effect on oil-impacted concrete mechanical properties, in both compressive and flexural loading steel fibre-reinforced concrete was the best performing. Therefore, for the purpose of the next stage, steel fibre-reinforced concrete will be investigated at varied dosage volume rates to determine the optimum. The results of this study is presented next section.

Chapter 6

Optimum Fibre Dosage for Concrete with Oil Contaminated Sand

6.1 Introduction

The investigation into the properties of oil contaminated concrete with short fibres in Chapter 5 concluded that steel fibres are the best performing. Using the recommended dosage for steel fibres outlined in Section 2.4.5.1 as 15-30 kg/m^3 by concrete volume, the optimum steel fibre dosage will be investigated in oil-impacted concrete. The fibre dosages investigated are; 0.00115%, 0.2%, 0.3%, 0.4% and 0.5% (0.9 - 39.65 kg/m^3) by concrete volume.

As outlined in Section 2.5.5, the load bearing capacity of fibre-reinforced concrete (FRC) is dependent on the volume dosage rate applied to the concrete matrix. The steel fibre-reinforced concrete (SFRC) are tested under compressive and flexural loading following the procedures outlined in Sections 3.7 and 3.8, respectively. The testing program is further outlined in Section 3.3.4. The purpose of this study is to determine the fibre volume dosage which most improves the mechanical properties of oil contaminated concrete.

6.2 Results and Observations

6.2.1 Physical Properties

The physical properties of SFRC at varied dosages is visually unaffected. Figure 6.1 shows the compressive cylinder specimens after curing. As fibre dosage increases, there is no noticeable increase in surface porosity.

Figure 6.1: Compressive specimens at varied dosages (0.5% - 0.00115% fibre dosage left to right)

The density of specimens was estimated through their weight and volume after 28 days of curing. The results are outlined in Table 6.1. Non-fibrous and 0.1% fibre dosage densities from Chapter 5 are also shown in the table for comparison.

Table 6.1: Density of compressive specimens at varied dosages (kg/m^3)

Fibre Dosage (% by Volume)	**Specimen Density (kg/m^3)**			**Average**	**Standard Deviation**
	1	**2**	**3**		
0	2322.74	2322.48	2329.11	2324.78	3.75
0.0015	2320.5	2307.7	2314.1	2314.1	6.37
0.1	2324.4	2320.8	2322.0	2322.4	1.84
0.2	2333.2	2336.4	2339.6	2336.4	3.18
0.3	2339.6	2342.8	2323.7	2335.3	10.23
0.4	2336.4	2323.7	2336.4	2332.2	7.35
0.5	2339.6	2330.0	2336.4	2335.3	4.86

From Table 6.1, the densities attained from specimens containing fibre dosages of 0% and 0.1% are higher due to the thicker cement capping of specimens in Programme 2. It can be noted that density slightly increases with increased steel fibre dosage.

6.2.2 Workability

The slump test was undertaken on each fibre dosage batch to compare the effect of fibre dosage on concrete workability is outlined in Section 3.6. The slump of each fibre dosage is outlined in Table 6.2:

Table 6.2: Slump of concrete with varied fibre dosages (mm)

Fibre Dosage (% by Volume)	Slump (mm)
0.00115	28
0.2	22
0.3	21
0.4	19
0.5	15

From Table 6.2, it can be noted that concrete slump decreases with the increase of steel fibre volume.

6.2.3 Compressive Behaviour

The compressive behaviour results of the influence of steel fibre dosage on oil-impacted concrete are outlined below in sections. Results will be discussed further in Section 6.3.3.

6.2.3.1 Failure Load

The ultimate recorded compressive stress of specimens is outlined in Table 6.3. The deviation in strength of specimens with the same fibre dosage is minor, with 0.00115% specimens having the largest deviation due to the high strength of specimen 1, which also increased its average strength. Like in Chapter 5 results, specimen 1 of control was considered an outlier and not included in the average strength calculation.

Table 6.3: Compressive strength (MPa) of specimens with varied fibre dosages

Fibre Dosage (% by Volume)	**Specimen Strength (MPa)**			**Average**	**Standard Deviation**
	1	**2**	**3**		
0	13.39	16.30	16.29	16.30	1.68
0.00115	18.93	15.21	15.84	16.66	1.99
0.1	19.01	17.64	17.49	18.05	0.84
0.2	15.90	14.28	17.58	15.92	1.65
0.3	15.31	16.36	15.92	15.87	0.53
0.4	15.39	15.62	17.44	16.15	1.12
0.5	14.06	17.03	16.77	15.95	1.64

Fibre dosage showed to have minimal effect on oil-impacted concrete compressive strength. The highest average strength was seen at a steel fibre dosage of 0.1%.

6.2.3.2 Stress-Displacement Behaviour

The stress-displacement relationship of specimens was analysed to compare influence of fibre dosage on concrete compressive behaviour. Overall, fibres improved concrete post-peak softening response and also increased specimen displacement at maximum stress.

The stress-displacement curves for specimens containing a steel fibre dosage of 0.00115% are shown in Figure 6.2. All specimens displayed comparable elastic and post-peak displacement-softening behaviour. Moreover, these specimens exhibited the most consistent stress-displacement behaviour among all fibre dosages considered. Specimen 1 reached ultimate stress at a displacement of 1.098 mm while specimens 2 and 3 had a slightly lower displacement of 1.061 mm at ultimate stress.

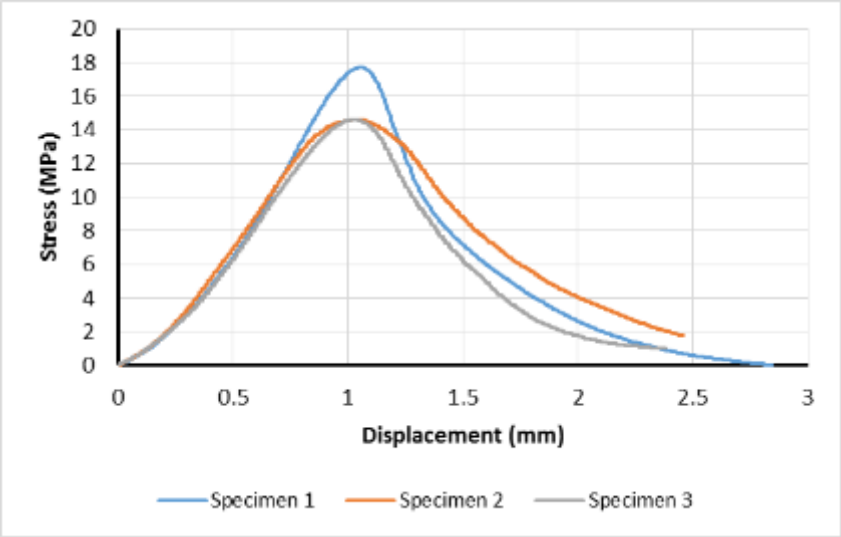

Figure 6.2: Stress-displacement behaviour of 0.00115% SFRC specimens

The deformation of concrete containing 0.2% of steel fibres under compressive loading is shown in Figure 6.3. Specimens 2 and 3 displayed similar elastic behaviour, indicated from the initial linear region of the stress-displacement curves, while specimen 1 experienced increased displacement at lower loads. Specimen 2, unlike

the others, exhibited brittle post-peak behaviour. The specimen's displacement at maximum stress is 1.820 mm, 1.086 mm and 0.860 mm, respectively.

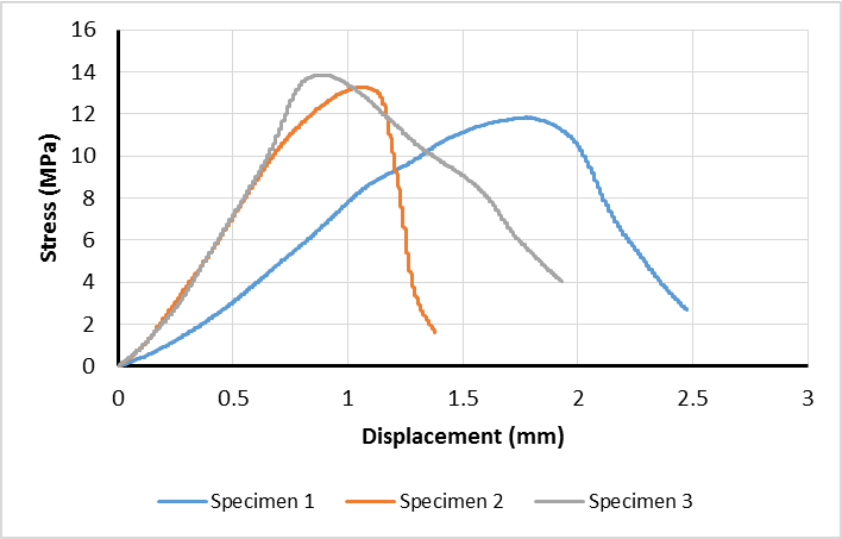

Figure 6.3: Stress-displacement behaviour of 0.2% SFRC specimens

The stress-displacement behaviour of specimens containing 0.3% of fibres can be seen in Figure 6.4. The elasticity of specimens 1 and 2 is comparable, while specimen 3 showed increased resistance to displacement before all exhibiting a displacement-softening post-peak behaviour. The displacement of specimens at ultimate stress was 1.084 mm, 1.310 mm and 0.905 mm, respectively.

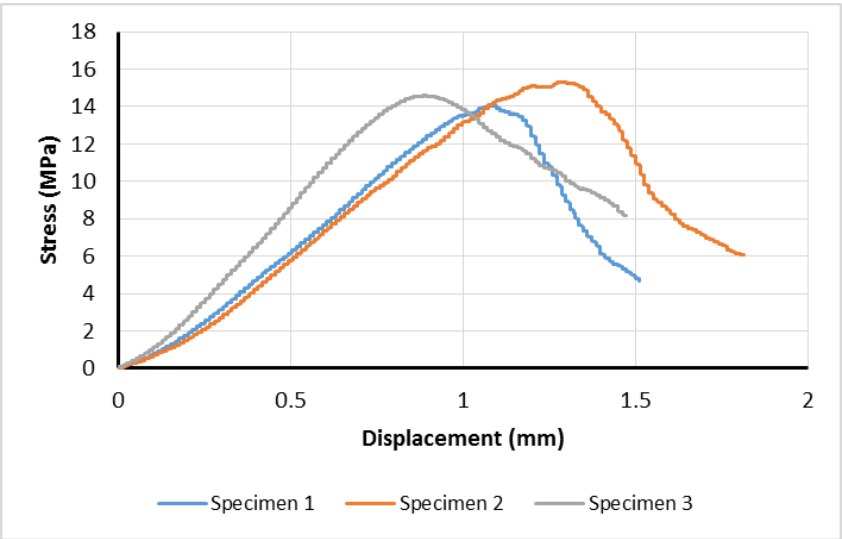

Figure 6.4: Stress-displacement behaviour of 0.3% SFRC specimens

Specimens with a 0.4% steel fibre dosage showed comparable stress-displacement behaviour, with all specimens exhibiting a ductile post-peak behaviour (Figure 6.5). At maximum stress, specimen displacement is 1.096 mm, 1.197 mm and 1.185 mm, respectively.

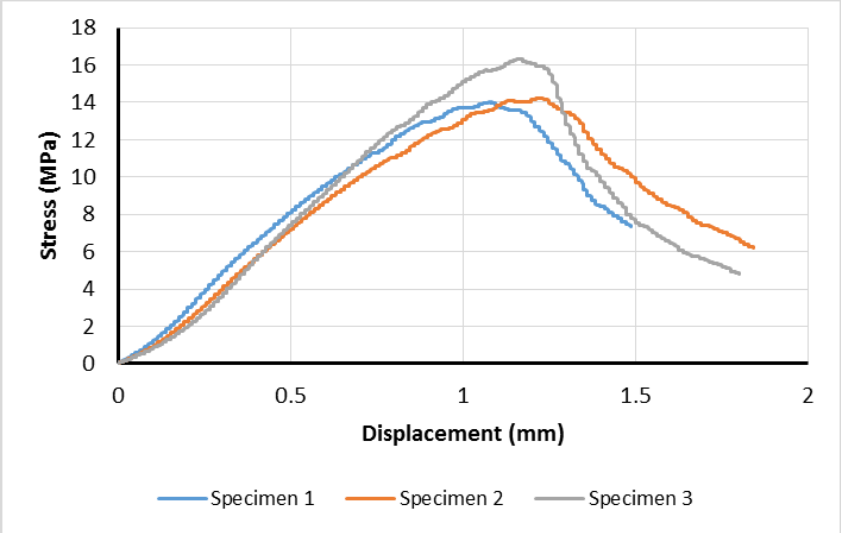

Figure 6.5: Stress-displacement behaviour of 0.4% SFRC specimens

The specimens containing the maximum dosage of 0.5% by concrete volume displayed similar elastic deformation (Figure 6.6). Additionally, all exhibited displacement-softening post-peak behaviour. Specimens reached an ultimate compressive stress at displacements of 1.174 mm, 1.263 mm and 1.023 mm, respectively.

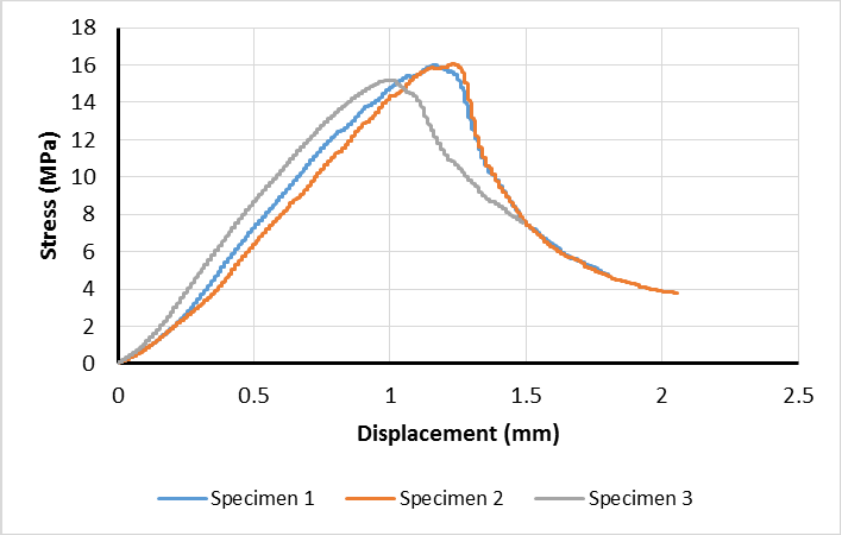

Figure 6.6: Stress-displacement behaviour of 0.5% SFRC specimens

The relative stiffness for steel fibre-reinforced concrete was determined from the linear slope of the elastic region in the above curves. The relative stiffness gives an indication of the elasticity of each concrete specimen. Results are shown in Table 6.4:

Table 6.4: Relative stiffness of specimens with varied fibre dosage (MPa/mm)

Fibre Dosage (% by Volume)	**Specimen Stiffness (MPa/mm)**			**Average**	**Standard Deviation**
	1	**2**	**3**		
0	9.42 R^2=0.999	16.39 R^2=0.9991	18.00 R^2=0.9993	17.20	4.56
0.00115	23.83 R^2=0.9991	19.13 R^2=0.9992	19.22 R^2=0.9989	20.73	2.69
0.1	19.81 R^2=0.9996	20.68 R^2=0.9997	18.00 R^2=0.9996	19.50	1.37
0.2	21.43 R^2=0.9992	14.09 R^2=0.9963	21.09 R^2=0.9992	18.87	4.14
0.3	15.33 R^2=0.9994	14.66 R^2=0.9986	20.32 R^2=0.9992	16.77	3.09
0.4	14.65 R^2=0.9922	13.66 R^2=0.9923	18.02 R^2=0.9992	15.44	2.29
0.5	17.12 R^2=0.9979	15.59 R^2=0.9981	18.13 R^2=0.9975	16.95	1.28

Across the entire spectrum of results there is a close correlation to a linear fit ensuring an accurate approximation of concrete stiffness (as noted by R^2 approaching 1). It is

noted that the addition of steel fibres decreases the relative stiffness of oil-impacted concrete.

6.2.3.3 Proportional Limit

Analysis of the proportional limit will determine if steel fibre dosage effects the service strength of oil contaminated concrete. The estimated proportional limit derived from the linear limit of the stress-displacement curves is outlined in Table 6.5. The non-fibrous specimen 1 proportional limit was considered an outlier as in Chapter 5 and was not included in the average calculation.

Table 6.5: Proportional limit of specimens with varied fibre dosage (MPa)

Fibre Dosage (% by Volume)	**Specimen Proportional Limit (MPa)**			**Average**	**Standard Deviation**
	1	**2**	**3**		
0	8.6	10.63	10.12	10.38	1.06
0.00115	15.74	12.86	12.84	13.61	1.87
0.1	16.37	14.34	13.34	14.68	1.54
0.2	11.86	10.62	15.59	12.69	2.59
0.3	13.49	14.27	12.91	13.56	0.68
0.4	12.87	12.58	12.37	12.61	0.25
0.5	13.77	15.72	13.14	14.21	1.35

There is a close correlation between the derived proportional limit between relative fibre dosages as indicted by the low standard deviation.

6.2.3.4 Failure Behaviour

Steel fibre-reinforced specimens at all dosages primarily exhibited shear failure. As fibre dosage increased, crumbling due to oil saturation decreased. The 0.00115% and the 0.5% dosage specimens are shown in Figure 6.7 after compressive failure. A combination of splitting and conical failure can be seen in the lower dosed specimens (a), while specimens with the highest fibre dosage experienced a combination of splitting and shear failure with reduced crack widths (b) as a result of reduced crumbling.

(a) (b)

Figure 6.7: Splitting/conical failure of 0.00115% (a) and splitting/shear failure of 0.5% (b) SFRC specimens

The thickness of the cement top capping was decreased for specimens tested in Programme 3 to ensure that it does not surpass concrete strength and influence results (Figure 6.8).

Figure 6.8: Thinner cement mortar top capping

6.2.4 Flexural Behaviour

The flexural behaviour results of the influence of fibres on oil-impacted concrete is outlined below in sections. Results will be discussed further is Section 6.3.4.

6.2.4.1 Failure Load

The flexural failure load of specimens with varied steel fibre dosage is outlined in Table 6.6. The standard deviation between specimens of the same dosage volume is minimal ensuring an accurate representation of flexural strength. Due to testing problems, specimen 1 of 0.1% fibre volume and specimen 3 of 0.3% fibre volume could not be included in the flexural analysis.

Table 6.6: Flexural strength (MPa) of specimens with varied fibre types

Fibre Dosage (% by Volume)	**Specimen Strength (MPa)**			**Average**	**Standard Deviation**
	1	**2**	**3**		
0	5.93	6.83	6.71	6.49	0.49
0.00115	6.04	6.29	6.87	6.40	0.43
0.1	-	6.76	6.84	6.80	0.06
0.2	6.07	6.14	7.24	6.48	0.66
0.3	6.67	6.54	-	6.61	0.09
0.4	6.55	6.35	6.72	6.54	0.19
0.5	7.17	7.10	7.07	7.11	0.05

It can be noted that the addition of steel fibres increase the flexural strength of oil-impacted concrete. The highest flexural strength is seen at a dosage of 0.5% by concrete volume.

6.2.4.2 Load-displacement Behaviour

The load-displacement relationship of specimens under four-point flexural loading was plotted for a comparison of the fibre-matrix interaction. Overall, specimen's experienced brittle failure after peak load was reached which is evident in the sudden load decrease at a constant displacement after ultimate load.

The load-displacement behaviour of specimens at 0.00115% steel fibre dosage is shown in Figure 6.9. Specimens 1 and 2 exhibited similar deformation while specimen 3 showed increased resistance to displacement. Specimen 1 experienced failure at a displacement of 1.43 mm, specimen 2 at 1.41 mm and specimen 3 at 1.10 mm.

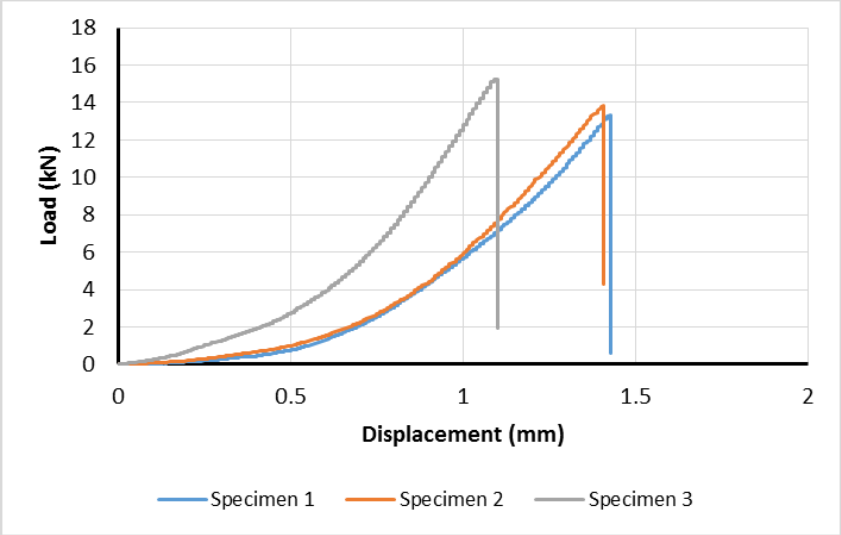

Figure 6.9: Load-displacement behaviour of 0.00115% SFRC specimens

When the steel fibre dosage was increased to 0.2% by concrete volume, overall, specimens showed no increase in ductility in comparison to 0.00115% dosage (Figure 6.10). Specimens failed at displacements of 1.41 mm, 0.97 mm and 1.00 mm, respectively.

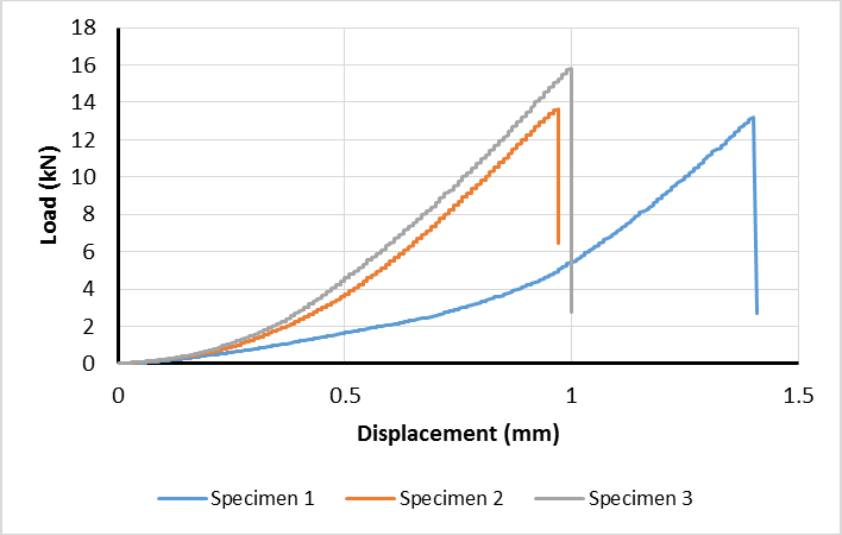

Figure 6.10: Load-displacement behaviour of 0.2% SFRC specimens

The load-displacement behaviour of 0.3% dosage volume specimens can be seen in Figure 6.11. The failure displacement of specimen 1 was 1.12 mm while specimen 2 failed at a displacement of 1.04 mm.

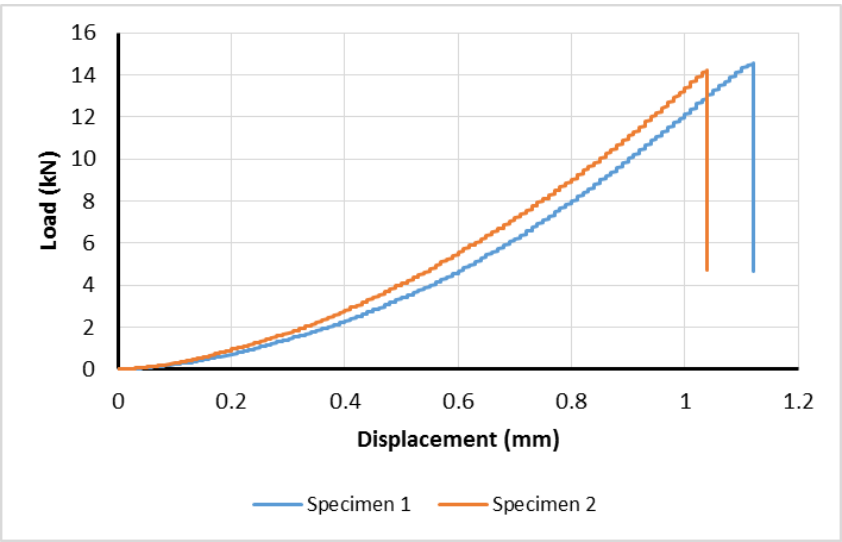

Figure 6.11: Load-displacement behaviour of 0.3% SFRC specimens

The load-displacement relationship of concrete containing 0.4% of steel fibres can be seen in Figure 6.12. Specimens exhibited varied deformation indicated by the dissimilar slopes before failure. Additionally, fibre bridging is evident from 0.4% fibre dosage where a shift in the load-displacement behaviour can be seen due to fibres

resisting crack propagation following initial cracking. This behaviour is most evident in specimen 2 after 0.5 mm displacement. Specimens had a corresponding displacement of 1.24 mm, 1.52 mm and 1.64 mm at ultimate load, respectively.

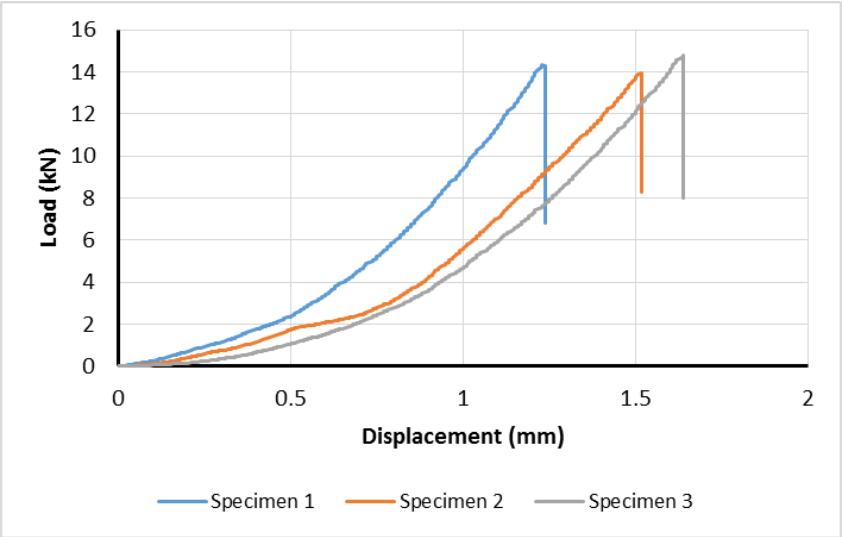

Figure 6.12: Load-displacement behaviour of 0.4% SFRC specimens

Specimens containing the maximum fibre dosage of 0.5% by concrete volume showed varied flexural behaviour as indicated by Figure 6.13. Overall, specimens exhibited increased ductility with displacements of 1.13 mm, 1.58 mm and 1.31 mm at failure, respectively.

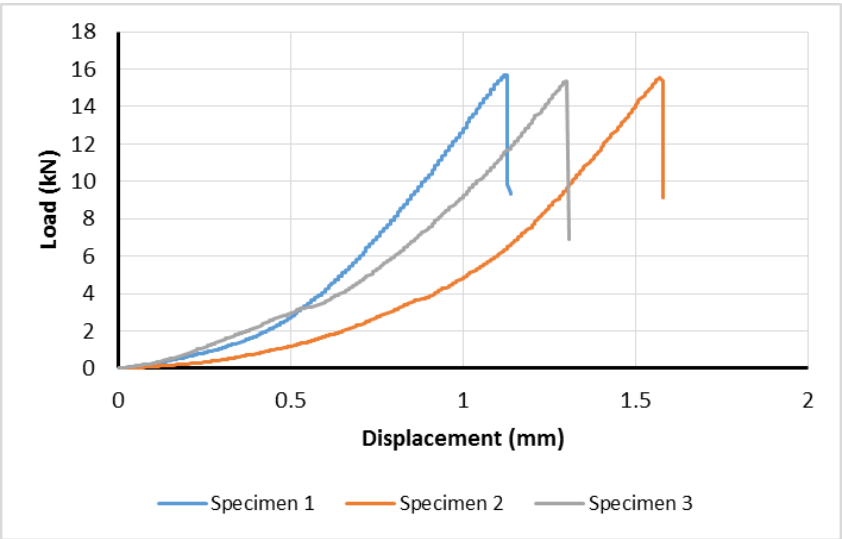

Figure 6.13: Load-displacement behaviour of 0.5% SFRC specimens

6.2.4.3 Failure Behaviour

When the specimens are loaded in bending setup, the maximum tension stress occurs at the bottom where the first crack would usually develop. However, as seen in Chapter 5, the addition of fibres increased concrete ductility and tensile strength which caused a redistribution of stress during loading at times causing failure to occur off-centre.

As steel fibre dosage increased, crack width at failure was reduced. A comparison of 0.00115% and 0.5% fibre volume specimens at failure can be seen in Figure 6.14:

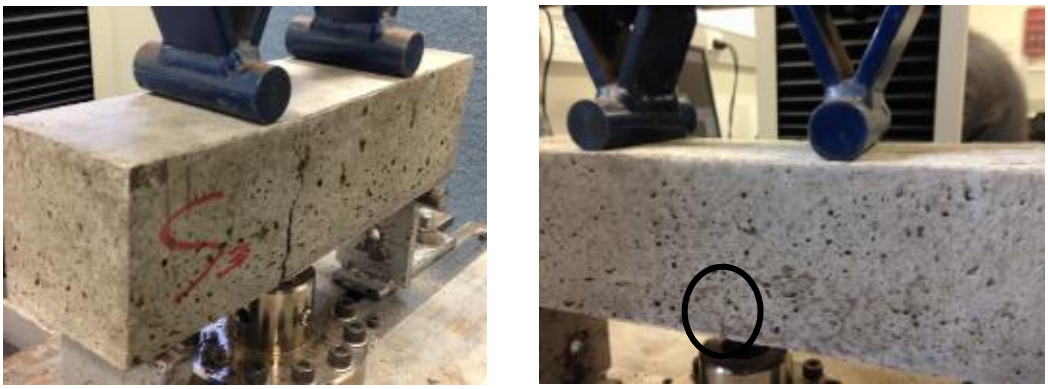

(a) (b)

Figure 6.14: Flexural failure at 0.00115% dosage (a) and 0.5% dosage (b)

Compared to the minimum fibre dosage of 0.00115%, the maximum dosage of 0.5% controlled crack propagation much more effectively.

Analysis of fractured surfaces shows that failure takes place primarily due to fibre pull-out. However, generally fibres still had hooked-ends after failure indicating a poor fibre-matrix bond (Figure 6.15).

Figure 6.15: Steel fibre after flexural failure

6.3 Discussion

Results are discussed in sections for clarity, making reference to the findings outlined in the previous section.

6.3.1 Effect of Fibre Dosage on Density

The effect of steel fibre dosage on oil contaminated concrete physical properties was analysed in Section 6.2.1. As illustrated in Figure 6.1, fibre dosage has no visual effect on concrete as noted by the unaffected surface porosity and saturation. The average density of specimens is outlined in Figure 6.16. The red horizontal line depicts the average non-fibrous density attained from Chapter 5. It can be noted that the specimens tested in programme 3 may have weighed less than the control and 0.1% fibre dosage specimens due to the thickness of the cement capping used in programme 2. The increased weight would have a minor effect on density estimates when compared to the thinner capped specimens.

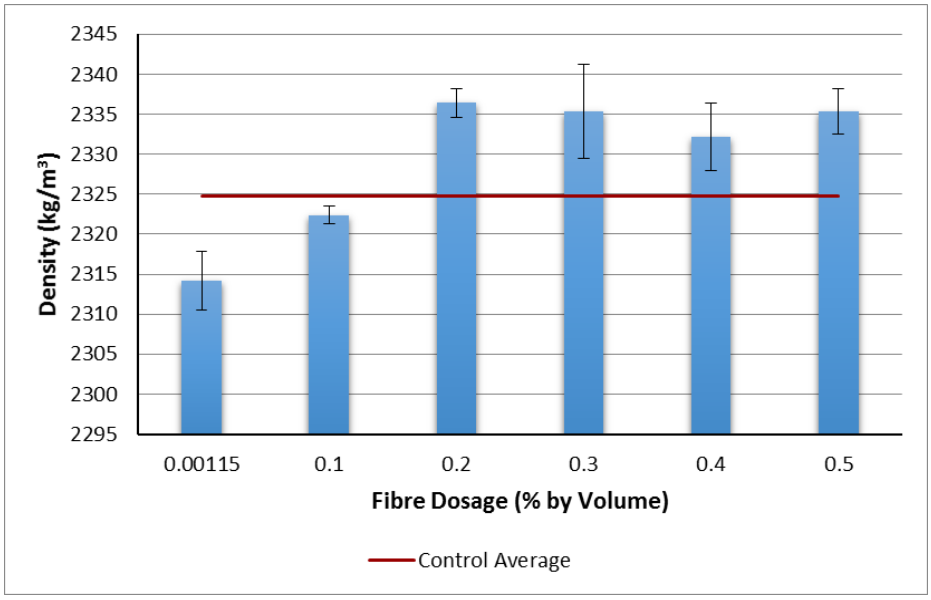

Figure 6.16: Average density of specimens with varied steel fibre dosages (kg/m^3)

In general, increased fibre dosage increases concrete density. Specimens containing 0.00115% and 0.1% dosage decreased concrete density by 0.46% and 0.10%,

respectively, when compared to the control average. Whereas, fibre dosages between 0.2%-0.5% increased concrete density by 0.50%, 0.45%, 0.32% and 0.45%, respectively. The increase in average density is smaller for the 0.3% dosage due to the lighter weight of specimen 3 (refer to Table 6.1).

Unlike results found in Chapter 5 (Section 5.3.1), fibre dosage was found to have an effect on oil-impacted concrete density. The maximum density increase was seen at a fibre dosage of 0.2% by concrete volume. Fibre dosages from 0.2% to 0.5% showed minimal deviation in concrete density, however, concrete weight would increase with the addition of steel fibres. From Section 2.5, investigations by Löfgren (2005) and Neves & Gonµalves (2000) found that fibre addition causes some perturbation of the matrix which can result in more air voids. Therefore, it is suspected that fibre dosages exceeding 0.2% induced voids within the matrix which decreased concrete density.

6.3.2 Effect of Fibre Dosage on Workability

The determination of SFRC workability is determined using a standard cone test. The slump test was carried out on each fresh fibre dosage batch as a comparison of oil-impacted concrete workability at various steel fibre dosage rates. Slump results are graphically summarised in Figure 6.17:

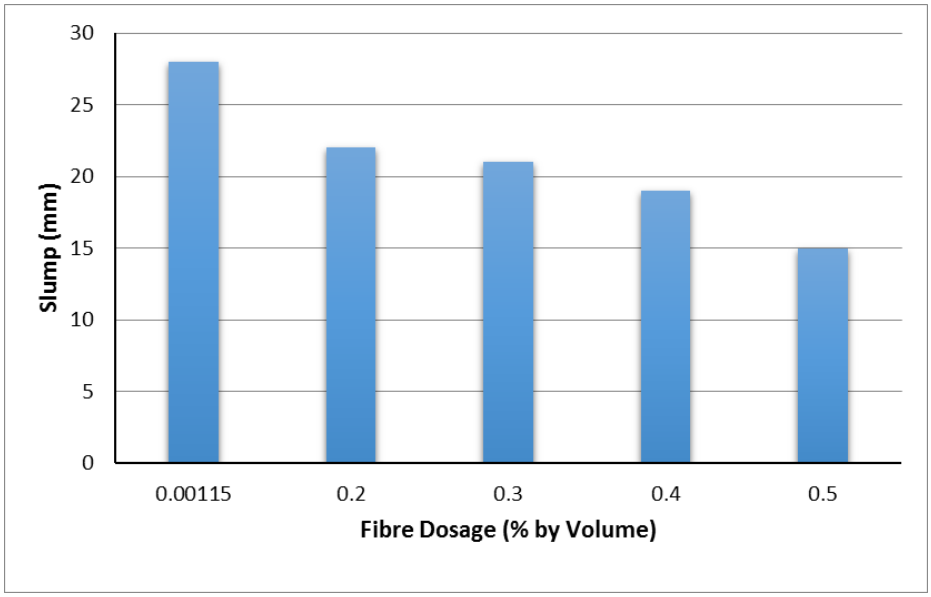

Figure 6.17: Slump of oil-impacted concrete with varied steel fibre dosage (mm)

In agreement with a study by Sarbini, Ibrahim & Saim (2013) (Section 2.5.6), results show that concrete workability is reduced with the increase of fibre content. When compared to the minimum fibre dosage, the addition of fibres reduced concrete slump by 21%, 25%, 32% and 46%, respectively. The decrease in workability is associated with difficulty in compacting concrete, thus, affecting the chances to produce a uniformly distributed concrete. However, as concrete is mechanically vibrated and the slump test is primarily a measure of stability under static conditions, concrete is considered satisfactory from a mobility point of view (Lamond & Pielert (eds.) 2006).

6.3.3 Effect of Fibre Dosage on Compressive Behaviour

6.3.3.1 Effect on Compressive Strength

The findings from the compressive failure load results are graphically summarised in Figure 6.18. The red line represents the non-fibrous average compressive strength attained from Chapter 5 results. The results show that 0.1% fibre dosage volume resulted in the highest average compressive strength. However, concrete strength may

have been influenced as a result of thicker cement top capping compared to specimens tested in this programme (Figure 6.8).

A slight increase in compressive strength of 2.2% and 10.8% was seen at dosages of 0.00155% and 0.1%, respectively, when compared to the control average strength. However, the strength of fibre dosages exceeding 0.1% fell below the non-fibrous average. A minimal loss in strength of 2.3%, 2.6%, 0.9% and 2.1% was exhibited by fibre dosages from 0.2% to 0.5% by concrete volume, respectively.

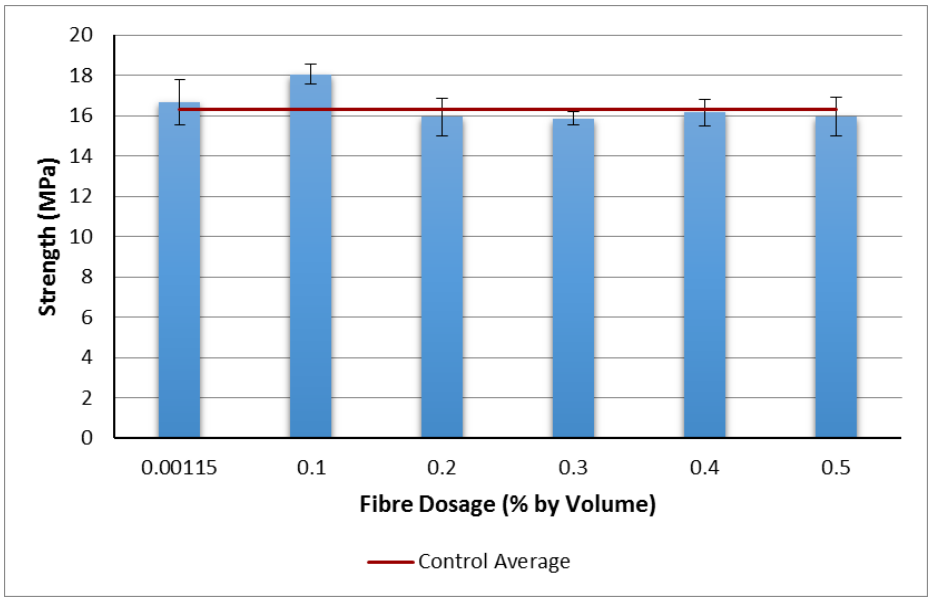

Figure 6.18: Average compressive strength of specimens with varied steel fibre dosages (MPa)

In agreement with literature reported by Mansour, Parniani & Ibrahim (2011) and Hsu & Hsu (1994) in Section 2.5.6, results show that increasing steel fibre dosage does not contribute to an increase in concrete compressive strength. Hsu & Hsu (1994) reported that reduced workability due to increased fibre volume produced voids within the matrix which restricted strength enhancement. From the slump results reported in Figure 6.17, it can be noted that concrete workability decreases as fibre dosage increases. However, as concrete was mechanically vibrated and the variation in

strength is minimal between dosages, it is assumed that the strength deviation is due to natural inconsistencies in a heterogeneous material such as concrete.

6.3.3.2 Effect on Stress-Displacement Behaviour

The stress-displacement behaviour of oil-impacted concrete can be a measure of concrete ductility at varied steel fibre dosage rates. A comparison of the representative stress-displacement curve for each fibre dosage volume is shown in Figure 6.19; including the control and 0.1% stress-displacement specimen behaviour from Chapter 5. All specimens exhibited ductile behaviour through extending the softening branch of concrete post-peak behaviour. However, increased fibre dosage did not result in a less brittle post-peak behaviour when compared to the minimum fibre dosage. It can be noted that specimens containing higher fibre volumes experienced increased displacements at failure load, hence, increasing concrete ductility.

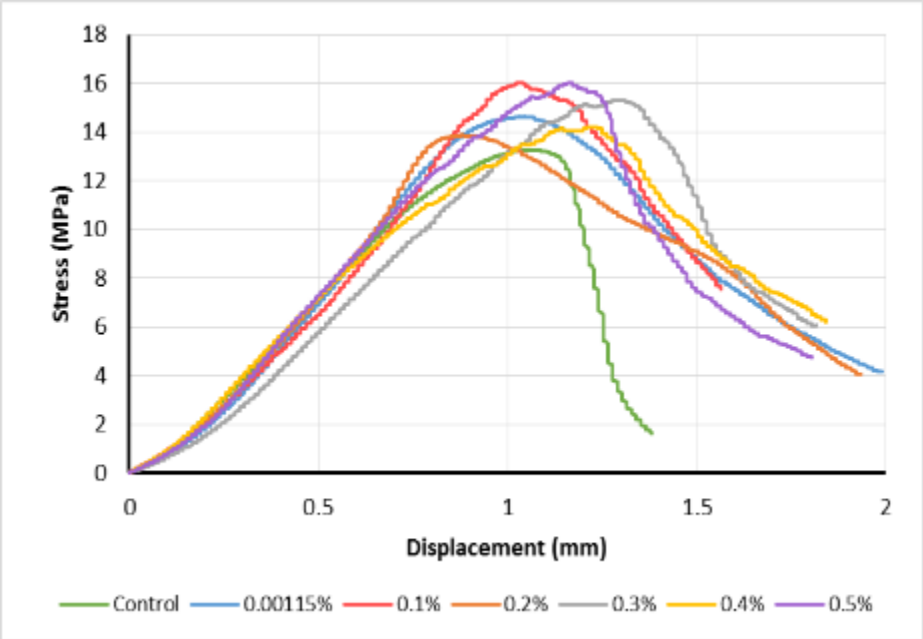

Figure 6.19: Stress-displacement relationship of compressive specimens at varied steel fibre dosages

Research by Lee, Oh & Cho (2015) outlined in Section 2.5.7, concluded that SFRC exhibited ductile behaviour after reaching compressive failure load and that the

displacement at this load generally increased along with an increase of fibre volume ratio. From the displacements at ultimate load reported in Section 6.2.3.2, similar results are found where displacements at failure increase with fibre addition. From Figure 6.19, concrete with a 0.5% fibre volume ratio experienced failure at a displacement of 1.263 mm compared to the failure displacement of 1.061 mm at the minimum fibre dosage of 0.00115%.

Moreover, from failure behaviour results (refer to Figure 6.7), it is noted that as fibre volume increases crack widths and crumbling due to saturation are reduced. Therefore, it can be assumed that increased concrete ductility is a result of a reduction in lateral deformation. At greater fibre dosages, there is a greater probability of fibres restraining axial cracking which increased the energy required for crack propagation.

6.3.3.3 Effect on Relative Stiffness

The relative elasticity of specimens outlined in Table 6.5 is graphically presented in Figure 6.20. The red horizontal line represents the average stiffness attained from the non-fibrous 10% oil contaminated specimens in Chapter 5. Initially, concrete elasticity is increased at low fibre dosages but decreases with the addition of steel fibres. The minimum fibre dosage of 0.00115% showed to have the highest elasticity out of fibre dosages considered with a 20.5% increase compared to the control average. Fibre dosages of 0.1% and 0.2% also increased concrete stiffness by 13.4% and 9.7%, respectively. At 0.3% fibre dosage, concrete stiffness decreased by 2.5%. Specimens containing 0.4% fibre dosage volume experienced the largest elasticity decrease of 10.2%, while 0.5% dosage specimens saw a 1.4% decrease in elasticity compared to the non-fibrous average.

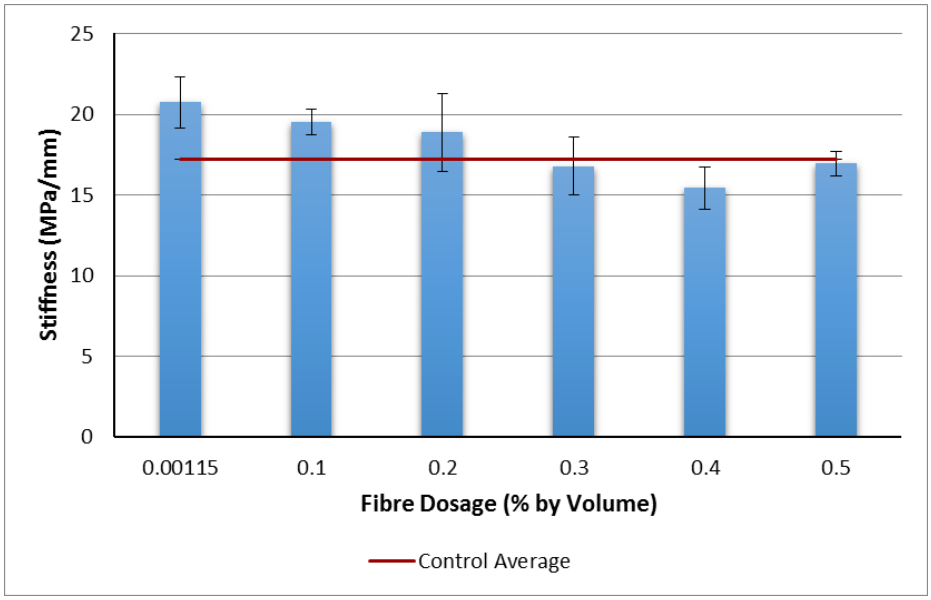

Figure 6.20: Average stiffness of specimens with varied steel fibre dosages (MPa/mm)

In agreement with findings by Neves & Fernandes de Almeida (2005) and Lee, Oh & Cho (2015) outlined in Section 2.5, the addition of steel fibres slightly reduced concrete elasticity. Neves & Fernandes de Almeida (2005) established that the reduction in elasticity is because fibres parallel to the load direction can act like voids and the eventual addition of voids caused by fibre addition. It is assumed that the probability of parallel fibres increases with the addition of fibres, hence, decreasing concrete stiffness. The increased ductility of concrete due to fibre addition causing a more gradual failure also may have decreased concrete elastic capacity.

6.3.3.4 Effect on Proportional Limit

While the ultimate compressive strength is an important factor, analysis of the proportional strength can determine the effect of fibre dosage on the service strength of concrete in its applications. Figure 6.21 outlines the average proportional limit derived from the stress-displacement curves (Table 6.5). The red line depicts the non-fibrous proportional limit average from Chapter 5 results.

Initially, the introduction of steel fibres increased the proportional limit of oil-impacted concrete, however, variation in fibre dosages had minimal effect. A fibre dosage of 0.1% exhibited the optimum proportional limit of 14.68 MPa, which may have been influenced by cement capping. Other fibre dosages showed minimal deviation in comparison, having a minimum 21.5% increase (at 0.4% dosage) to a maximum 37.0% increase (at 0.5% dosage) compared to the control average proportional limit.

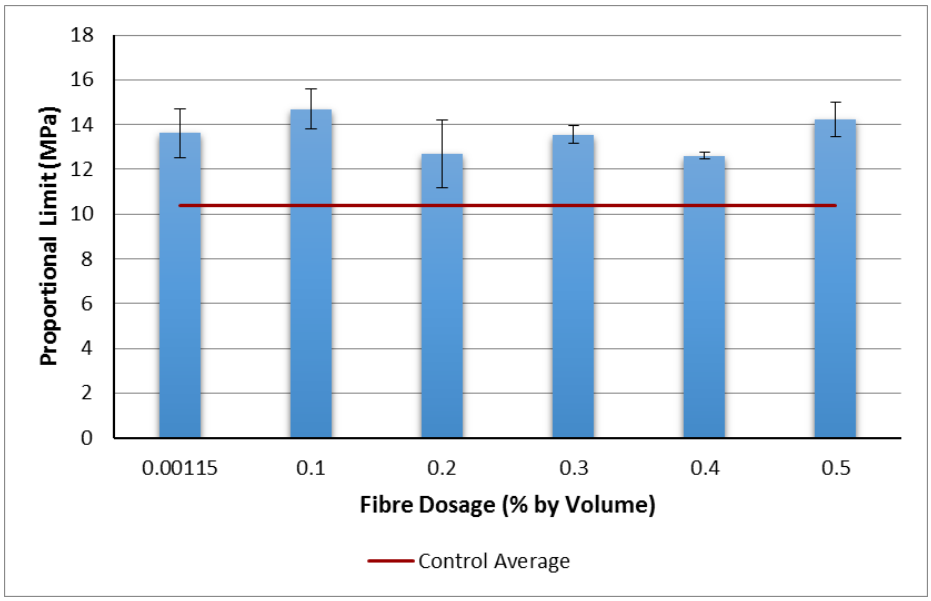

Figure 6.21: Average proportional limit of specimens with varied steel fibre dosages (MPa)

Although the elasticity of concrete decreased with the addition of fibres, the proportional limit did not decrease as a result due to the increased ductility of concrete. However, a maximum 20% deviation was seen between the fibre dosages considered (0.1%-0.5% fibre dosage) with no clear trend. Therefore, it can be concluded that steel fibre dosage has an insignificant effect on concrete proportional limit due to induced voids within the matrix as fibre dosage volume increases. Fibre volume had a more significant effect on concrete permanent deformation.

6.3.4 Effect of Fibre Dosage on Flexural Behaviour

6.3.4.1 Effect on Flexural Strength

The effect of steel fibre dosage on the flexural strength of oil-impacted concrete is summarised in Figure 6.22. The red line shows the average flexural strength of normal oil contaminated concrete from Chapter 5. The trend followed that the addition of steel fibres slightly increases concrete 28 day flexural strength. The optimum strength improvement of 9.60%, compared to the control average, was seen at the maximum fibre dosage of 0.5% by concrete volume. Interestingly, concrete containing 0.1% fibre volume showed a strength increase of 4.78%. While specimens containing 0.00115%, 0.2%, 0.3% and 0.4% fibre dosages showed a maximum strength improvement of 1.77% to the control average (0.3% fibre dosage). Overall, a flexural strength increase of 0.71 MPa was seen between the minimum and maximum fibre dosages (0.00115%-0.5%).

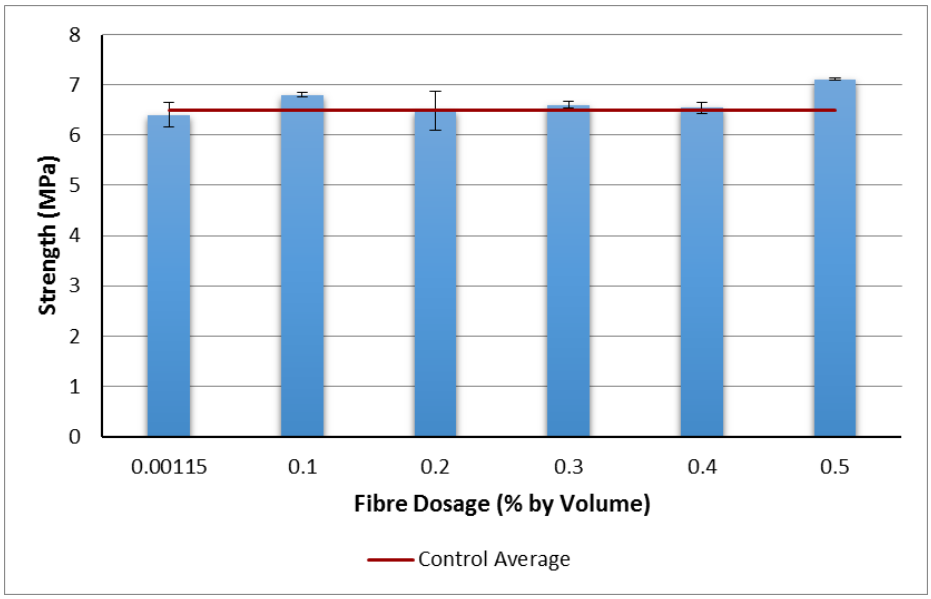

Figure 6.22: Average flexural strength of specimens with varied steel fibre dosage (MPa)

From literature outlined in Section 2.5, similar results were seen in studies by Mansour, Parniani & Ibrahim (2011), Wang & Wang (2013) and Yazıcı, İnan & Takak

(2007). All studies found that the addition of steel hooked-end fibres increase the 28 day flexural strength of ordinary Portland cement concrete. It was concluded that the increase in flexural strength is influenced by a softening response due to fibre bridging making concrete more ductile.

Referring to Figure 6.14, analysis of concrete flexural failure behaviour showed that the addition of fibres enhanced crack bridging efficiency which is evident in the reduced crack widths and crack propagation at failure. Load transfer through crack bridging becomes more effective with fibre addition as fibres are more likely cross the failure path as fibre volume increases, hence, increasing concrete tensile capacity.

However, from the fibre dosages analysed, flexural strength increased by a maximum of 0.62 MPa (9.6% increase at 0.5% fibre dosage) compared to non-fibrous concrete, which is not a significant improvement. Analysis of the failure surface (Figure 6.15) showed that fibres generally kept their hooked-end fibre pull-out after failure. If the fibre-matrix bond is strong, generally, a considerable amount of energy dissipation takes place as fibres are straightened and plastically deformed during fibre pull-out. From Chapter 4 (Section 4.3), a significant decrease in concrete density and strength was seen at 10% oil contamination. Therefore, it is suspected that oil saturation hindered the ability of concrete to hold fibres under tensile stress causing a bond-slip effect. Due to fibre-matrix slippage, the tensile strength of steel fibres could not be used effectively to increase concrete flexural strength, which is why only a minimal improvement in strength was seen.

6.3.4.2 Effect on Load-Displacement Behaviour

The load-displacement behaviour of concrete under flexural loading is an indication of its ductility. Figure 6.23 depicts the typical load-displacement relationship of each fibre dosage from the curves presented in Section 6.2.4.2. Also included is the control and 0.1% fibre dosage load-displacement behaviour of specimens from Chapter 5.

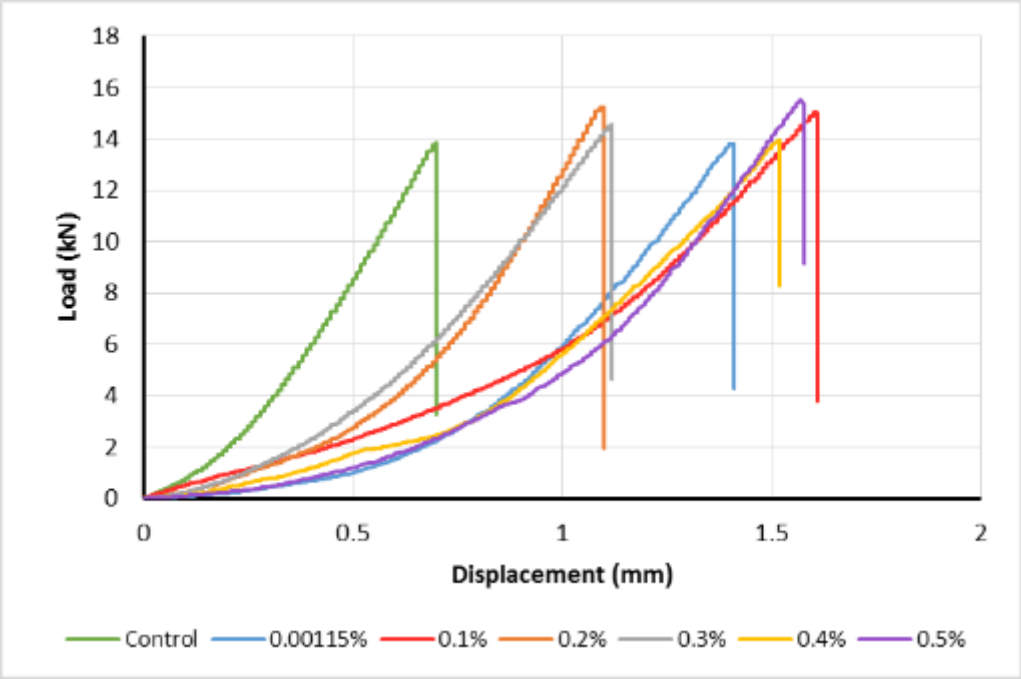

Figure 6.23: Load-displacement relationship of flexural specimens with varied steel fibre dosages

Overall, the introduction of steel fibres improve the ductility of concrete, however, there is no trend noticed from the influence of fibre volume ratio on FRC flexural behaviour from the curves. The displacement at ultimate load of specimens containing 0.2% and 0.3% steel fibre dosages of 1.10 mm and 1.12 mm, respectively, is less than the failure displacement exhibited by specimens containing smaller dosages (0.00115% and 0.1%). These specimens exhibited a more brittle behaviour showing increased resistance to displacement as indicated by their steeper slope before failure.

A more ductile behaviour was observed for specimens containing 0.4% and 0.5% fibre dosages. These specimens displayed increased failure displacements of 1.52 mm and

1.58 mm, respectively. Interestingly, the 0.1% fibre dosage specimen exhibited the maximum displacement of 1.61 mm at failure, however, this may be due to the possible varied test conditions of the separate programmes.

It is evident that steel fibres increase the ductility of concrete by increasing specimen displacement at failure loads through fibre bridging. However, the effect of steel fibre dosage showed to have varied effects on concrete ductility. This may be due to the relatively small dosage increments investigated as well as the typical variation between concrete mixes. However, as fibre dosage did not have a significant effect on oil-impacted concrete flexural strength, the load-displacement behaviour was not expected to show an obvious trend, as flexural strength is dependent on concrete ductility.

6.4 Summary and Conclusion

This chapter has provided insight into the properties of steel fibre-reinforced concrete with oil contaminated sand at varied dosage rates.

It has been noted that fibre dosage volumes does not affect the physical properties of oil-impacted concrete, however, concrete density was altered. Fibre dosages exceeding 0.2% increased concrete density when compared to unreinforced concrete. However, as there was minimal deviation seen between 0.2% to 0.5% fibre dosages it was assumed that fibres at higher dosages induced voids within the matrix.

Analysis of compressive behaviour showed that the addition of steel fibres does not contribute to an increase in 28 day concrete compressive strength. The optimal improvement of concrete compressive strength of 10.8% was seen with a fibre dosage

of 0.1%, however, this result may have been influenced by the thicker cement capping of specimens in Programme 2. Otherwise, a strength deviation between +2.2% (0.00115% dosage) and -2.6% (0.3% dosage) was seen with other fibre dosages when compared to the unreinforced average strength. Due to the minor variation in strength it was assumed that the deviation is due to natural inconsistencies in concrete.

The compressive stress-displacement behaviour of FRC showed that all specimens exhibited ductile behaviour and extended the softening branch of concrete post-peak behaviour when compared to the non-fibrous specimen. However, increase in fibre dosage did not further extend the post-peak softening branch but rather increased specimen displacement at failure load. Greater crack control at higher fibre dosages was assumed to increase the energy required for crack propagation which increased concrete ductility.

The addition of fibres decreased the elasticity of concrete in compression while increasing its ductility during permanent deformation where crack arresting initiates. Initially, the introduction of steel fibres increased the proportional limit of oil-impacted concrete, however, variation in fibre dosages had minimal effect on its deviation. Therefore, in compression, fibre dosage played more of a role in the improvement of concrete post-yield behaviour.

Analysis of the effect of fibre dosage on concrete flexural strength showed that strength increased with the addition of steel fibres. An optimum strength improvement of 9.60% was seen at the maximum fibre dosage of 0.5% by concrete volume. It was assumed that the increase in flexural strength is influenced by a softening response due to fibre bridging making concrete more ductile. This increased ductility was seen through failure analysis where crack widths and propagation was reduced with

increased fibre dosage. However, due to the marginal improvement in concrete flexural strength (up to 0.62 MPa), it is suspected oil saturation encouraged bond-slippage between the fibres and matrix under tensile stresses.

Additionally, there was no clear trend seen through the analysis of load-displacement behaviour at varied fibre dosages. Minimal correlation between fibre dosage and concrete ductility was seen as the minimum fibre dosage of 0.00115% was found to have a larger failure displacement than specimens containing 0.2% and 0.3% fibre dosage volumes. The small fibre dosage increments in conjunction with the typical variations between concrete mixes were assumed to cause the mixed results.

Overall, the steel fibre dosages considered were found to have minimal effect on the properties of concrete with 10% oil contaminated sand. The maximum fibre dosage of 0.5% was the best performing when the varied specimen preparation (cement top capping) and possible test environment variations of 0.1% fibre dosage specimens was taken into account. The 0.5% fibre dosage most improved concrete flexural strength while causing minimal reduction to compressive strength.

Larger fibre dosages may further improve concrete flexural strength, however, the associating loss in compressive strength as well as the effect of oil saturation should be considered. However, 10% oil contaminated sand used as a constituent in concrete may hinder fibre features irrespective of fibre dosage.

Chapter 7

Conclusion

7.1 Review Project Objectives

This project set out to evaluate the prospects of the use of oil contaminated sand in concrete and investigate the possibility of the inclusion of fibres to regain or enhance the mechanical properties of oil-impacted concrete. With sand contamination so widely spread, recycling of contaminated soils could result in a cleaner environment as well as a cost effective construction material. The process to determine if this is a viable option requires accurate knowledge of the properties of oil contaminated concrete with and without fibre-reinforcement through experimentation. This was achieved by:

1. Performing a literature review to identify and understand the following:
    i. The causes, geotechnical properties and current remediation methods of crude oil contaminated sand
    ii. The mechanical properties and current application options for the use of oil contaminated sand in concrete
    iii. The purpose and applications of fibre-reinforced concrete
    iv. The mechanical behaviour of fibre-reinforced concrete

2. Determine the effect of oil contamination on the physical and mechanical properties of concrete through testing. Based on findings, decide on a maximum oil content that is still suitable for use in construction.
3. Having identified the maximum oil content, evaluate the compressive and flexural behaviour of crude oil-impacted sand in concrete with four different types of fibres. Determine the best performing fibre based on findings.
4. Having identified the best performing fibre, determine the optimum fibre dosage volume through investigation of the compressive and flexural behaviour.

The knowledge base surrounding the use of oil contaminated sand in concrete was improved and solutions for its use in construction applications have been made. The results of the project have allowed for the maximum oil content to be identified as noted in Chapter 4 in line with the second research objective. Likewise, the investigation of fibre types through experimentation have allowed for the optimum fibre type to be determined in Chapter 5 to satisfy the third research objective. Chapter 6 met the fourth research objective where the optimum fibre dosage was determined. Elements of the discussion from each chapter take knowledge of the information outlined in the literature review.

7.2 Project Conclusions

This project experimentally investigated the effect of the addition of short fibres on the physical and mechanical properties of concrete consisting of oil-impacted sand. Conclusions are made in sections as per the project objectives.

7.2.1 Review of Literature

Based on the extensive review of literature conducted, a detailed understanding on the following was gained:

- Approximately 80 percent of land is polluted by products of petroleum origin. The current remediation methods for contaminated sand such as incineration, thermal desorption, soil washing etc. is uneconomical and the long-term management of sand is unsustainable as a treatment solution.
- Sand cohesion and friction angle of oil contaminated sand decreased with increase in oil content. An optimum sand cohesion was seen at 1% oil content.
- Oil contamination decreases concrete compressive strength due to the oil coating of sand particles and inhibiting cement hydration.
- The addition of fibres has the potential to improve the mechanical properties of concrete consisting of oil contaminated sand.

7.2.2 Compressive Behaviour of Concrete with Oil Contaminated Sand

The results of the investigation in Chapter 4 confirmed that light crude oil contaminated sand has a direct effect on concrete physical and mechanical properties. The following are the main findings of this study:

- As oil contamination increased, concrete porosity and saturation worsened. Concrete density decreased by a maximum of 8.2% at 20% contamination compared to the uncontaminated specimens.
- Oil contamination in excess of 1% decreases concrete compressive strength. Concrete decreased in strength by 44% at 10% contamination and by 81% at 20% contamination compared to the uncontaminated average strength.

- 1% oil contamination increased concrete strength by 4.1% compared to the uncontaminated specimens due to sand reaching optimum cohesion as a result of oil bonding sand particles.
- Sand containing oil in excess of 1% over saturated sand particles which hindered the bond formation between mortar and aggregate and encouraged water seepage which increased concrete porosity.
- 10% oil contamination is the maximum oil content that is suitable for use in construction applications. Concrete contaminated up to 10% achieved a proportional limit above 10 MPa making it suitable for use in applications such as parking lots, footpaths, pathways and bus terminals.
- The poor physical properties of concrete at 20% contamination primarily contributed to its unsuitability for practical use.

7.2.3 Compressive and Flexural behaviour of Oil Contaminated Concrete with Short Fibres

Chapter 5 investigated concrete with 10% oil contaminated sand with the inclusion of Forta Ferro, polypropylene, ReoShore 45 and steel fibres at a dosage volume of 0.1% by concrete volume. The following are the main findings of this study:

- Fibres did not affect the physical properties of oil-impacted concrete, nor its density, due to the relatively low fibre dosage implemented.
- Fibres did not significantly affect the compressive strength of concrete. Steel fibres most improved concrete compressive strength by 11% due to their higher tensile strength and hooked geometry.

- Fibres improved the softening post-peak branch of concrete stress-displacement behaviour compared to plain concrete.
- Fibres had no significant effect on oil-impacted concrete flexural strength. Only steel fibres enhanced concrete flexural strength, with a 4.8% strength increase compared to the non-fibrous average.
- All fibre types, excluding ReoShore 45, improved concrete ductility through increasing displacement at failure loads.
- Although fibres enhanced concrete ductility, crack bridging efficiency was hindered due to matrix saturation.
- Steel fibres were concluded the best performing due to their optimal enhancement of concrete compressive and flexural strength.

7.2.4 Compressive and Flexural Behaviour of Oil Contaminated Concrete with varied Fibre Dosage

Chapter 6 investigated concrete with 10% oil contaminated sand with steel fibre dosages between 0.00115% - 0.5% by concrete volume (0.9 - 39.65 kg/m^3). The following are the main findings of this study:

- The addition of steel fibres did not contribute to an increase in compressive strength. The minor variation in strength of up to 4.19% was assumed to be result of natural inconsistencies between concrete specimens.
- The addition of fibres decreased concrete elasticity in compression while increasing its ductility during permanent deformation where crack arresting initiates.

- Concrete flexural strength increased with the addition of steel fibres. The optimum strength improvement of 9.6% was seen at the maximum fibre dosage of 0.5% by concrete volume.
- Concrete flexural strength increased by a maximum of 0.62 MPa (at 0.5% fibre dosage). Therefore, it is assumed that concrete offered no pull-out resistance to fibres due to saturation which hindered flexural strength development through crack bridging.
- The maximum fibre volume dosage of 0.5% most improved concrete flexural strength while causing minimal reduction to compressive strength.

7.2.5 Overall Remarks

From the results of this investigation, it was found that concrete saturation when using 10% oil contaminated sand hindered the crack stabilisation and load transfer features of fibres which usually improve concrete strength. Therefore, minimal recovery of concrete mechanical properties with 10% oil contaminated sand was seen with the inclusion of fibres or their respective dosage volumes. Using oil contaminated sand as a constituent in concrete should only be considered in low strength applications. Further investigations are required to determine the maximum oil contamination level in sand that will not hinder the enhancement provided by short fibres on concrete properties to make this waste material applicable in building and construction applications.

7.3 Further Research

Further investigations are highly recommended to gain further understanding of the effects of oil contaminated sand in concrete and to investigate further solutions to regain or enhance the loss in its mechanical properties. Several recommendations for further research are outlined below:

- Investigate the maximum level of oil contamination that will not hinder the enhancement provided by short fibres on concrete properties.
- Investigate the effect of oil contamination on the physical and mechanical properties of concrete with an increased curing length. A study by Almabrok et al. (2013) found that oil contamination increased concrete setting time. Hence, oil-impacted concrete may not reach optimum strength at 28 days.
- Further laboratory tests should be undertaken to investigate the effects of oil contamination on abrasion, impact, blasting, shatter, shear, tensile splitting or concrete creep as well as testing of structural elements, such as concrete slabs, beams and walls.
- Investigate the effect of other fibre types such as glass and various steel fibre geometries on oil-impacted concrete mechanical properties. Also, the combination of short fibre types may provide a more efficient mechanical structure.
- Investigate the effect of increased steel fibre volume dosage on oil-impacted concrete mechanical properties.
- Investigate the durability of oil-impacted concrete as well as the effect of oil on steel fibres; e.g. steel corrosion.

List of References

Abousnina, R 2015, 'An Overview on Oil Contaminated Sand and its Engineering Applications', *International Journal of GEOMATE*, vol 10, no. 19, pp. 1615-1622.

Abousnina, R, Shiau, J, Manalo, A & Lokuge, W 2014, 'Effect of Light Hydrocarbons Contamination on Shear Stength of Fine Sand', *Fourth International Conference on Geotechnique, Construction Materials and Environment*, Brisbane.

ACI Committee 54.1R 1996, 'Fibre Reinforced Concrete', American Concrete Institute, Michigan.

ACIFC 1999, *An Introduction Guide: Steel Fibre Reinforced Concrete Industrial Ground Floors*, Warwickshire.

ADFIL Construction Fibres 2012, *Products*, viewed 15 June 2015, <http://www.adfil.co.uk/products_fibrillated.php>.

Ajagbe, W, Omokehinde, O, Alade, G & Agbede, O 2011, 'Effect of Crude Oil Impacted Sand of compressive strength of concrete', *Construction and Building Materials*, vol 26, no. 1, pp. 9-12, <http://www.sciencedirect.com/science/article/pii/S0950061811002911>.

Alhozaimy, A, Soroushian, P & Mirza, F 1996, 'Mechanical properties of polypropylene fibre reinforced concrete and the effects of pozzolanic materials', *Cement and Concrete Composites*, vol 18, no. 2, pp. 85-92.

Almabrok, M, McLaughlan, R & Vessalas, K 2013, 'Chacterisation of cement mortar containing oil-contaminated aggregates', Faculty of Engineering and Information Technology, University of Technology Sydney, 978-0-415-63318-5, Taylor & Francis Group, London.

Al-Matairi, N & Eid, W 1997, 'Utilisation of oil-contaminated sands in asphalt concrete for secondary roads', *Materials and Structures*, vol 30, no. 202, pp. 497-505.

Al-Sanad, H, Eid, W & Ismael, N 1995, 'Geotechnical Properties of Oil-Contaminated Kuwaiti Sand', *Journal of Geotechnical Engineering*, vol 121, no. 5, pp. 407-412, <http://ascelibrary.org/doi/abs/10.1061/(ASCE)0733-9410(1995)121%3A5(407)>.

ASTM 2014, 'ASTM C1231: Standard Practice for Use of Unbonded Caps in Determination of Compressive Strength of Hardened Concrete Cylinders', vol 4, no. 2.

ASTM International 2012, 'ASTM C1609 '.

Ayininuola, G 2008, 'Influence of diesel oil and bitumen on compressive strength of concrete', *Journal of Civil Engineering*, vol 37, no. 1, pp. 65-71, <http://jce-ieb.org.bd/pdfdown/3701006.pdf>.

Balaguru, P & Shah, S 1992, *Fiber-Reinforced Cement Composites*, McGraw-Hill Inc., New York, USA.

Barragán, B 2002, 'Failure Toughness of Steel Fibre Reinforced Concrete Under Tension and Shear', PhD Thesis, UPC, Barcelona.

BASF 2015, 'Forta Ferro'.

BASF 2015, 'Masterfibre Econo-Net'.

BASF 2015, 'Reoco 65/35'.

BASF 2015, 'ReoShore 45'.

Beaudoin, J 1990, *Handbook of Fibre-Reinforced Concrete: Principles, Properties, Development and Applications*, Noyes Publications, New Jersey.

Bentur, A & Mindess, S 1990, *Fibre Reinforced Cementitious Composites*, Elsevier Science Publishing Ltd., New York, USA.

Calsiu, I, Marinescu, M, Plopeanu, G, Tanase, V & Toti, M 2001, 'The effects of crude oil pollution on physical and chemical characteristics of soil', *Research Journal of Agrigcultural Science*, vol 43, no. 3, pp. 125-129.

Cement Australia 2012, *General Purpose Cement*, viewed 25 June 2015, <http://www.cementaustralia.com.au/wps/wcm/connect/website/packaged-products/resources/0f30f68046152743947995b796eb3285/PDS-GP-Rev-3-170212.pdf>.

ChampionMotoUK Ltd 2009, *Putoline HPX Off Road Fork & Suspension Oil*, viewed 20 April 2015, <http://www.championmotouk.com/product-info-t.php?Putoline-HPX-Fork-Suspension-Oil-pid10650.html>.

Chevron 2014, *Energy Supply and Demand*, viewed 1 April 2015, <http://www.chevron.com/globalissues/energysupplydemand/>.

Clarke, J, Vollum, R & Swannell, N 2007, 'Guidance for the Design of Steel-Fibre Reinforced Concrete', 63, Concrete Society, Camberly.

Collins, R 1992, 'Assimilation of Wastes and By-Products into Highway System: Status Report and Regulatory Influences', *Second Interagency Symposium on Stabilisation of Soils and Other Materials*, Department of the Interior, Washington, LA.

Devold, H 2013, *Oil and gas production handbook*, ABB, Oslo.

Domone, P, Illston, J (eds.) 2010, *Construction Materials: Their Nature and Behavior*, 4th edn, Spon Press, New York.

Dorf, R 2004, *The Engineering Handbook*, CRC Press, New York.

Døssland, A 2008, 'Fibre Reiforcement in Load Carrying Concrete Structures', PhD Thesis, Department of Structural Engineering, Norwegian University of Science and Technology, 1503-8181.

Dowa Eco-System 2006, *Soil Remediation*, viewed 1 June 2015, <http://www.dowa-eco.co.jp/en/soil.html>.

Dramix Guidelines 1995, *Design of concrete structures: steel wire reinforced concrete structures with or without ordinary reinforcement*.

Dupont, D 2003, 'Modelling and experimental validation of the constitutive law (σ−ε) and cracking behavior of steel fibre reinforced concrete', PhD Thesis, Department of Civil Engineering, Catholic University of Leuven, Leuven.

Ejeh, S & Uche, O 2009, 'Effect of Crude Oil Spill on Compressive Strength of Concrete Materials', *Journal of Applied Sciences Research*, vol 5, no. 10, pp. 1756-1761, <http://www.aensiweb.com/old/jasr/jasr/2009/1756-1761.pdf>.

Exporters India 2015, *Kasturi Metal Composites Private Limited*, viewed 15 June 2015, <http://www.exportersindia.com/kasturi-metal-composites1902273/products.htm>.

Ezeldin, S & Balaguru, P 1992, 'Normal- and High-Strength Fibre-Reinforced Concrete Under Compression', *Journal of Materials in Civil Engineering*, vol 4, no. 4, pp. 415-429.

Fibremesh 2011, *Fibremesh Micro-Reinforcement System*.

Fibrex 2015, *Fibrex Glued Steel Fibres*, <http://www.onwardchem.com/faqs.htm>.

Flynn, L 1992, 'Recycling: Will Roads Become 'Linear Landfills'?', Scranton Gillette Communications, Des Planes.

Gambhir, M 2009, *Concrete Technology: Theory and Practice* , 4th edn, Tata McGraw Hill Education Private Limited, New Delhi.

Hassan, H, Taha, R, Rawas, A, Shandoudi, B, Gheithi, K & Barami, A 2005, 'Potential uses of petroleum-contaminated soil in highway construction', *Construction and Building Materials*, vol 19, no. 8, pp. 646-652.

Holcim Australia 2015, *Fibre Reinforced Concrete*, viewed 20 April 2015, <http://www.holcim.com.au/en/products-and-services/concrete-readymix/high-performance/fibre-reinforced-concrete.html>.

Hsu, L & Hsu, C 1994, 'Stress-strain behaviour of steel-fibre high-strength concrete under compression', *ACI Structural*, vol 91, no. 4, pp. 448-457.

International Energy Agency 2014, *Key World Energy Statistics*, viewed 15 March 2015, <http://www.iea.org/publications/freepublications/publication/KeyWorld2014.pdf>.

International Energy Agency 2014, *World Energy Outlook 2014*, viewed 15 March 2015, <http://www.iea.org/textbase/npsum/weo2014sum.pdf>.

International Energy Agency 2015, *Oil Market Report*, viewed 1 April 2015, <https://www.iea.org/oilmarketreport/omrpublic/>.

Keer, J 1984, *New reinforced concretes: cocrete technology and design*, Surrey University Press, London.

Knapton, J 2003, *Ground Bearing Concrete Slabs: Specification, Design, Construction and Behaviour*, Telford.

Kooiman, A 2000, 'Modelling Steel Fibre Reinforced Concrete for Structural Design', PhD Thesis, Delft Technical University.

Labib, W & Eden, N 2006, 'An investigation into the use of fibres in concrete industrial ground-floor slabs', John Moores University, Liverpool.

Lamond, J, Pielert, J (eds.) 2006, *Significance of Tests and Properties of Concrete and Concrete Making Materials*, ASTM International, West Conshohocken.

Lee, S, Oh, J & Cho, J 2015, 'Compressive Behaviour of Fibre-Reinforced Concrete with End-Hooked Steel Fibres', *Materials*, vol 8, pp. 1442-1458.

Löfgren, I 2005, 'Fibre-reinforced Concrete for Industrial Construction', PhD Thesis, Department of Civil and Environmental Engineering, Chalmers University of Technology, Göteborg.

Maccaferri 2015, *Fibers as Structural Element for the Reinforcement of Concrete*, viewed 20 April 2015, <http://maccaferribalkans.com/al/docs/documents/broshura/fibers.pdf>.

Madderom, F 1980, 'Excess water can be a costly ingredient in concrete', The Aberdeen Group.

Madhavi, T, Raju, L & Mathur, D 2014, 'Polypropylene Fibre Reinforced Concrete - A Review', *Emerging Technology and Advanced Engineering*, vol 4, no. 4.

Mansour, F, Parniani, S & Ibrahim, I 2011, 'Experimental Study on Effects of Steel Fibre Volume on Mechanical Properties of SFRC', *Advanced Materials Research*, vol 214, pp. 144-148.

Markeset, G & Hillerborg, A 1995, 'Softening of concrete in compression - Localization and size effects', *Cement and Concrete Research*, vol 24, no. 4, pp. 702-708.

Mashalah, K, Amir, H & Majid, T 2006, 'The effects of crude oil contamination on geological properties of Bushehr coastal soils in Iran', *The Geological Society of London*, vol 214.

Naaman, A 2000, 'Fibre Reinforcements for Concrete: Looking Back, Looking Ahead', *Fibre-Reinforced Concretes (FRC)*, RILEM Publications, Michigan.

Neves, R & Fernandes de Almeida, J 2005, 'Compressive Behaviour of Steel Fibre Reinforced Concrete', *Structural Concrete*, vol 6, no. 1, pp. 1464-4177.

Neves, R & Gonµalves, A 2000, *Steel Fibre Reinforced Concrete - Durability Related Properties*, LNEC, Lisbon.

Nigerian National Petroleum Corporation 2015, *Oil Production*, viewed 1 April 2015, <http://www.nnpcgroup.com/nnpcbusiness/upstreamventures/oilproduction.aspx>.

Oluremi, J & Osuolale, O 2014, 'Oil Contaminated Soil as Potential Applicable Material in Civil Engineering Construction', *Journal of Environment and Earth Science*, vol 4, no. 10, pp. 2224-3216.

Organization of the Petroleum Exporting Countries 2015, *Libya*, <http://www.opec.org/opec_web/en/about_us/166.htm>.

Osuji, S & Nwankwo, E 2015, 'Effect of Crude Contamination on the Compressive Strength of Concrete', *Nigerian Journal of Technology*, vol 34, no. 2, pp. 259-265.

Petesch, C 2013, *Shell Niger Delta Oil Spill: Company to Negotiate Compensation and Cleanup with Nigerians*, viewed 1 April 2015, <http://www.huffingtonpost.com/2013/09/09/shell-niger-delta-oil-spill_n_3892264.html>.

Radmix 2009, *Technical Manual*, viewed 20 April 2015, <http://www.radmix.com/files/Radmix_Technical_Manual.pdf>.

Rahman, A, Hamzah, U, Taha, M, Ithnain, N & Ahmad, N 2010, 'Influence of Oil Contamination on Geotechnical Properties of Basaltic Residual Soil', *American Journal of Applied Sciences*, vol 7, no. 7, pp. 954-961.

Rai, A & Joshi, Y 2014, 'Applications and Properties of Fibre Reinforced Concrete', *Journal of Engineering Research and Applications*, vol 4, no. 5, pp. 123-131.

Saint-Gobain 2011, *Vetrotex Texturised and Voluminized Glass Yarns*, viewed 15 June 2015, <http://www.vetrotextextiles.com/Products/TexturizedandVoluminized>.

Sarbini, N, Ibrahim, I & Saim, A 2013, 'Enhancement on Strength Properties of Steel Fibre Reinforced Concrete', Faculty of Civil Engineering, University of Technology Malaysia, Johor Bahru.

Shah, S, Shroff, A, Patel, J, Tiwari, K & Ramakrishnan, D 2003, 'Stabilisation of fuel oil contaminated soil', *Geotechnical and Geological Engineering*, vol 21, no. 4, pp. 415-427.

Shan, H & Meegonda, J 1998, 'Construction Use of Abandoned Soil', *Journal of Hazardous Materials*, vol 50, pp. 133-145.

Shell Nigeria 2015, *Oil Spill Data*, viewed 1 April 2015, <http://www.shell.com.ng/environment-society/environment-tpkg/oil-spills.html>.

Simetric 2011, *Specific Gravity of Liquids* , viewed 20 April 2015, <http://www.simetric.co.uk/si_liquids.htm>.

Sinclair Knight Marz 2013, 'Management of Contaminated Soils in South Australia', Adelaide.

Song, P & Tu, C 2014, 'Effect of Different Types of Polypropylene Fibres on the Properties of Mortar', *Journal of C.C.I.T*, vol 43, no. 2.

Sriravindrarajah, R, Do, H, Nguyen, L & Aoki, Y 2011, 'Effect of clogging on the water permeability of pervious concrete', in S Fragomeni, S Venkatesan (eds.), *Incorporating Sustainable Practice in Mechanics and Structures of Materials*, Taylor & Francis Group, London.

Standards Australia 2000, 'AS 1012.11: Methods of Testing Concrete'.

T. F. S. B. Products 2008, *Storage Tank Fire Protection - Leave Nothing to Chance*.

The Telegraph 2008, *Oil and Gas Related Pollution in Libya*, <http://www.telegraph.co.uk/news/wikileaks-files/libya-wikileaks/8294826/OIL-AND-GAS-RELATED-POLLUTION-IN-LIBYA.html>.

Tuncan, A, Tuncan, M & Koyuncu, H 1997, 'Stabilisation of Petroleum Contaminated Drilling Wastes by Additives', *International Offshore and Polar Engineering Conference*, Honolulu.

U. S. E. P. Agency 1997, 'Office of Pollution Prevention and Toxics', Washington.

United States Environmental Protection Agency 1996, 'A Citizen's Guide to Soil Washing', Technology Information Office.

United States Environmental Protection Agency 2006, 'In Situ Treatment Technologies for Contaminated Soil', Engineering Forum Issue Paper, Solid Waste and Emergency Response.

Wang, H & Wang, L 2013, 'Experimental study on static and dynamic mechanical properties of steel fibre reinforced lightweight aggregate concrete', *Construction and Building Materials*, vol 38, pp. 1146-1151.

Weiss, J 2012, *Stress-Strain Behaviour of Concrete*, <http://www.theconcreteportal.com/cons_rel.html>.

Wikipedia 2015, *Oil Reserves in Libya*, <https://en.wikipedia.org/wiki/Oil_reserves_in_Libya>.

Wong, C 2004, 'Use of Short Fibres in Structural Concrete to Enhance Mechanical Properties', Thesis, Faculty of Engineering and Surveying, University of Southern Queensland.

Yazıcı, Ş, İnan, G & Takak, V 2007, 'Effect of aspect ratio and volume fraction of steel fibre on the mechanical properties of SFRC', *Construction and Building Materials*, vol 21, no. 6, pp. 1250-1253.

List of Appendices

Appendix A: Project Specification

University of Southern Queensland
Faculty of Health, Engineering and Sciences

Engineering Research Project 2015
PROJECT SPECIFICATION

FOR:	Ashleigh Braden
TOPIC:	THE EFFECT OF FIBRES ON THE PROPERTIES OF CONCRETE WITH OIL CONTAMINATED SAND
SUPERVISOR:	Allan Manalo and Weena Lokuge
ENROLEMENT:	ENG 4111 – S1, ONC, 2015 ENG 4112 – S2, ONC, 2015
PROJECT AIM:	To examine the effect of fibres on the mechanical and physical characteristics of concrete with oil contaminated sand, which will give a better understanding on the properties of concrete with COIS, its potential application as structural concrete and solutions for it to meet strength requirements through the addition fibres.
SPONSORSHIP:	University of Southern Queensland
PROGRAMME:	Issue A - March 2014

1. Review current and related literature. Research the problems that arise with using oil contaminated sand in concrete, the current use fibre-reinforced concrete (FRC) in construction and the mechanical characteristics of FRC.
2. Determine the effect of oil contamination on the physical and mechanical properties of concrete. Through compressive testing, determine the percentage of oil contamination that significantly impacts the strength of concrete, however, retains adequate physical properties.
3. Evaluate the compressive and flexural behaviour of crude-oil impacted sand in concrete with four different fibre types to determine the best performing.
4. Determine the optimum dosage of the best performing fibre through investigation of compressive and flexural behaviour.
5. Writing and submission of thesis.